CHARACTERIZATION OF CELLULOSE ESTERS
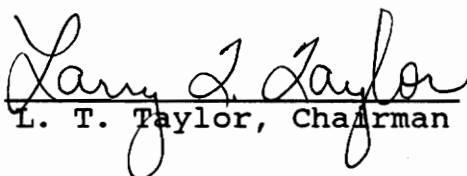
VIA GPC/FT-IR

by

Charles William Saunders

Dissertation submitted to the Faculty of the
Virginia Polytechnic Institute and State University
in partial fulfillment of the requirements
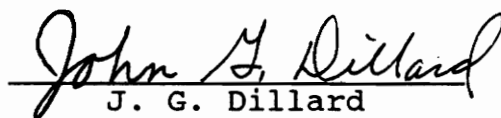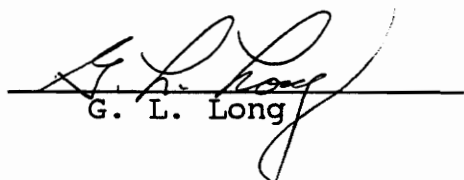for the degree of

DOCTOR OF PHILOSOPHY

in

Chemistry

APPROVED:

L. T. Taylor, Chairman

J. G. Mason

J. G. Dillard

G. L. Long

H. M. McNair

April, 1990

Blacksburg, Virginia

CHARACTERIZATION OF CELLULOSE ESTERS

VIA GPC/FT-IR

by

Charles William Saunders

Larry T. Taylor, Chairman

Chemistry

(ABSTRACT)

The object of this research was the development of on-line methods for the determination of the degree of substitution of cellulose esters. The focus of the effort was on the application of a Fourier transform infrared spectrometer (FT-IR) as an in-line detector for quantitative gel permeation chromatography (GPC). GPC/FT-IR has been used in the analysis of polymeric materials in the past, but not for quantifying the substituent content of cellulosics.

This work has identified the infrared asymmetric nitrate absorptions of cellulose nitrates observed in THF and acetonitrile solutions. Independent absorptions for the primary nitrate at C_6 and secondary nitrate at C_3 were observed at 1651 cm^{-1} and 1639 cm^{-1} respectively. In addition, a third absorption at 1667 cm^{-1} was observed to be dependent upon the degree of nitration

of the cellulose nitrate. This absorption was found to be due to steric hindrance between secondary nitrate groups on the C_2 and C_3 sites.

The infrared absorptions of cellulose acetate butyrates in THF, acetonitrile, and methylene chloride were also characterized. Separate absorptions for the acetyl and butyryl C-O-C asymmetric stretch were observed at 1235 cm^{-1} and 1176 cm^{-1} respectively. In acetonitrile and methylene chloride the carbonyl asymmetric stretching mode frequency observed at $\approx$1753 cm^{-1} was found to be dependent upon the extent of acetyl substitution.

This work developed a method for the quantitative determination of the degree of nitration of cellulose nitrates as a function of the polymer molecular weight using the asymmetric nitrate stretch. Methods for the determination of the acetyl and butyryl substitution of cellulose acetate butyrates were developed as well. Examples of each method applied to real world samples were carried out.

ACKNOWLEDGMENTS

Table of Contents

List of Figures

List of Tables

Chapter 1

Introduction

Introduction

Cellulose esters have been important commercial polymers since their discovery in 1846. It was then that cellulose nitrate (CN) was invented by C. F. Schöenbein[1]. CN quickly replaced blackpowder as the propellant for munitions and explosives. The first plastic, celluloid, was a combination of CN and camphor and was used as a base for photographic emulsions. Another cellulose ester, cellulose acetate (CA), eventually replaced celluloid due to the flammability of CN. Many lacquers and product coatings contain a cellulose ester of some type, such as CN, CA, cellulose propionate (CP), cellulose acetate propionate (CAP), or cellulose acetate butyrate (CAB).

Cellulose esters can be divided into two categories, inorganic and organic. CN is the only inorganic ester of cellulose to achieve commercial significance[2]. The lower nitrogen containing soluble CNs are utilized in wood and automotive coatings, while the higher nitrogen content smokeless powders are used in the production of propellants. CN differs in its production compared to organic esters of cellulose in that the cellulose starting material never dissolves in the reaction medium. This means that chemical and physical

variations in the starting material are retained and thereby influence the end product. Commercial cellulose can be obtained from either wood pulp or cotton. Wood pulp contains a lower amount of alpha cellulose than cotton. Alpha cellulose is considered to be pure cellulose and in the presence of more impurities harsher chemical treatment is needed for purification. This harsher treatment results in lower average molecular weights and greater polydispersity, which affect the mechanical properties of the CN produced from wood pulp[3].

The analysis of CN includes those parameters common to all polymers, such as molecular weight distribution (MWD) and intrinsic viscosity. Presently gel permeation chromatography (GPC) is the method of choice for determining the MWD, despite disagreement among some as to the validity of current calibration methods. The question appears to center around the solvent/solute interaction of polymers in solution. Presently the MWD relative to polystyrene standards is accepted. In addition to MWD, the percent nitrogen of the material is of importance, since this controls the solubility characteristics of the CN. The end use of the CN is governed by its solubility in various solvents. The nitrate nitrogen content is determined using

a Du Pont nitrometer[4]. This method is based upon reacting the nitrate with sulfuric acid and mercury, generating sulfate salts and evolving NO gas. It is the volume of evolved gas which is actually measured. This method yields only the average nitrogen content for the polymer and gives no information as to the uniformity of the nitrogen content throughout the polymer MWD. The additional tests performed on CN focuses on the physical and mechanical properties of the polymer.

Organic esters of cellulose include CA, CP, and the mixed esters CAP, CAB, cellulose acetate phthalates, succionates, and others. The acetates of cellulose have achieved the greatest commercial significance, with CA being the most widely used cellulose ester. Aside from photographic film bases, it is used in the production of cigarette filters and acetate fibers in the textile industry[5].

Analysis of CA and the mixed acetate esters is essentially the same, so that individual discussions would be redundant. As with CN and most other polymers, the MWD and intrinsic viscosity are of importance. In addition, tests for the acetyl and, in the case of mixed esters, additional ester groups are performed. The official methods, as set forth by the American Society for Testing and Materials (ASTM), involve

saponification of the ester functionality with excess NaOH and back titration with standard acid[5,6]. This method can take as long as three days to obtain results. In addition to the amount of ester substitution, the amount of remaining unesterified hydroxyls is important. The hydroxyl content is the controlling factor in solubility characteristics of organic cellulose esters[7]. The ASTM method for measuring residual hydroxyl involves reacting with phenyl isocyanate and measuring the ultraviolet absorbance of the resulting carbanilate[6].

Infrared spectrometry has been used in the analysis of cellulosics, but for the most part been restricted to qualitative interpretations. Generally, a film of the polymer is cast from solution and transmission infrared analysis performed. Interpretation consists of observing the presence or absence of specific functional groups. Despite the advent of improved instrumentation with Fourier transform infrared spectrometers (FT-IR), and their potential when coupled with chromatographic techniques, relatively little work has been performed in this area[8]. Infrared absorption is specific to the functional group present, and as such can yield a wealth of information about how the environment of an analyte influences its chemical

conformation.

THESIS STATEMENT

The goal of this research is to develop an on-line GPC method for determining the degree of substitution of cellulose esters as a function of the polymer molecular weight. The method development will focus upon characterizing the infrared absorptions of cellulose nitrates and cellulose acetate butyrates in solution, and identifying those absorptions which are ester substituent specific.

RESEARCH OBJECTIVES

The following objectives were established for this research:

[1] Characterize cellulose nitrate and cellulose acetate butyrate via FT-IR and GPC/FT-IR.

[2] Correlate observed infrared and chromatographic data with chemical and/or physical properties of the cellulose ester.

[3] Develop qualitative and if possible quantitative
     methods for the characterization and/or substituent
     analysis of cellulose esters using FT-IR detection.

[4] Apply these methods to real world samples to
     determine the usefulness of FT-IR and GPC/FT-IR as
     an analytical tool for cellulose esters.

Chapter 2

Literature Review

LITERATURE REVIEW

Chromatography of Cellulose Esters

Cellulose Nitrate

The earliest efforts to separate different molecular weight fractions of cellulose nitrate were performed by fractionation methods[9,10]. This method could be either solution fractionation or precipitation fractionation. Solution fractionation consists of incremental addition of solvent of increasing solvent strength. Each incremental fraction consists of polymer of increasing molecular weight. An uncertainty with the technique is whether sufficient time has passed for complete solubilization of a given fraction. In contrast, precipitation fractionation is achieved by first dissolving all of the polymer in a suitable solvent and then adding increasing amounts of a non-solvent to precipitate the fractions. In this method, it is the higher molecular weight material which is obtained first. In studies to evaluate fractionation methods for CN, it was found that most laboratories preferred precipitation fractionation over solution fractionation[11,12]. The preferred solvent was a mixture of

acetone:water (91:9), with incremental additions of water to precipitate the fractions. It was also found that precipitation fractionation yielded more fractions than did solution fractionation, particularly in the high molecular weight region. Figure 1 shows the cumulative percent of cellulose nitrate fractions where the same worker carried out the fractionations using the same methods. Both techniques were reproducible, giving consistent though different values for the same samples. The different lines in each graph represent replicate measurements.

Fractionation methods have for the most part been replaced by chromatographic techniques, particularly GPC. In GPC, separation of the individual fractions is accomplished by passing the polymer through a column(s) packed with material of defined pore size. Based upon the hydrodynamic volume of the polymer molecules, the smaller molecules which fit within the pores are retained and the larger molecules are excluded and pass through the column bed. Thus, the higher molecular weight material elutes first. Common detectors used with GPC include differential refractive index (DRI), ultraviolet (UV), and differential viscometric.

The first application of GPC for CN was in 1965[13]. In many of the early papers the objective was not to
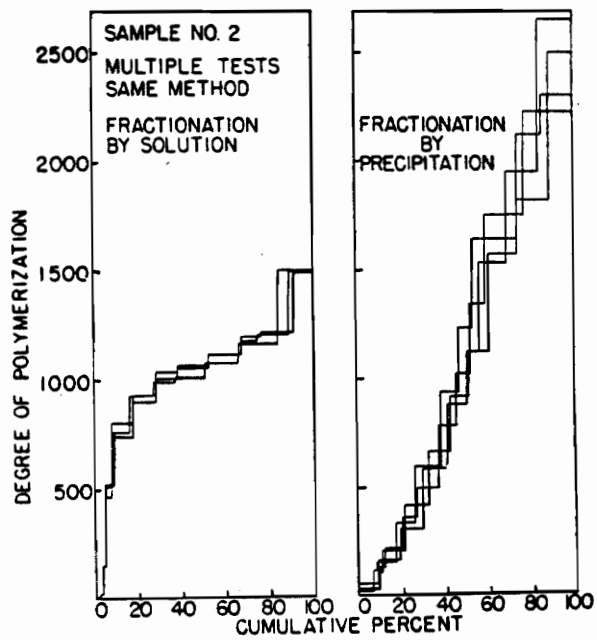
Figure 1. Comparison of solution and precipitation
fractionation methods performed by the same
worker [11]

obtain molecular weight data for the CN itself, but to use the nitrate derivative to obtain information about the original cellulose[13-19]. This was ostensibly due to the lack of degradation of the cellulose when nitrated with proper care[16]. The cellulose was nitrated to a level of ≈13.4 % nitrogen, very near the theoretical maximum of 14.15 %.

Of the papers which dealt with the nitrate itself, most were concerned with propellant grade CN[20-25]. For these, the nitrogen content varies over the range of 11.0 to 13.5 % nitrogen. A major concern in these reports was whether data obtained on a highly nitrated CN could be extrapolated for use with lower nitrated species. Since GPC is based upon hydrodynamic volume, such an extrapolation assumed that all CNs behaved the same in solution regardless of the degree of nitration. The elution volume of the polymer was thought to be a function solely of the chain length, however, calculated weight average molecular weights were consistently higher than values obtained by intrinsic viscosity measurements. Calibration for the system consisted of using narrow molecular weight polystyrene standards, and relating the elution volume of the sample to the molecular weight of polystyrene which would elute at the same volume. A solution to this dilemma appeared in

1967 in a report by Benoit, Grubisic, and Rempp[26]. They suggested that the universal calibration parameter for GPC was the hydrodynamic volume of the polymer, measured as the product of intrinsic viscosity and molecular weight, and not chain length. The logarithm of this product plotted against elution volume for a number of different polymers all fell on a single curve, shown in Figure 2. This suggested that a set of narrow molecular weight standards for a well defined system, such as polystyrene, could be used to arrive at accurate molecular weight values for systems where no such standards exist for the polymer in question, as in the case of cellulose nitrate.

Holt et al. investigated the validity of this calibration technique specifically for high molecular weight cellulose nitrate[27]. They found that when ethyl acetate was the solvent the elution volume of the CN was dependent upon the injected sample concentration. If the elution volume were extrapolated to zero concentration, then the universal calibration of Benoit et al. held true. French and Nauflett[24] and Marx-Figini and Soubelet[19] found that when $\log [\eta] M_n$ was used, the curve for CN was parallel but displaced from that of polystyrene. Each group found that the displacement was equal to the dispersity of the polymer, M_w/M_n.
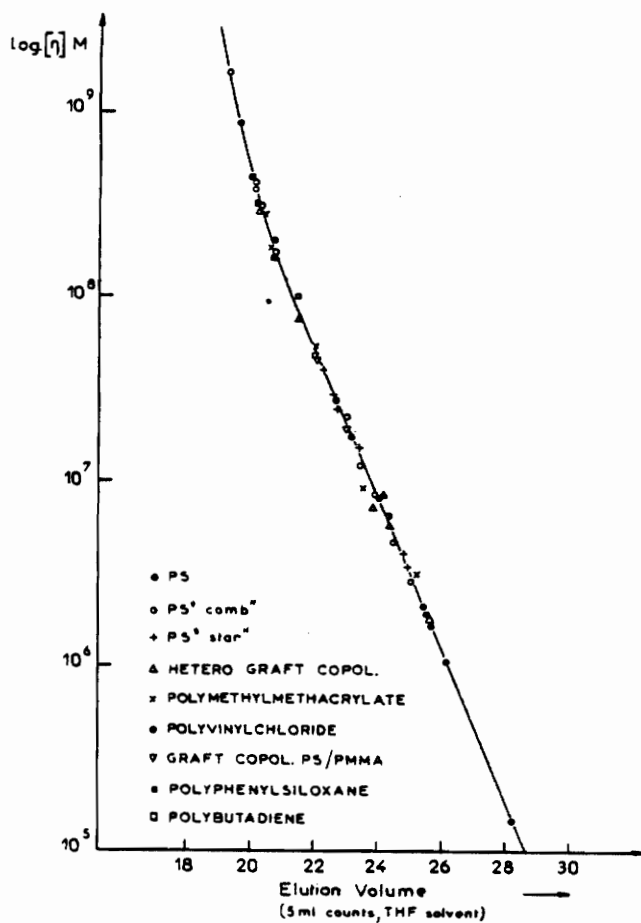
Figure 2. Universal GPC calibration for several poly-

mers based upon hydrodynamic volume [14]

In order to circumvent the problems associated with using polystyrene to calibrate GPC data for CN, it is necessary to identify a different polymer which has solution properties closer to those of CN, and for which a series of narrow molecular weight standards can be prepared. Since such a material has not been found, attempts have been made to use CN itself to calibrate the GPC data. Goetz et al. have used broad molecular weight CN samples which have been well characterized by independent means, such as light scattering and membrane osmometry, as calibration standards[28]. They derived an equation which relates the elution volume of the broad molecular weight CN to that of narrow molecular weight polystyrene as:

$$C_x(V_x) = \alpha C_{ps}(V_{ps})\beta$$

where V is the elution volume, C_x and C_{ps} are constants related to the molecular weight of the CN and polystyrene standards respectively, and α and β are constants combining the Mark-Houwink constants for the polymers in question. Using the independently derived molecular weight data for CN and polystyrene and the GPC elution data, a computer algorithm computes the constants. With this type of calibration, they found that computed molecular weights and polydispersities were much closer

to those obtained by viscometry and osmometry. A drawback observed was the need to use a CN standard which contained the same nitrogen content as the sample being analyzed.

In addition to calibration, problems associated with detection of CN in GPC have been reported. These stem mostly from the widespread use of differential refractive index (DRI) as the universal GPC detector. Most of the early reports on GPC of CN used THF as the mobile phase. Indeed, THF is still one of the most common GPC solvents. With CN the problem lies in the very small refractive index difference between THF and CN[10,18]. Efforts to alleviate this problem have taken two approaches. The first was to explore alternative solvents which might have a greater refractive index difference, and hence improve the overall signal to noise ratio. As mentioned earlier, Holt et al. used ethyl acetate as a solvent[27]. The major drawback here was the much greater dependence of the elution volume upon the injected sample concentration. This would make accurate molecular weight information difficult to obtain. Meyerhoff has explored the use of acetone as a solvent[18,29]. Acetone is a better solvent for CN than THF and also possesses a greater refractive index difference. When Styragel[TM] columns were used, acetone

consistently gave a broader elution profile than did THF. Separation of individual molecular weight fractions was also better with acetone than THF and the expected improvement in signal to noise ratio was obtained. The drawback with acetone is the effect it has on the swelling characteristics of the cross-linked polymer gels. Acetone tends to cause the gels to contract to some extent, so that a separate column for which the gels have been conditioned for use with acetone is necessary.

A corollary to the examination of different solvents for the GPC of CN is the examination of the solvation of CN in the solvents themselves. It has been noted for some time that solutions of CN demonstrate what has been termed an aging effect. This effect manifests itself as a decrease in solution viscosity with time. Spurlin devoted a section of his classic work to the subject [30]. Reviewing work performed to that time, he came to the conclusion that aging was the result of degradation of the CN chain resulting in the production of lower molecular weight material. Siochi has more recently studied this problem[10]. Using low angle laser light scattering and GPC she came to the conclusion that the decrease in solution viscosity arose not from degradation of the CN but from a break-

ing-up of aggregates of CN molecules as the solvent more fully penetrated the fibrous structure. Such a break-up would result in an apparent increase in the low molecular weight fraction of the polymer.

The second approach to solving the detection problem has been to explore different detectors for use with GPC in the analysis of CN. The ultraviolet detector (UV) has been used for CN, where the absorption of the nitrate moiety gives rise to the signal response[21,22]. Here the difficulty is in the different absorption which one would get from CNs of similar molecular weight but different degrees of nitration. More recently, Carlson et al. have utilized a photo diode array UV detector for the GPC of CN[23]. This enabled them to observe changes in the chromatogram throughout the UV spectrum. They were able to verify that the degree of nitration of the CN does indeed influence the UV absorption, particularly at 270 nm, a secondary absorption maximum for CN.

Lloyd has demonstrated the utility of electrochemical detection for the analysis of CN residues of forensic interest[31,32]. The CN was detected with a pendent mercury drop electrode which was connected directly to the GPC system. The hydrodynamic voltammogram generated was sensitive to as little as 1 ng of CN

present in firearm residues. This system consisted of a single 25 cm column packed with silanized bare silica and a mobile phase composition of acetonitrile:water (100:5, v/v) containing 0.01 M tetramethylammonium perchlorate. The water served to reduce adsorption effects on the silica column and to provide a source of protons for reduction at the electrode. The perchlorate was added as a supporting electrolyte and was selected for the low residual current it provided. Operating at a flowrate of 1.5 mL/min. samples could be screened for the presence of propellant grade CN in as little as 3 minutes after sample preparation.

Other detectors used for the GPC of CN have included the differential viscometer and the Fourier transform infrared spectrometer (FT-IR). Siochi utilized the differential viscometer in tandem with a DRI for her work[10]. This detector measures the pressure of the eluting species and relates the differential pressure with the viscosity of the eluting species as:

$$DP/P_i = n_{sp}/4$$

where DP is the differential pressure, P_i is the inlet pressure, and n_{sp} is the specific viscosity. The specific viscosity can then be used with the universal calibration to arrive at absolute molecular weight information.

Raisor and Law used an FT-IR coupled to GPC to obtain molecular weight information for propellant lacquers which contained polymers which overlapped sufficiently so as to make quantitation difficult using conventional detectors[33]. By integrating the GPC chromatogram over selected wavenumber regions they were able to obtain separate elution profiles for each polymer contained in the lacquer, and then determine the molecular weights of each.

GPC has not been the only chromatographic technique applied to CN. Forestier and coworkers[34,35] and Douse[36] have demonstrated the utility of thin layer chromatography (TLC) for the separation and identification of CN in residues from explosions and handswabs. After separation on silica gel plates using either trichloroethylene:acetone (80:20)[34,35] or acetone:methanol (60:40)[36], the CN spot was visualized using Griess' reagent. Kamide et al. used both open TLC and vapor programmed TLC (VP-TLC) to determine the nitrogen content of CNs[37]. In open TLC the developing chamber is open to the atmosphere and the vapor phase surrounding the TLC plate is not saturated with mobile phase. In VP-TLC the chamber is closed and the vapor phase saturated with mobile phase under controlled conditions. Both techniques were able to separate CN by

nitrogen content but the mechanisms involved were different. Open TLC operated more on adsorption-desorption while VP-TLC operated more from phase separation.

Cellulose Acetates

The separation techniques applied to cellulose acetates (CA) have for the most been the same through the years as those for CN. The major difference is the lack of the calibration problems which have plagued CN. Brewer et al. compared GPC and fractional precipitation for determining the molecular weight distribution of cellulose acetates and cellulose carbanilates[38]. They found that both methods gave comparable results. Kamide and coworkers have continued to utilize successive solutional fractionation (SSF) in the characterization of cellulose triacetate and water soluble incompletely substituted cellulose acetate[39,40,41]. For the triacetate 1-chloro-2,3-epoxypropane was used as the solvent and hexane as the non-solvent. For the water soluble acetate water was used as the solvent and methanol the non-solvent. This same group used SSF in combination

with GPC in the characterization of cellulose diacetate[42]. The SSF fractions were analyzed by light scattering and membrane osmometry and the results compared with GPC. Here again there was good agreement between the techniques. Alexander and Muller also found that the combination of fractionation methods with GPC aided in the characterization of very low and very high degree of polymerization regions of cellulosics[43].

Charcoal[44] and aluminum filings and quartz sand[45] were investigated as early substrates for the chromatography of CAs, however, they appear to have had only limited success. Mano and Cunha Lima reported a paper chromatographic method for the identification of several cellulose esters[46]. Cellulose acetates and acetate butyrates were first saponified and the acetic and butyric acids detected by paper chromatography with an ethanol:ammonium hydroxide solvent folowed by development in bromocresol green.

Wilson and Floyd have taken a different approach to the chromatography of cellulose acetates[47]. They have been working on the separation of mixtures of cellulose acetates by the percentage acetyl content using gradient HPLC. Using a PRP-1 column and a mobile phase of acetone:water:methanol (4:3:1) programmed to 100 % acetone at 0.8 mL/min over 15 min. they were able

to separate several cellulose acetates containing from 38 to 43 percent acetyl groups by weight. Figure 3 shows the graph they obtained of retention time versus percent acetyl.

A method based upon the hydrolysis of the ester groups followed by gas chromatography was reported by Williams and Siggia[48]. The polymer was first reacted with molten phosphoric acid at elevated temperature. The volatile products were trapped in a loop immersed in liquid nitrogen. After completion of the reaction the loop is heated and the condensed products swept into a gas chromatograph for detection. Reported recoveries were close to 100 %.

Infrared Spectroscopy of Cellulose Esters

Cellulose Nitrate

Employment of infrared spectroscopy (IR) to the characterization of cellulosics was one of the first applications of IR. Kuhn examined the infrared spectra of 79 carbohydrates in 1950[49]. Among those was a sample of nitrocellulose. The samples were all examined as

RETENTION TIME (MIN)

Y = 0.491*X - 10.2

Weight Percent Acetyl
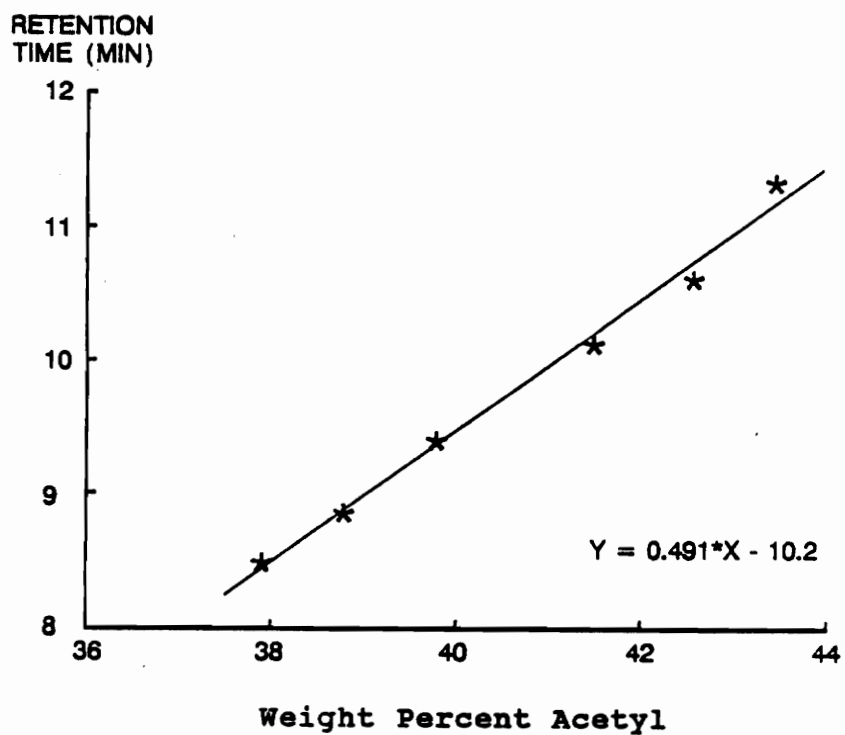
Figure 3. Correlation of percent acetyl in cellulose
acetate versus HPLC retention time [47]

solids in mulls of mineral oil or as viscous liquids placed between salt plates. A great deal of useful information concerning the absorption frequencies of substituents was learned from such early studies. Pristera et al. also examined nitrocellulose in a study of the infrared spectra of some 68 explosive ingredients[50]. The objective was to evaluate IR for the analysis of explosive mixtures with the possibility of developing a rapid and quantitative procedure. There were several early attempts to use infrared spectroscopy to quantitate the percent nitrogen in a cellulose nitrate. In 1959 Rosenberger and Shoemaker used the 11.92 micron (840 cm^{-1}) O-N absorption band to determine the percent nitrogen of cellulose nitrate in mixtures of cellulose resins[51]. Levitsky and Norwitz used the asymmetric N-O stretch of cellulose nitrate at 6.0 microns (1660 cm^{-1}) for the determination of percent nitrogen[52,53]. Rather than casting the CN as a film on a salt plate, as had been done in all previous work, they ran their samples in a liquid cell with the CN dissolved in THF. This avoided the previously reported problem of total absorption of CN at the 6 micron band. Norwitz continued to develop the technique into the 1970's with a method to determine the percent nitrogen of CNs contained in propellant formulations[54].

Aside from efforts to develop quantitative methods IR has also been used to probe some of the fundamental properties of CN. Jutier et al. used FT-IR to follow the kinetics of the thermal degradation of CN derived from wood pulp and cotton[55]. They followed the increase in the absorbance of a band at 1740 cm^{-1} as a function of temperature to arrive at kinetic parameters which describe the autocatalytic degradation of CN. This band arises from the cleavage of the $O-NO_2$ bond during combustion, resulting in the formation of aldehydes which give rise to the carbonyl stretching absorption at 1740 cm^{-1}.

In addition to kinetic studies IR has been used to examine the hydrogen bonding characteristics of cellulose nitrates. Brodman, Devine, and co-workers have published several articles relating to the hydrogen bonding of CN^{56-61}. The majority of these dealt with the hydrogen bonding of deterrents to the unesterified hydroxyl groups of the CN. Deterrents are materials which interact with the CN so as to decrease the burning rate. Among those materials which were examined were di-n-butyl phthalate, camphor, N,N'-diethyl-N,N'-diphenylurea, N,N'-dimethyl-N,N'-diphenylurea, and 2,4-dinitrotoluene. The extent of hydrogen bonding was monitored by observing the shift in the absorption

maximum of the hydroxyl stretching region in the area of 3500 to 3300 cm^{-1}. The diphenylureas exhibited the greatest hydrogen bonding of the five while 2,4-dinitrotoluene exhibited the least. In all cases it was hypothesized that interaction occurred between the unesterified hydroxyls of the CN and either the nitrogen of the ureas, the nitro group of 2,4 dinitrotoluene, or the carbonyl group for the others. Further studies with di-n-butyl phthalate presented experimental support for the postulation of a transition of predominant intermolecular forces from hydrogen bonding to van der Waals on going from intermediate to highly nitrated celluloses. In this case the hydroxyl stretching frequency was observed to increase from 3525 cm^{-1} for a 12.1 % nitrogen CN to 3560 cm^{-1} for a 13.1 % nitrogen CN. The transition, while not a sharp one, appeared to occur for CN containing 12.5 % nitrogen.

Having established that infrared analysis could be used to rank the strengths of known deterrents, this same group set out to evaluate classes of compounds which might prove useful as deterrents. Two series, one of benzoic acid esters and one of phthalic acid esters, were examined to measure the extent of hydrogen bonding as a function of the ester side chain length. For the benzoic acid esters a correlation was observed between

the hydroxyl stretching absorption shift and the Taft σ^* constant. The Taft σ^* constant is an empirical measure of the compound's electron donating ability. With increasingly negative Taft σ^* value the electron donating effect of the compound increases and the strength of the hydrogen bond increases as reflected by the shift in the hydroxyl absorption frequency.

Deterrents have not been the only type of compounds which hydrogen bond to CN examined by infrared analysis. The energetic nitramines octahydro-1,3,5,7-tetranitro-s-tetrazine (HMX) and hexahydro-1,3,5-trinitro-s-triazine (RDX) have also been examined. The interaction of these materials with CN was deemed important to the understanding of propellant formulations. It was found that a hydrogen bond of the CN hydroxyl to an oxygen of the nitramine existed and that RDX appeared to form a stronger bond with CN than did HMX.

Brodman's group has not been the only ones exploring the hydrogen bonding characteristics of CN. Nauflett and Gill have described another case of a nitramine acting as a plasticizer with CN through hydrogen bonding[62]. In this case the nitramine was N,N'-dimethyl methylenedinitroamine (DMMD).

Cangelosi and Shaw used monofunctional electron

donating probes to examine the extent of hydrogen bonding in a number of polymer systems including CN[63]. They found that for probes containing carbonyl functional groups the strength of the hydrogen bonds correlated with solubility parameter comparisons. This correlation indicates that hydrogen bonding is a major force in the solubility of these polymers.

Panov, Zhbankov, and Malakhov have explored the infrared absorptions in the hydroxyl and methylene regions of CNs in an effort to study the fine structure of the polymer [64,65]. Examining CNs of varying degrees of nitration they found that unesterified hydroxyls are involved in some form of hydrogen bonding even in highly nitrated CNs. They also found the hygroscopic nature of CN resulted in the adsorption of water from the environment, which gave rise to the appearance of a non-bonded hydroxyl absorption in the 3600 cm^{-1} region.

Cellulose Acetates

The use of infrared spectroscopy in the analysis of cellulose acetates has focused more upon the quantitation of the residual hydroxyls than upon the degree of substitution as in CN. This is due to the importance

of the residual hydroxyls in the solubility of the product in various solvents. Brown et al. examined the infrared spectra of several organic cellulose derivatives in the 4000 - 3000 cm^{-1} region, the fundamental hydroxyl stretching region[66]. Measuring cast films of several cellulose acetate butyrates they found that the hydroxyl absorption region contained three bands at 3490, 3553, and 3631 cm^{-1}. The intensity of the 3490 cm^{-1} band increased relative to the others as the butyryl content increased. This variation was attributed to the decreased incorporation of water in esters of greater butyryl content.

Mitchell et al. developed a method for the determination of the acetyl content of cellulose acetates by measuring the first overtone of the hydroxyl stretching absorption at 1.445 μ[67]. They found that this overtone varied inversely with the acetyl content of the cellulose acetate under investigation when pyrrole was used as the solvent. Hilton extended the application of near infrared analysis to the determination of hydroxyl numbers in polyesters and polyethers and found the results were less than one percent different than those obtained by chemical methods with the added benefit of reduced man hours[68].

Some more fundamental studies have been carried

out. Cangelosi and Shaw examined cellulose acetate
butyrate (CAB) in the same fashion as they did CN[63]. As
with CN they found that CAB exhibited strong hydrogen
bonding characteristics with electron donating probe
compounds. Ivanova and Zhbankov examined cellulose
acetates and, as did Panov and coworkers with CN, found
no evidence of free hyroxyls[69]. They found that the
extent of hydrogen bonding was proportional to the
degree of esterification and that celluloses acetylated
in a homogeneous medium had a hydroxyl absorption
maximum at 3350 cm^{-1} corresponding to intermolecular
hydrogen bonding. Marupov examined cellulose esters and
ethers in the 1300 to 900 cm^{-1} region[70]. They identi-
fied several absorptions which they were able to assign
to the asymmetric stretching mode of the C-O-C(=)
structure of the ester groups.

Applications of Fourier Transform Infrared Detection to Chromatographic Analyses

The first demonstration of coupling a FT-IR to a chro-
matographic system was in 1967 when Low and Freeman passed
the eluate from a packed GC column through a 4 mm i.d.
x 5 cm long flowcell[71]. Since that time a number of
improvements to the GC "lightpipe" designs have been
made and the technique has been extended to LC and

SFC[72].

GPC (a form of LC) was one of the earliest and easiest LC methods adapted for on-line IR analysis[73]. The isocratic mobile phase of GPC made spectral subtraction of the solvent absorption from analyte absorption simple and straightforward compared with the difficulties associated with gradient mobile phases. In this early work the separation and identification of silicone oils, paraffin oils, and benzene was demonstrated using μ-Styragel GPC columns and THF as the mobile phase. The infrared detector was a dispersive instrument and thus only a single frequency could be monitored as opposed to collection of the full IR spectrum. The C-H stretching mode at 2940 cm^{-1} was selected for its universality and sensitivity for a wide range of organic compounds.

Terry and Rodriguez used a similar instrumental setup to measure several functional groups contained in a polymer as a function of molecular weight[74]. They successfully measured the amounts of polystyrene and polymethyl methacrylate in a mixture even though the polymers coeluted by monitoring the IR absorption at 1731 cm^{-1} and 698 cm^{-1} independantly. They also measured both the free and bonded hydroxyls and the ether functionality of polyethylene oxide by measuring the

absorptions at 3610 cm^{-1}, 3510 cm^{-1}, and 1132 cm^{-1} respectively.

With the development of Fourier transform instruments the ability to obtain full spectrum analysis became possible. Vidrine and Mattson demonstrated the separation of butyl acrylate polymer from polystyrene using THF as the solvent[75]. Real time chromatograms were generated by the monitoring of specific wavenumber regions and full spectra from different elution volumes were compared for identification of the polymers. They also looked at a mixture of silicone and mineral oils in carbon tetrachloride. Vidrine later demonstrated the power of FT instruments by the use of spectral subtraction to identify coeluting analytes[76].

Since its development two schools of thought on the collection of LC-IR data have arisen. The first, used in the early examples, is to collect the spectra "on the fly" using an in-line flowcell and accept the loss of some regions from complete solvent absorption. The advantages of this method are simplicity, the ability to analyze labile compounds, and the ability to quantitate[77]. The alternate method, developed by Griffiths and coworkers, is to deposit the column effluent onto a moving belt or similar track from which the solvent is removed by thermal processes[8]. The advantage

of this method is the ability to obtain complete spectra. The disadvantages are the complexity of the instrumental setup, memory effects from from previous compounds deposited on the belt, and the loss of labile compounds during the solvent removal process[8,77]. Most commercial instruments utilize the flowcell method.

One of the prime considerations in collecting chromatographic information on the fly is the identification of the chromatographic peak from background data. In FT techniques data are collected in the frequency domain and interferograms are what is actually stored. Different schemes for converting the interferometric data into conventional chromatographic data have been proposed.

The two popular methods for generation of chromatographic data from FT-IR detection in use today were introduced in back-to-back papers presented at the International Conference on FT-IR held in Columbia, SC, June 1977[78,79]. Coffey and Mattson devised a method which consisted of transforming a small portion of the data points collected per interferogram and integrating the absorbance over several specific infrared regions[80]. The result was a set of low resolution chromatograms which were monitored in real time (the calculations taking less than one second of computer

time) and also gave some information about the func-
tional group characteristics of the eluting compounds.
In their original work five spectral regions covering
the most common functional groups were monitored: the
OH region from 3600-3570 cm^{-1}, the CH region from 3080-
3020 cm^{-1}, the carbonyl region from 1760-1680 cm^{-1}, the
aromatic C-C region from 1560-1520 cm^{-1}, and the COC
region from 1170-1155 cm^{-1}. Most manufacturers of
instruments today offer this technique for obtaining
chromatograms in the form of several user selectable
spectral regions.

The second technique introduced at the conference
in 1977 was by de Haseth and Isenhour and is based upon
Gram-Schmidt vector orthogonalization[81]. In this case
the vector consists of the number of data points which
comprise the digitized interferogram. If two orthonor-
mal equivalent vectors are summed the resultant vector
is zero. If the vectors are nonequivalent the resulting
vector will be non-zero. In the case of FT-IR data the
non-zero amount will be proportional to the amount of
infrared absorbing analyte present in the flowcell at
that point in time. Since Gram-Schmidt orthogonaliza-
tion operates on the interferogram information over the
entire spectral range is included in the data. Thus,
the resulting chromatogram contains all peaks which

absorbed at any region of the spectral range. This is quite different from the previous case where each resulting chromatogram contained only those peaks which absorbed in the defined spectral region. The Gram-Schmidt technique is also available on all present day commercial equipment and the two methods are often used in combination.

Chapter 3

Characterization of Cellulose Nitrates via GPC/FT-IR

Introduction

The nitration of cellulose is a complex equilibrium reaction where each hydroxyl reacts at a different rate and is influenced by the presence of a nitrate group at the adjacent position. This leads to eight possible combinations of nitrate and hydroxyl groups on any anhydroglucose unit. Figure 4 shows these possible combinations and the corresponding degree of nitration. In addition, these substituted glucose units may be distributed randomly along a cellulose nitrate chain. Thus any cellulose nitrate is really composed of a mixture of units of varying degrees of nitration placed randomly along the molecular chain. It is this fact which has led to the difficulties reported in the analysis of CNs and to its unique and complex chemistry.

The mechanism for the separation process in GPC is accepted as being principally due to the hydrodynamic volume of the polymer in the solvent system in use. Thus polymers of like molecular composition and weight would sweep out the same volume and demonstrate the same chromatographic retention characteristics. The
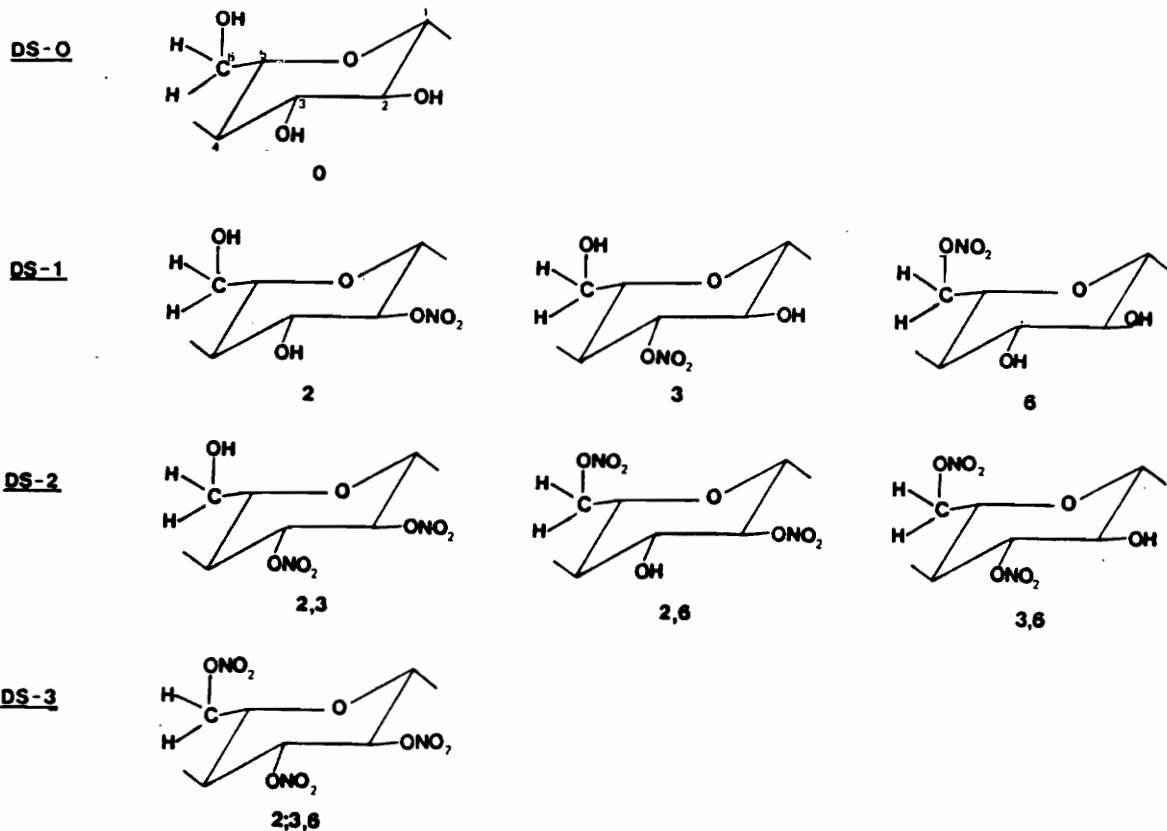
Figure 4. Eight possible substitution patterns for nitrated anhydroglucose units of cellulose.

nitration of cellulose carries it through a sequence of changes not only in weight and substitution but also in inter- and intramolecular interactions. Spurlin described the sequence in terms of the regularity of the cellulose chain and the associated interactions[82].

This is best illustrated by examining a projection of the cellulose chain and considering the changes introduced as the nitration progresses. Figure 5a shows the cellulose backbone with the three hydroxyl sites fully substituted. The chain appears the same in the case of the fully unsubstituted material. Initially all sites are occupied by hydroxyls and hydrogen bonding is the principal interaction force between and among anhydroglucose units. The regularity of the polymer allows for significant interaction, as the insolubility of cellulose in many common solvents attests. As the nitration proceeds, hydroxyls are replaced by nitrato groups, leading to an irregular chain sequence in the partially substituted molecule (Figure 5b). This reduces the possibility for hydrogen bonding and restricts the amount of intermolecular interaction which can occur. When nitration is complete, again a regular structure is obtained since all sites are now occupied by nitrato groups Figure 5a again). Intermolecular

(a) Completely substituted derivatives

(b) Derivatives of substitution 2.3

○ Oxygen   ● Hydrogen   ⊘ Substituents
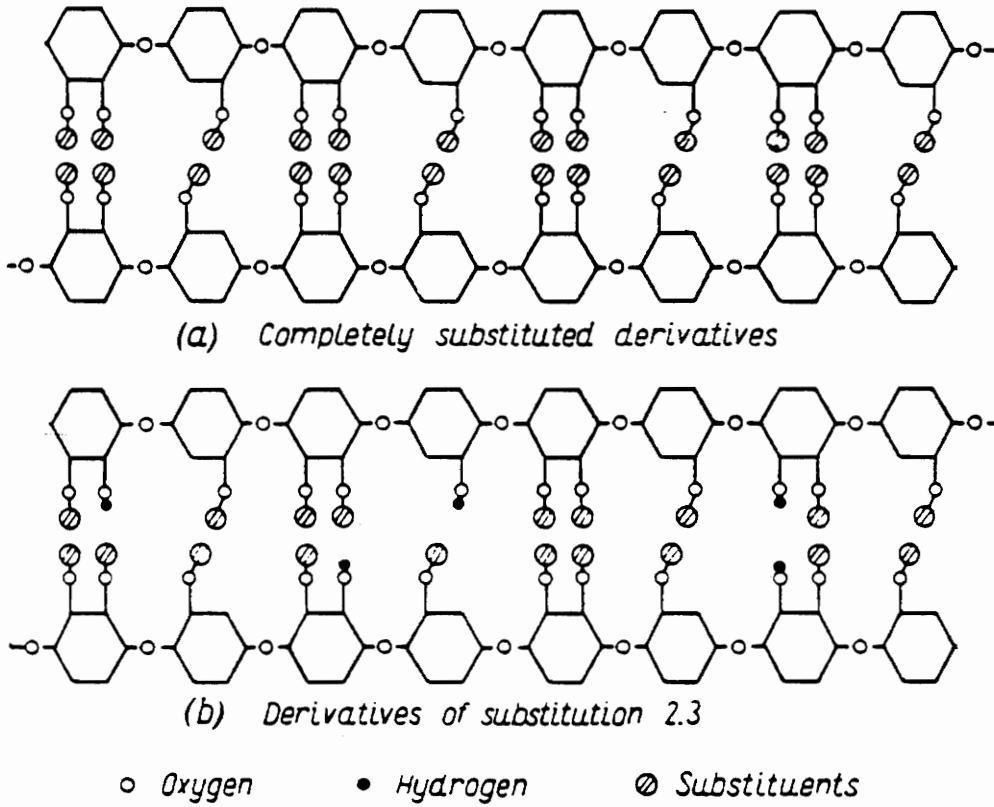
Figure 5. Illustration of regularity of cellulose
chain.[82]

41

interaction is now more likely than the intermediate case but now the forces involved are van der Waal's rather than hydrogen bonding. With CNs of different but intermediate substitution one can envision a multitude of intermediate and possible combinations of the forces involved, which lead to the different solubilities of the CNs and may influence the GPC of them as well.

In order to characterize CN via GPC/FT-IR it is first necessary to evaluate the chromatography of CNs of varying degrees of nitration to evaluate the influence, if any, of increasing nitration on the chromatographic separation of CN when FT-IR is used as the detector. Conventional detectors for GPC include differential refractive index (DRI) and ultraviolet (UV). Since the refractive index difference between THF and CN is small, UV detection has been more commonly employed to achieve greater signal to noise ratio. As a part of the development of on-line infrared detection of the GPC of CN a comparison of IR and UV as detectors has been performed.

One of the advantages of on-line infrared detection is that not only is chromatographic information available but spectrometric information as well. Given sufficient infrared windows this can mean positive identification of unknown peaks is available without

additional outside analyses. In the infrared analysis of polymers generally only qualitative information is sought and the samples are usually examined in the solid state as thin films. Obtaining infrared spectra on the fly as the chromatography is being carried out means that spectral information concerning different regions of the chromatographic peak are available and a more detailed study of the polymer is possible. In this work an examination of changes which may be present in the infrared spectra have been examined as a function of the polymer molecular weight distribution.

Experimental

For this work a single mixed bed polystyrene divinylbenzene GPC column was selected. Such a column gives a medium separation of polymeric distributions in a reasonably short period of time. A Perkin Elmer PL-Gel mixed bed column, 30 cm by 7.5 mm i.d. was used (Perkin Elmer Corp., Norwalk, CT). The mobile phase was HPLC grade THF (Fisher Scientific, Raliegh, N.C.) at a flowrate of 1 mL/min. HPLC grade THF was chosen since it does not contain the preservative butylated hydroxy-toluene, which absorbs strongly in the ultraviolet. A Perkin Elmer LC-10 HPLC pump was used to deliver the

mobile phase to the column.

The detector used was a Nicolet 5SXC FT-IR (Nicolet Instruments, Madison, WI.) fitted with an in-line flowcell. This flowcell is made of zinc selenide and is cylindrical in design, creating a multiplicity of pathlengths depending upon the positioning of the cell in the infrared beam path. Through the center a pathlength of 1.0 mm is obtained. The illuminated cell volume is 0.5 μL and the overall cell volume is 4 μL. The Nicolet standard GC/IR software was used without modification. This yields a spectral resolution of 8 cm^{-1} and co-adds 4 scans into each data file, a data file being collected each second of the chromatographic run. Chromatograms were generated either by the Gram-Schmidt orthoganolization method or by integrating the absorbance over the 1666-1651 cm^{-1} region. When only CN is present no difference was found between the two methods. Spectral deconvolution was achieved through the taking of the second derivative of the absorbance spectrum, and baseline correcting the resultant spectrum.

For the comparison with UV detection, an Applied Biosystems Spectroflow 757 variable wavelength UV was connected in-line after the FT-IR (Applied Biosystems, Foster City, CA.). The flowcell in this unit had a

pathlength of 8 mm and a volume of 6 μL. The maximum
absorption line for CN, 210 nm, was monitored. Chromat-
ograms were recorded on a Spectra Physics model 4270
integrator (Spectra Physics Corp., San Jose, CA.).

The CN samples evaluated were obtained from the
Naval Surface Warfare Center, Indian Head, MD. They
consisted of CNs of degrees of nitration (DN) from 2.11
(11.5 % nitrogen) to 2.78 (13.53 % nitrogen) and are
listed in Table I. Samples were prepared in THF at
concentrations of $\approx$ 0.2 % wt./wt. These were allowed to
stand for two days to achieve complete dissolution of
the polymer. Prior to analysis, the samples were fil-
tered through a 0.45 μm membrane filter to remove any
particulate matter prior to chromatography. Sample
volumes of 100 μL were injected on the chromatographic
column via a Rheodyne external HPLC sample injection
loop (Rheodyne Corp., Cotati, CA.). For the solvent
comparison study, samples were prepared as described
above using HPLC grade acetonitrile.

The denitration experiments were carried out
according to the procedure developed by Purves et
al.[83,84]. For these, 3 grams of 13.53 % nitrogen CN
(DN=2.78) and 2.0 grams of 11.5 % nitrogen CN (DN=2.11)
were denitrated by the action of an excess (3.3 grams
and 2.5 grams) of free hydroxylamine dissolved in

TABLE I

Percent Nitrogen and Degree of Nitration (DN) of CNs Examined

Percent Nitrogen	DN
11.5	2.11
12.2	2.32
12.6	2.45
13.15	2.63
13.53	2.78

pyridine. The resulting products, 2.3 grams (89.5 % theoretical yield) and 1.15 grams (87.1 % theoretical yield), were identified by ^{13}C-NMR and % nitrogen analysis. The NMR used was a 50 MHz Bruker model 200 spectrometer, collecting 11 000 scans overnight at 80 ^{o}C on a 10 % solution of polymer dissolved in deuterated DMSO (Aldrich Chemical Co., Milwaukee, WI.). Spectral lines were identified based upon the works of Wu[85] and Reeder[86] and the obtained spectra were compared to predicted spectra generated with a program developed by Dr. Harold Bell of VPI & SU, using the chemical shift data of Reeder and Bell.

For all quantitative work regression curves were calculated using propagation of errors and t-statistics. A minimum of five replicate analyses for each substituent level were taken and standard deviations plotted with the data. Where quantitation is performed the 95 % confidence interval was calculated as $x \pm tS_x$. S_x was calculated as:

$$(S_a^2 + S_y^2 + (x)S_b^2)^{\frac{1}{2}}/b$$

where S_a and S_b are the errors in the slope and intercept respectively of the regression line $y = a + bx$.

Results and Discussion

For the evaluation of the influence of DN on the GPC/FT-IR of CNs several commercial CNs were chromatographed under the same conditions and the chromatograms and infrared spectra compared. Since not all samples were available at the outset of this study, only the first three (DNs 2.11, 2.32, and 2.63) are included in the chromatographic study.

Comparison of Chromatographies of CNs of Differing Degrees of Nitration

The initial chromatographic evaluation of the CNs was carried out by injection of solutions of the same concentration of three CNs of differing nitration onto a single mixed bed GPC column. The Gram-Schmidt reconstructed chromatograms (GSR) of these are shown in Figure 6. Note that there appears to be a bimodal separation in the form of a shoulder on the high molecular weight side of the 2.63 DN and 2.32 DN CNs, and that the 2.11 DN CN appears to tail in the low molecular weight region. The observance of a shoulder or "hump" on the high molecular weight portion of the GPC peak of CN has been reported previously[87,88]. It has also been reported previously that polar polymers can exhibit anomalous elution behavior in GPC[89] and that
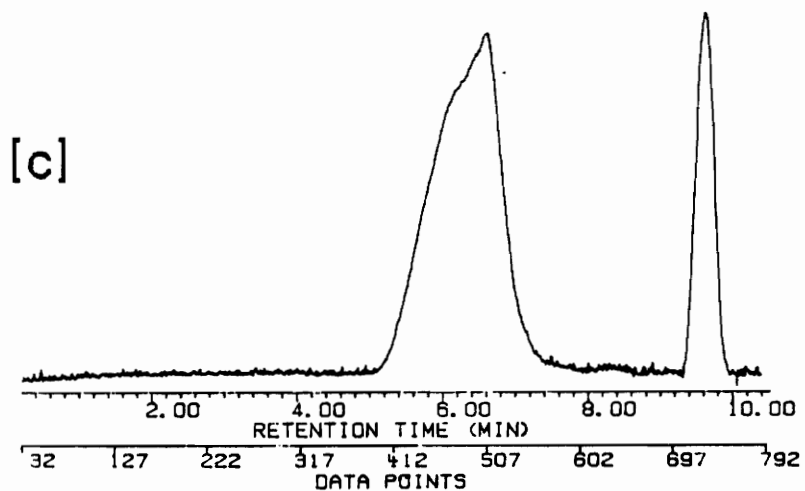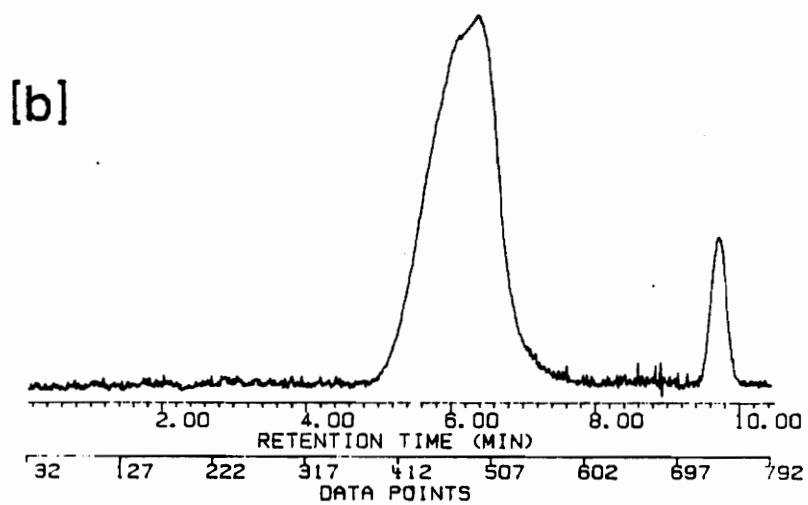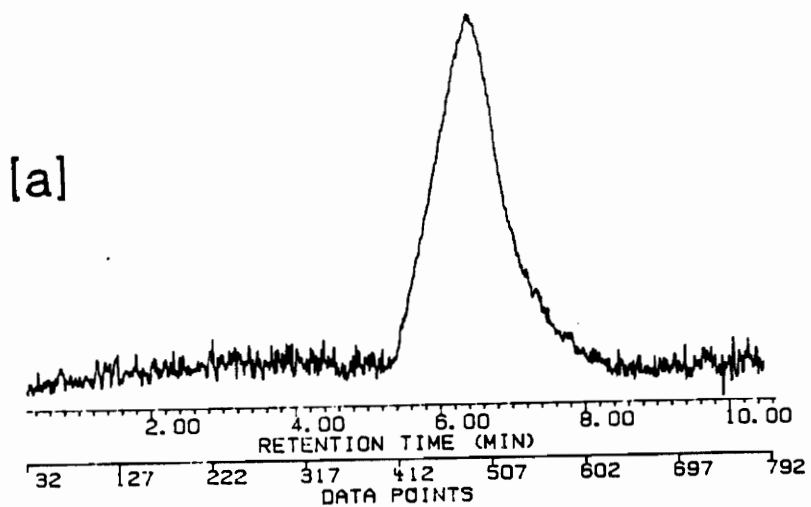
Figure 6. GSRs of CNs of DN [a] 2.11, [b] 2.32, and [c] 2.63

CN in particular demonstrates unusual and non-reproducible behavior[22]. This was mostly in the form of tailing peaks which did not return to baseline and degradation of columns after repeated injections of CN solutions. To evaluate whether the observed phenomena are real or if some interaction with the column bed is occurring, two additional experiments using first a different column of the same design and second a column which had been washed with a solution of triphenylphosphine in THF to reduce any oxidized sites were carried out.

The GPC chromatograms of the same three CNs on a second PL-gel mixed bed column are shown in Figure 7. Note that while the elution is slightly different the observed phenomena are still present. This leads one to believe that it was not a poor column in the first case and that perhaps something else is responsible for the observed elution behavior. The manufacturer of the gels used in these columns, Polymer Laboratories (Amherst, MA.), recommends against the use or storage of styrene-divinylbenzene columns with unstabilized THF. This is due to the potential formation of peroxides associated with THF (a potential inhibited by the use of butylated hydroxytoluene as a preservative), which can attack and oxidize the surface of the gel creating interaction sites which can alter the column properties and eventu
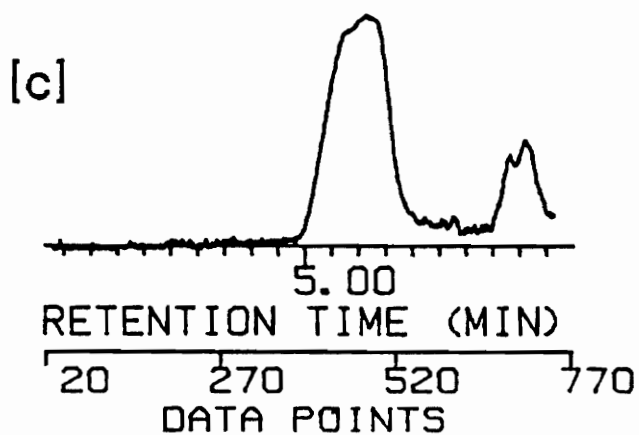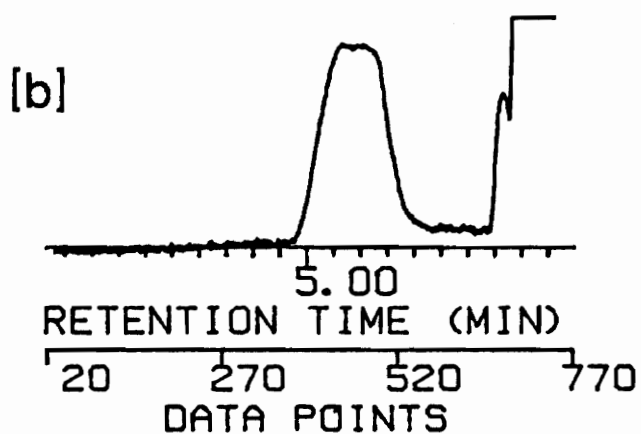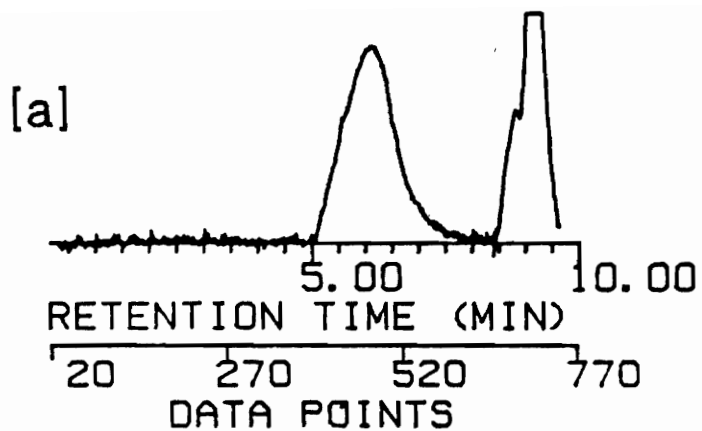
Figure 7. GSRs of the same CNs on a second GPC column. Identifications are the same as in Figure 6.

ally reduce its overall efficiency. To counter the effects of peroxides they recommend that a suspect column be flushed with a 0.1 % solution of triphenylphosphine in THF at a slow flowrate to reduce any oxidized surfaces. Figure 8 shows the GPC chromatograms of the same CNs on the treated column. The elution profile for the CNs is different only in the observance of increased resolution of the "humps" on the high molecular weight region. It can then be concluded that the observed bimodal separation is not a function of the column or solvent but the nature of the polymers themselves. The tailing associated with the 2.11 DN CN is still present in all cases and may be due to the increased number of residual hydroxyls on the polymer chain as compared to the more highly nitrated species.

As mentioned previously, polymers with polar end groups have been known to tail in GPC through interaction with the column bed, possibly with small numbers of carboxylic acid groups which have been reported to exist on some organic gels[90,91]. Certainly CN can be ranked among these, since the end groups will posses either a hydroxyl or a nitrate on any of the four sites available (C_2, C_3, C_4, C_6). In addition, it has been theorized that the nitration process does not proceed uniformly along the entire length of the cellulose
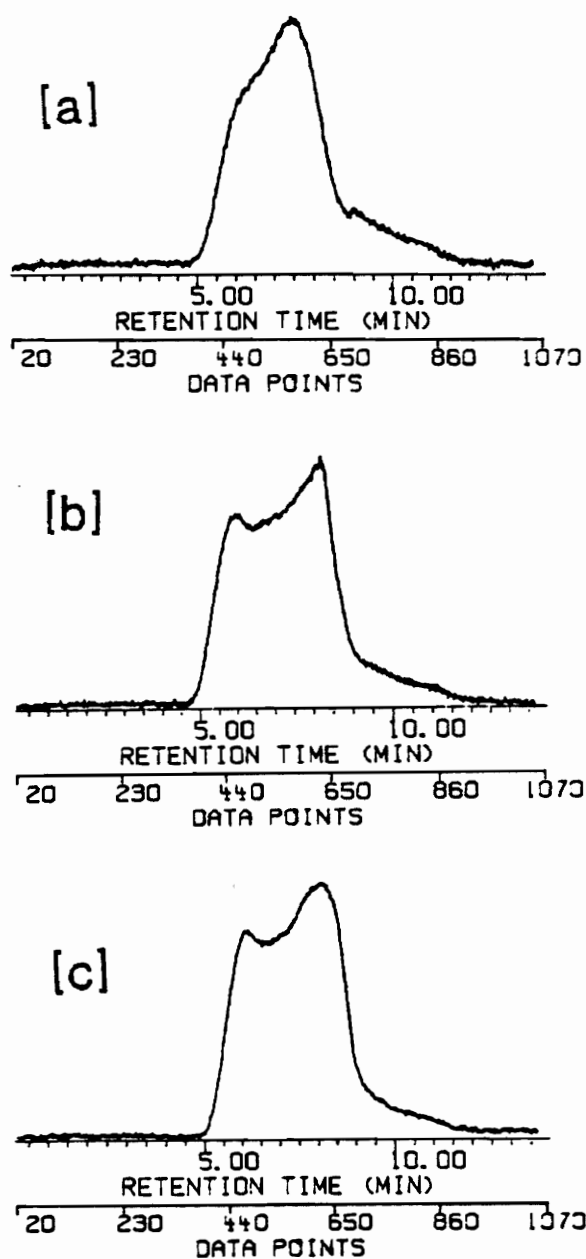
Figure 8. Reconstructed Chromatograms of the same CNs
on column two treated with a solution of
triphenyl phosphine. See Figure 6 for identi-
fications.

chain. There has been some evidence to suggest that the nitration of one glucose unit influences the rate of nitration at adjacent units, such that blocks of highly nitrated and of non-nitrated units exist within the same molecule[92]. Such a molecule could potentially posses several sites which might interact with the column bed, particularly the lower nitrated species.

This possibility was tested by chromatographing the denitrated CNs and looking for evidence of increased tailing. Figures 9 and 10 show the comparisons of chromatograms for the 2.78 and 2.11 DN CNs respectively before and after the denitration process. The denitrated materials had DNs of 1.80 and 1.72. Note that in neither case does there appear to be evidence of increased tailing due to the increased number of hydroxyl groups. This suggests that when the integrity of the GPC column is maintained there is no interaction between residual hydroxyls of CN and the column bed.

Comparison of IR With UV Detection

This portion of the study was designed to evaluate whether the observed elution behavior was a function of using an infrared spectrometer as a detector as opposed to the more conventional UV. This was carried out by
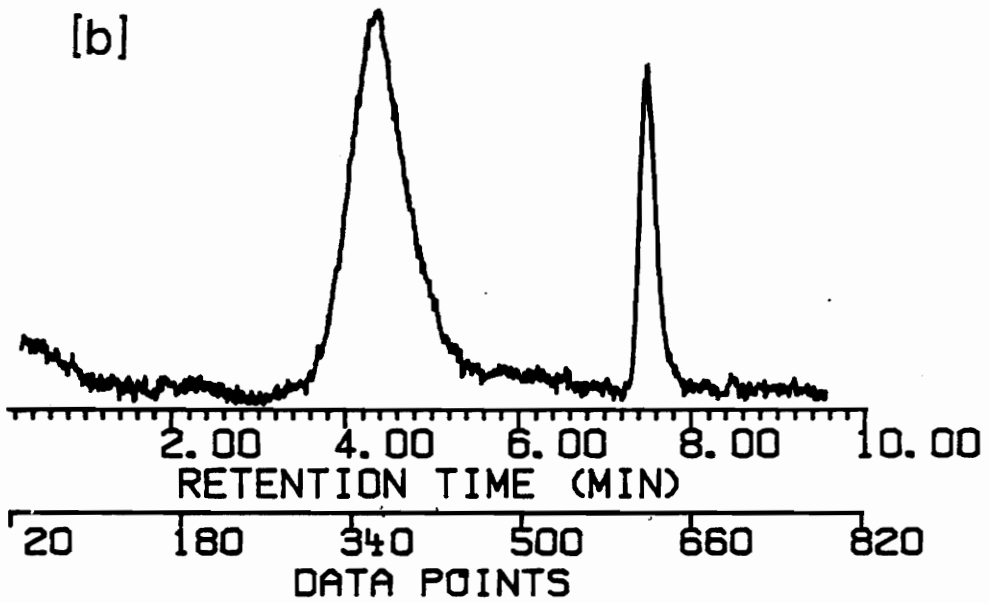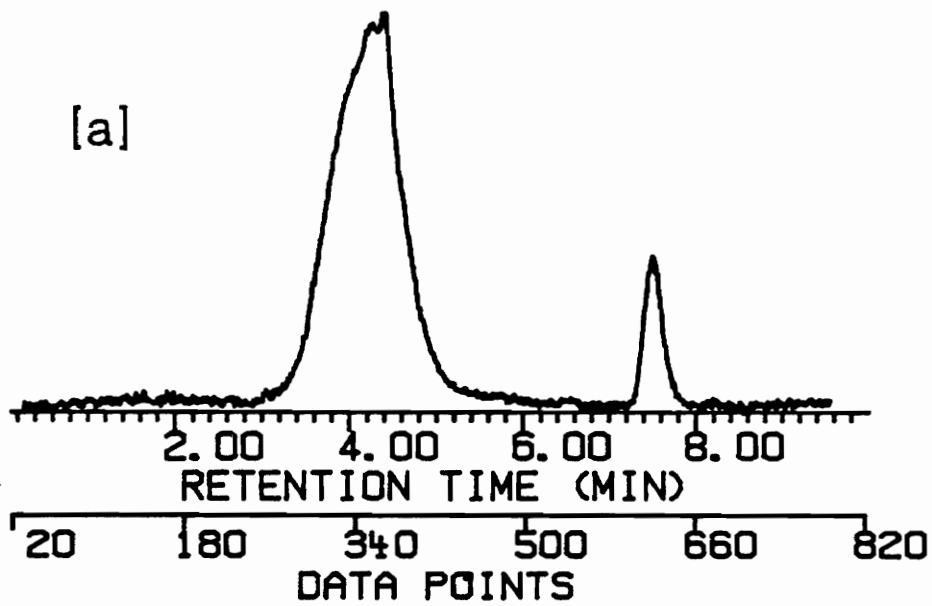
Figure 9. Comparison of GSRs of [a] 2.78 DN CN and [b]
its Denitrated Counterpart (1.80 DN)

55
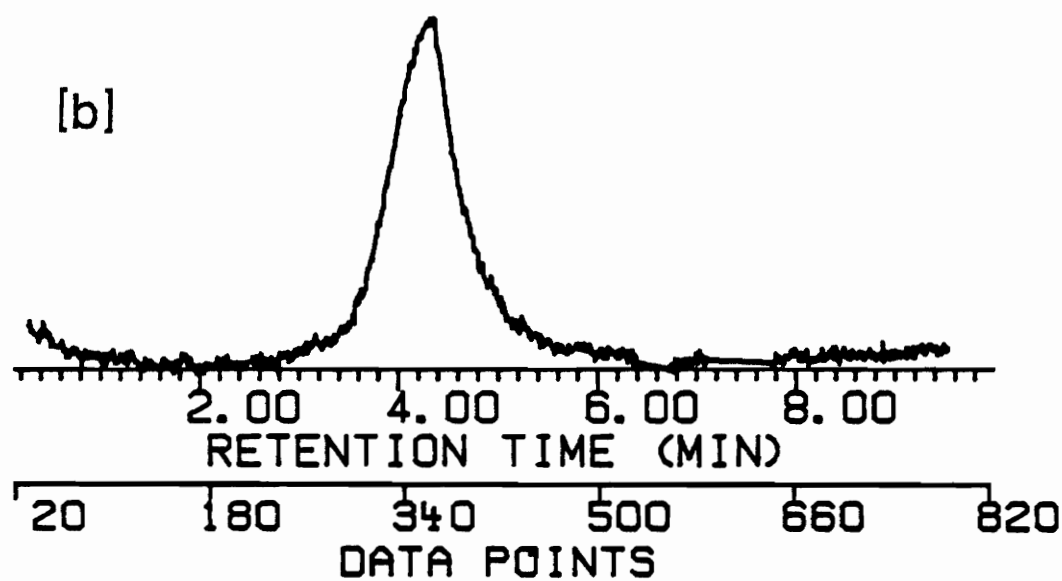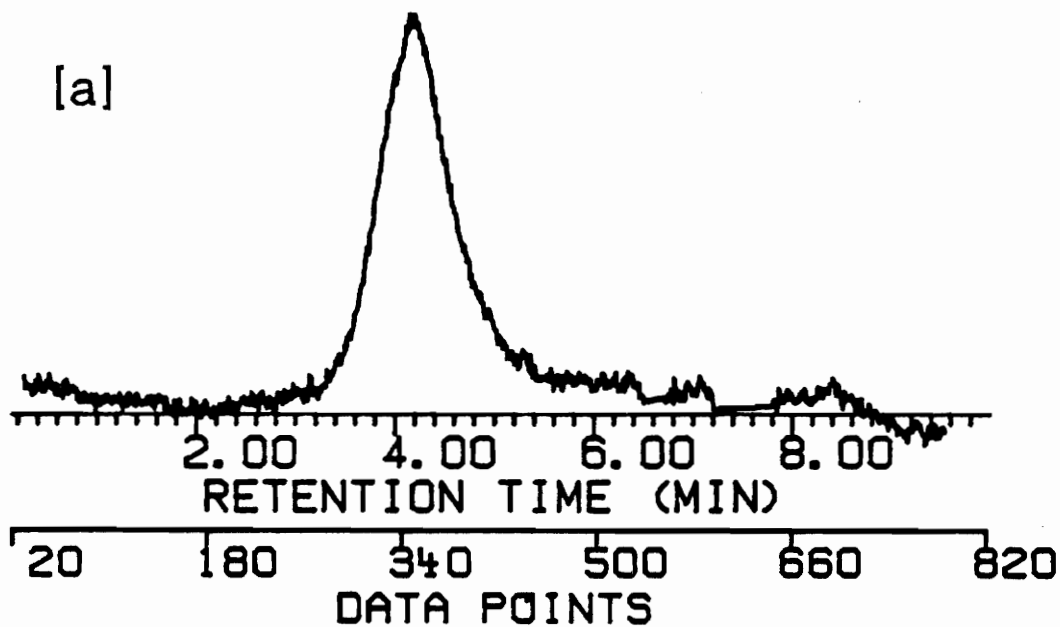
Figure 10. Comparison of GSRs of [a] 2.11 DN CN and [b]
its Denitrated Counterpart (1.72 DN)

placing a UV detector in-line after the FT-IR and collecting both responses on the same chromatographic runs.

In order to validate the wavelength to be monitored in the UV a set of test runs at 254, 230 and 210 nm was carried out. The conventional wavelength for UV detection is 254 nm and it is the only wavelength available on fixed wavelength UV detectors. This is the region of maximum absorbance for aromatic compounds. CN contains no aromatic functionality but does exhibit some absorption at 254 nm. In fact, the maximum absorbance for CN dissolved in THF is at 210 nm, observed in this study and elsewhere[23]. Since the same chromatographic trace is observed at each wavelength, but the signal to noise ratio (SNR) is higher at 210 nm, comparisons were made using 210 nm.

Figures 11 and 12 show the comparisons of the integrated IR absorbance over the 1666-1651 cm^{-1} region and the absorbance at 210 nm for the 2.11, 2.32, 2.45, and 2.63 DN CNs. Since the UV detector was in-line after the IR there is a small offset in the elution time of the polymers, however the peak widths are the same (4.5 min.) and the shape of the elution profile is in each case the same. This should not be a surprise since the absorption in both cases is related to the

nitrate functionality. The IR absorbance arises from the asymmetric stretching mode of the nitrate group and the UV absorption from the $\pi_2 \rightarrow \pi_3$ (anti-bonding to non-bonding) transition[93].

Elution Profile of CNs as a Function of Dissolution Time

One advantage of the UV detection system is the ability to obtain an integrated area of all eluting peaks. This is something which is not presently available in FT-IR chromatographic software packages. With the UV already in-line a study to evaluate the elution profile as a function of sample dissolution time was conducted. The desire for this stems from a controversy as to (1) whether CN dissolves completely in THF in the normal sample preparation time frame prior to chromatography, and (2) whether the DN of the CN alters the dissolution rate. Previous researchers have examined this problem using different techniques. Early researchers referred to the phenomena as the aging of CN solutions. Spurlin devoted a section of his classic work to the subject[30]. In reviewing work performed at that time, he came to the conclusion that the aging phenomena, observed as a decrease in solution viscosity
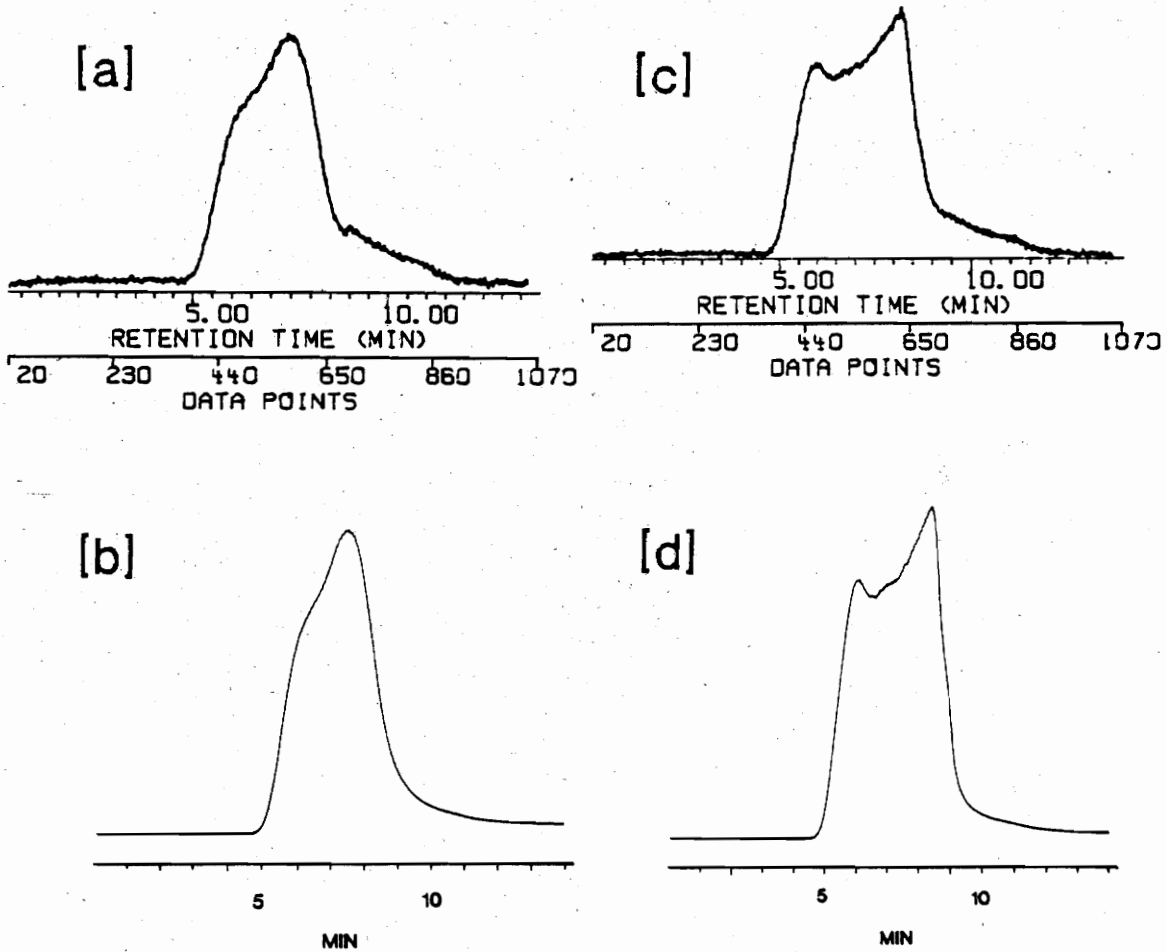
Figure 11. Comparison of the GPC traces obtained for
CNs of 2.11 [a,b] and 2.32 [c,d] DN using
infrared [a,c] and UV [b,d] detection.

59
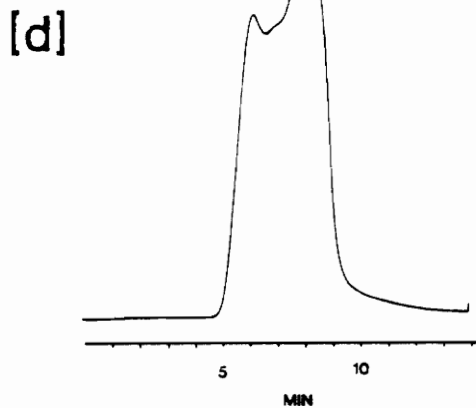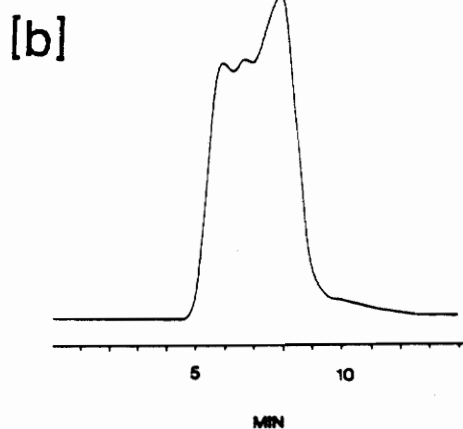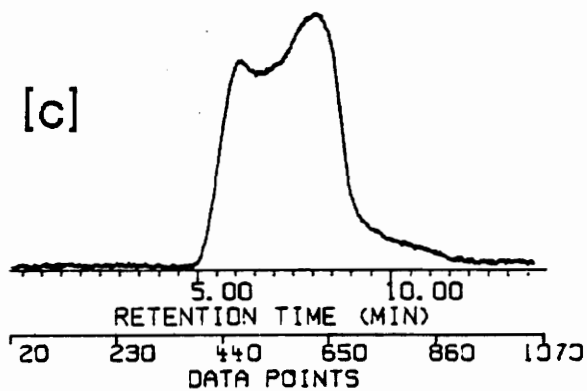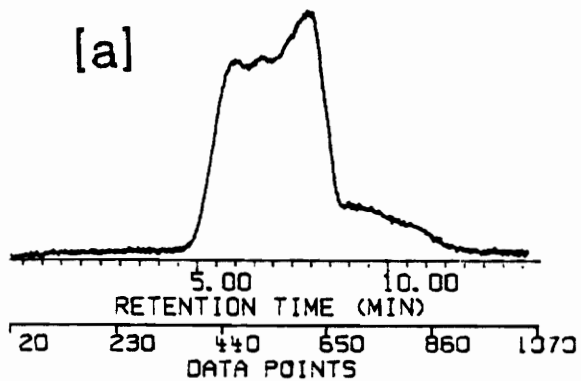
Figure 12. Comparison of the GPC traces obtained for CNs of 2.45 [a,b] and 2.63 [c,d] DN using infrared [a,c] and UV [b,d] detection.

with time, was due to the degradation of the CN chain. This would result in the formation of additional lower molecular weight species. This degradation was thought to arise from residual acids from the commercial processes. This phenomenon was examined more recently by Siochi[10]. She came to the conclusion that the reduction in viscosity arose from a breaking up of aggregates of CN molecules as the solvent fully permeated the fibrous structure. Such a breakup would result in an apparent increase in the lower molecular weight fraction of the polymer.

The study performed here was designed not to arrive at specific molecular weight information, but to see if changes could be observed in the GPC chromatograms with time using in-line spectrometric detection. For this, the integrated areas from the UV detector signal were collected in triplicate runs on a daily basis for a six day period for both the 2.45 and 2.63 DN CNs. Figure 13 shows the comparison of day 1 and day 6 chromatograms for the 2.63 DN CN. Similar results were obtained for the 2.45 DN CN. The chromatographic trace obtained on day 6 shows an obvious increase in the low molecular weight fraction of the polymer. This is in agreement with the observed trend in solution viscosity discussed earlier. This increase results in a
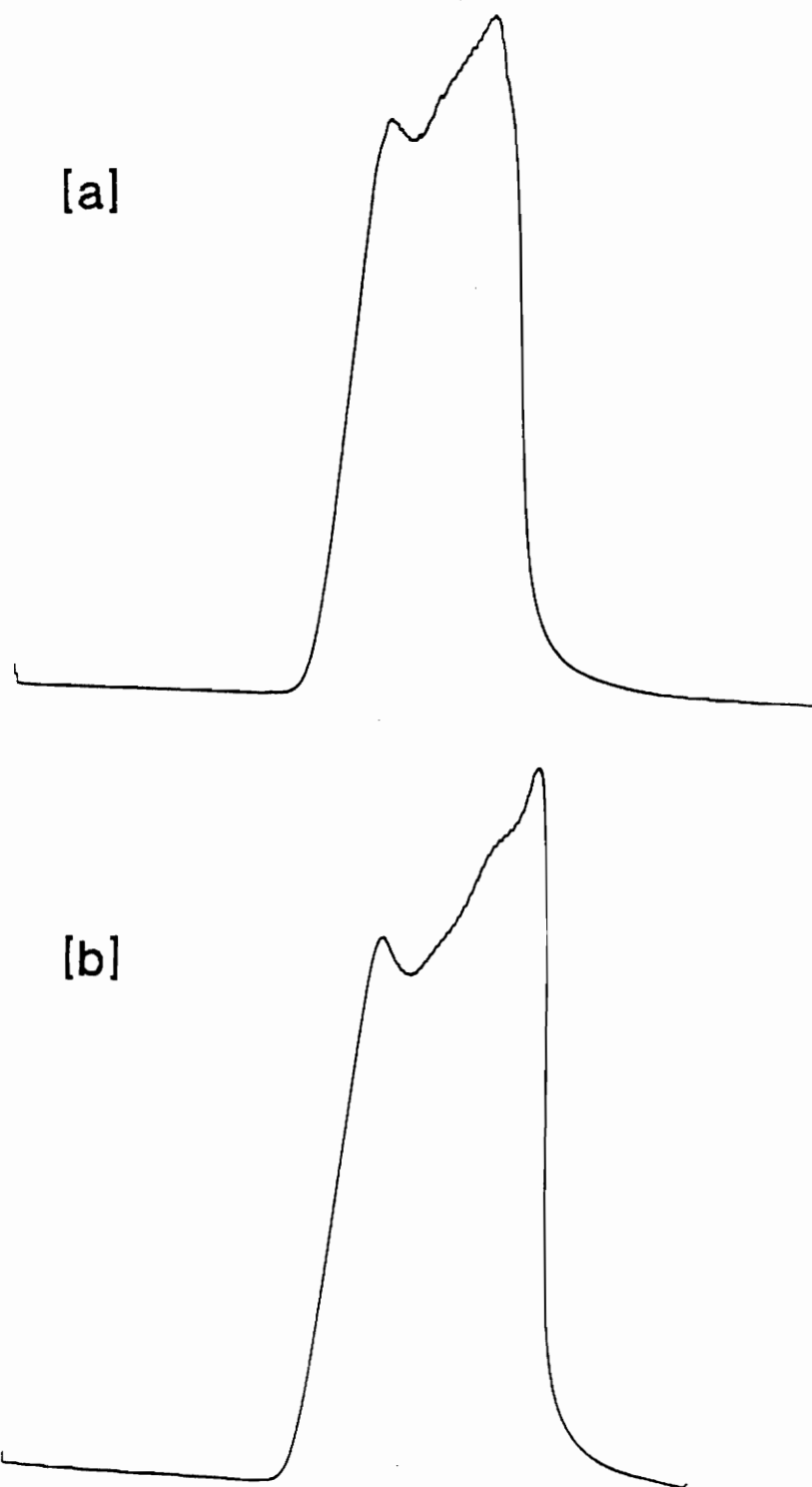
Figure 13. Comparison of the GPC chromatograms of [a] day 1 and [b] day 6 for 2.63 DN CN.

broader distribution and a larger chromatographic trace. For the overall integrated areas then, an increase is observed as dissolution time increases. Figure 14 shows the trends observed for both samples carried through the process. Note that it takes about four days to approach an equilibrium value, indicating that only after this time might reproducible molecular weight numbers be obtainable by GPC. This is in agreement with Siochi's work where almost seven days were required before equilibrium viscosity numbers were obtained.

Spectrometric Characterization of CNs of Differing DNs

As spectrometric techniques have evolved they have been increasingly applied to the characterization of cellulose derivatives in order to more fully understand their chemistry. Infrared spectrometry is no exception. Almost as soon as reliable infrared spectrometers were developed their capabilities were directed toward the study of cellulose and its derivatives, especially cellulose nitrate. Much of the early work consisted of qualitative evaluation of the spectra obtained from cast films of the polymers.

The objective of this part of the study was to
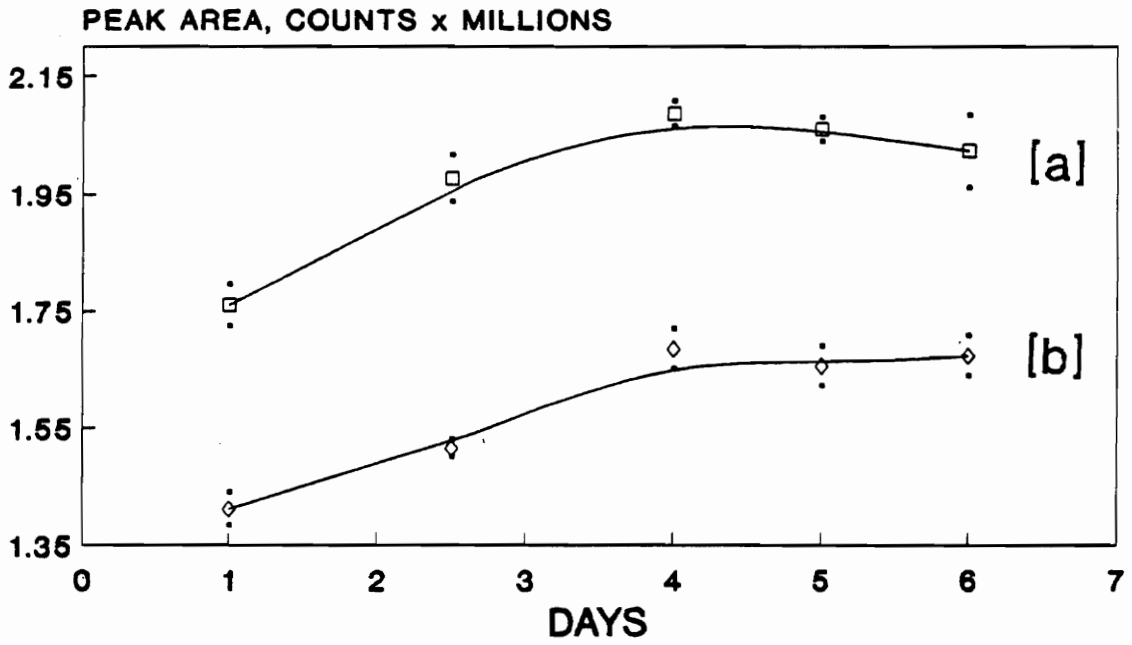
Figure 14. Observed trends in peak area for the [a]
2.45 and [b] 2.63 DN CNs.

obtain the infrared spectra of CNs in solution and evaluate them with respect to the DN and the MWD. This was carried out by connecting the GPC column in-line with the FT-IR spectrometer and collecting infrared spectra "on the fly".

Comparison of Infrared Spectra of CNs

The mid-infrared spectrum of CN in solution has to date not been studied in detail. This is due to the more conventional practice of studying polymers in the solid state or as cast films. Dilute solutions of polymers have an additional degree of freedom relative to solid state material which can influence the inter- and intramolecular forces among the polymer units.

A major consideration in coupling FT-IR to any liquid chromatographic technique is the infrared absorption regions of the mobile phase. THF, one of the most common GPC solvents, has several strong absorption regions in the infrared. These are shown in Figure 15. Note that the region below 1500 cm^{-1} is completely obscured due to total absorption by the solvent. No spectral information about the sample can be obtained in this region, as well as a small region around 2000 cm^{-1}, one around 3800 cm^{-1}, and a large region between
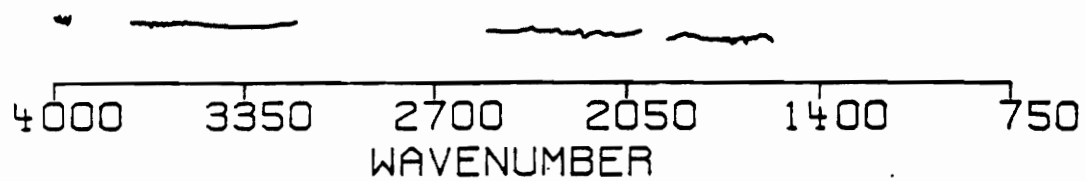
Figure 15. Spectral Windows of THF.

3200 and 2600 cm^{-1}. The only spectral window of any real value for CN is that from 1800 to 1600 cm^{-1}. The asymmetric stretching mode of the nitrate group of CN absorbs in this region. The appearance of this stretching mode for the CNs of DN 2.11, 2.32, 2.45, and 2.63 are shown in Figure 16. Note that as the DN increases there is an apparent increase in the high energy side of the absorption. This phenomena has not been previously reported in the infrared spectra of solid state or cast films of CN. Leider and Pane, as part of a study on the stability of the nitrate ester positions of CN examined the infrared spectra in THF of CN of DN 2.21 and the same material after additional nitration to DN 2.88[94]. They observed that upon additional nitration of the material an increase in the high energy side of the asymmetric stretch in THF occurred. They attributed the difference in the spectra to the position of the nitrate groups upon the anhydroglucose ring, assigning the high energy band to the secondary nitrates at C_2 and C_3, and the low energy band to the primary nitrate at C_6.

Panov et al. also examined CNs in THF solution and also in nitromethane[95]. While not observing a split of the asymmetric nitrate stretch, they did note that the absorption maximum shifted to higher energy with in
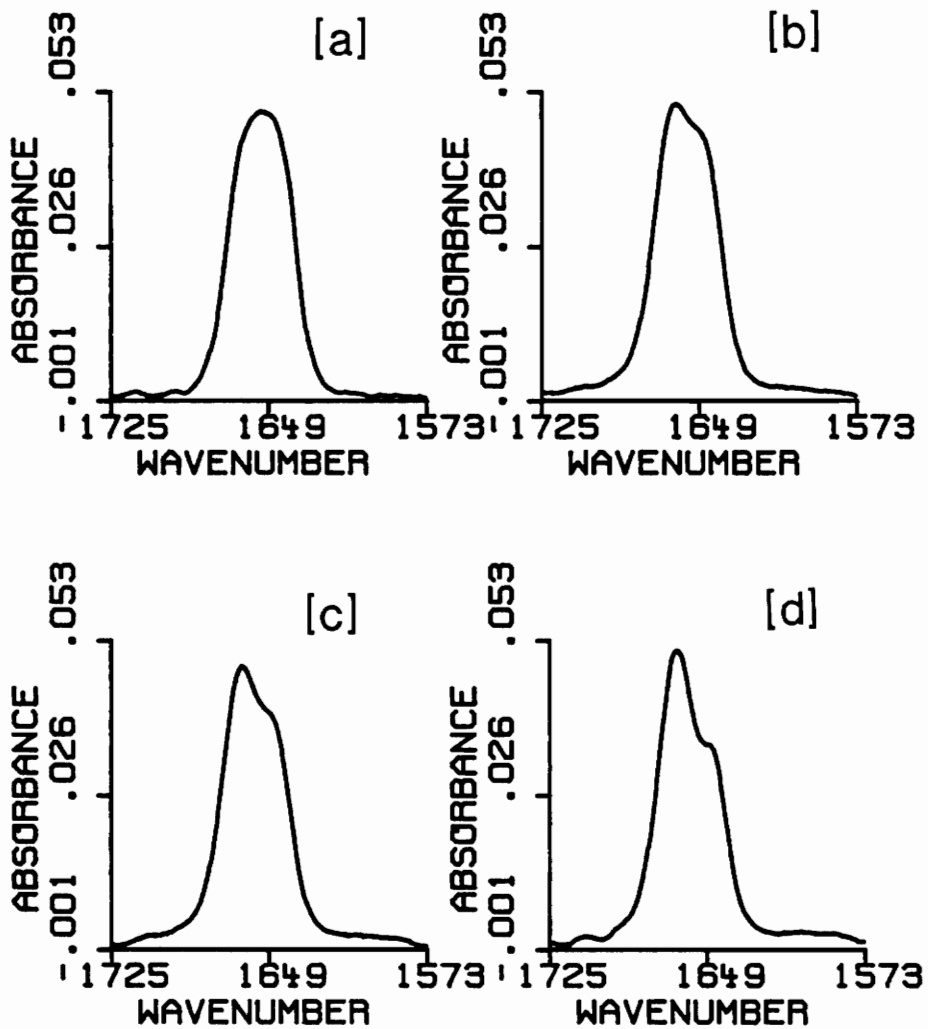
Figure 16. Infrared Spectra of the Asymmetric Stretch-
ing Region for CNs of [a] 2.11, [b] 2.32,
[c] 2.45, and [d] 2.63 DN

creasing nitration. Between 9.5 and 13.5 % nitrogen a shift from $\approx$ 1647 cm^{-1} to $\approx$ 1663 cm^{-1} was noted. This shift was attributed to the increase in the number of nitrate groups leading to a more rigid polymer, which would absorb at higher energy.

Kuznetsova et al. examined CNs as films pressed from fibers[96]. This is different from the normal procedure of casting films from solution. They did observe a splitting of the asymmetric nitrate stretch with an increase in the high energy band as the nitration level increased. Model compounds were employed to interprete the data. The model was 4,6 ethylidene α-methylglucoside which had been nitrated at the C_3 position in one case and both the C_3 and C_2 positions in the other. It was found that the higher energy band increased in intensity for the compound nitrated at both the C_3 and C_2 positions. Thus, the higher energy absorption was assigned to the C_2 nitrate group and the lower energy band to the C_3 nitrate group. The extrapolation to CN was somewhat incomplete as CN also has some nitrate groups on the C_6 position. With only two bands observed and the assignment based only on the C_2 and C_3 nitrate groups, it was assumed that the C_6 primary nitrate and the C_3 secondary nitrate possessed similar characteristics and the infrared absorptions would be coincident.

This last report was also interesting in that spectra taken of films cast from solution do not show a split of the nitrate absorption. To test this in our laboratory we compared solid state spectra with solution spectra. Samples of CN dissolved in THF were deposited on ground IR grade KBr using a home built deposition device. This device consisted of an airbrush which had been modified by the replacement of the central spindle with a length of 100 μm i.d. fused silica tubing. The other end of the tubing was connected to the outlet of the GPC column so that the column eluent passed through the airbrush and was dispersed as a fine mist on the KBr surface. This required a reduction in mobile phase flowrate from 1 mL/min to 0.3 mL/min. It was also necessary to pass heated nitrogen gas through the airbrush to disperse the eluent as a fine mist. The gas also facilitated removal of the solvent. With the tip of the airbrush held 0.5 cm from the KBr surface a spot size of 400 μm diameter was generated. Using this setup a sample of 2.45 DN CN was chromatographed and the infrared spectra collected using an infrared microscope in the reflectance mode. Figure 17 shows the spectrum obtained from this procedure, with assignments of principle absorption bands indicated. Note that with the solvent removed the
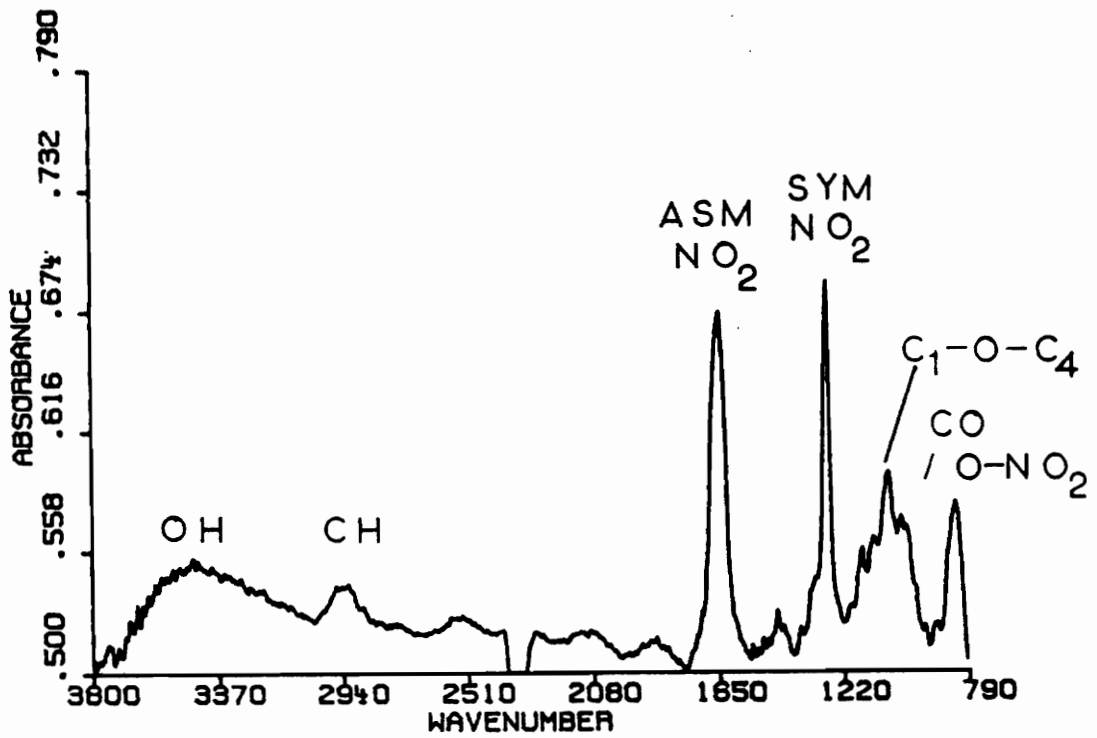
Figure 17. Diffuse reflectance infrared spectrum of
2.45 DN CN deposited on KBr

entire infrared region is observable. Figure 18 shows an expansion of the asymmetric nitrate region of this analysis compared to that of 2.45 DN CN in solution. Here the lack of splitting of this band in the case of the solid state spectrum is obvious. From this study it appears the splitting is only observed for CNs in solution.

In order to elucidate more spectral information concerning the observed splitting of the asymmetric nitrate stretch, analyses were conducted at 2 cm^{-1} resolution by direct injection of solutions of CN into the IR flowcell. This was carried out in this fashion in order to utilize all the same equipment for the study but circumvent the 8 cm^{-1} resolution restriction of the GC/IR software. All spectra collected were ratioed to a solvent background. Figure 19 shows the asymmetric stretching region for the same samples as Figure 16, only at 2 cm^{-1} resolution. Note that while some additional separation of the bands is obtained there remains a considerable amount of spectral over-lap.

Investigation of Solvent Influence on the Spectra of CNs

It was mentioned previously that the degree of
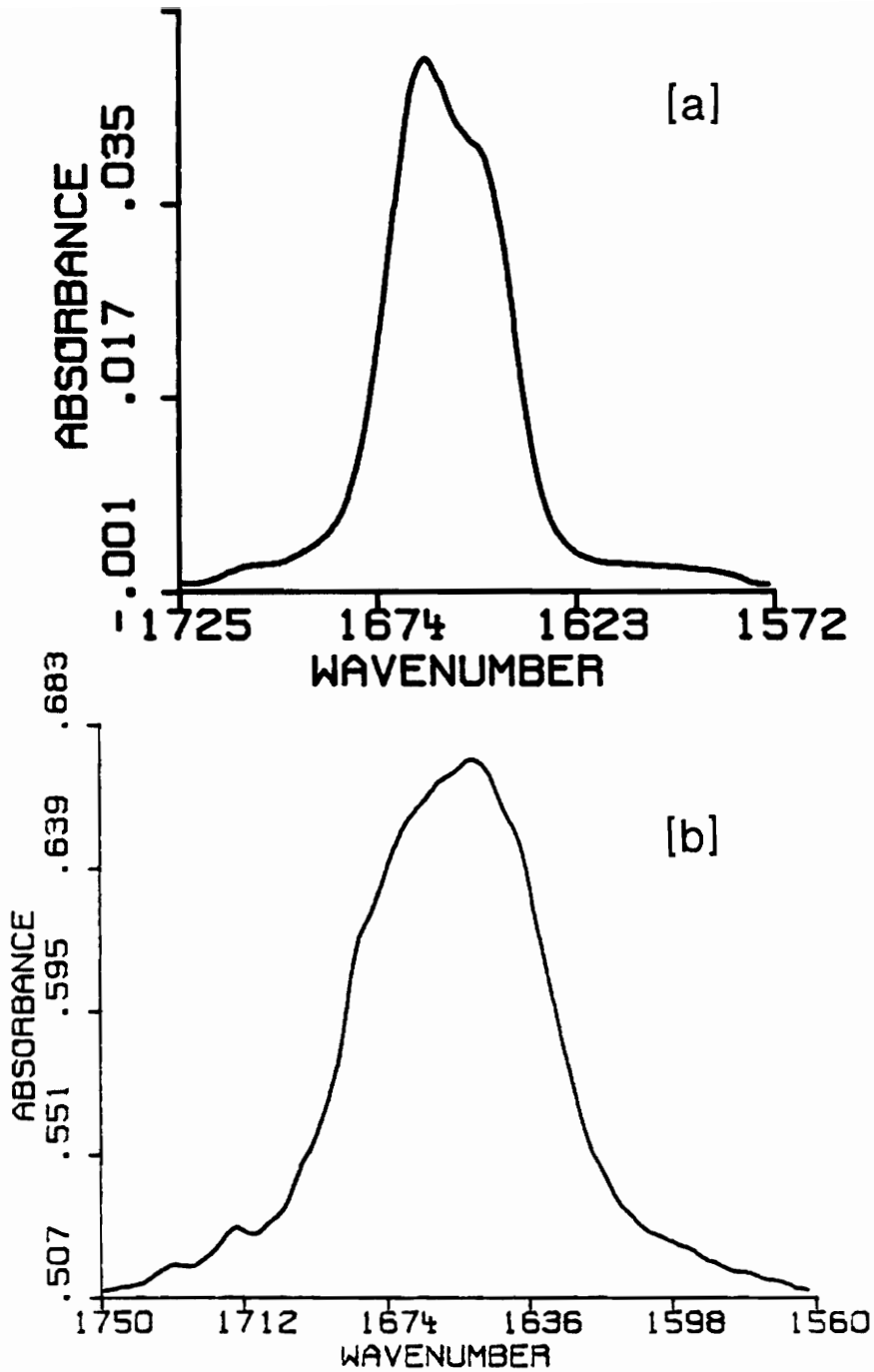
Figure 18. Comparison of the asymmetric nitrate
stretching region of 2.45 DN CN [a] in
solution and [b] by diffuse reflectance
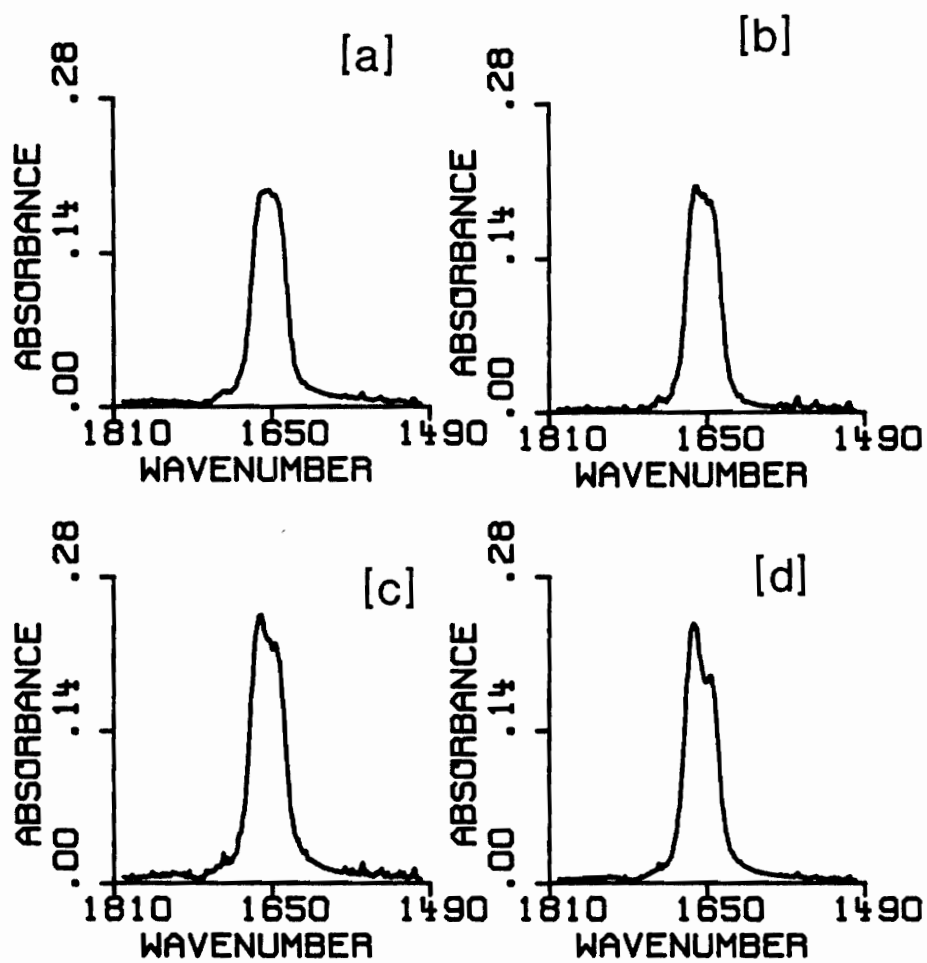
Figure 19. Spectra of [a] 2.11 [b] 2.32 [c] 2.45 and [d] 2.63 DN CNs at 2 cm^{-1} resolution

nitration of CN is the governing factor in the solubil
ity of the CN in a given solvent system. It is recog-
nized in the cellulose community that this is princi-
pally due to the remaining unesterified hydroxyls
interacting with solvent molecules. This is evidenced
by the fact that CN is only soluble in polar solvents
which might interact via hydrogen bonding with free
hydroxyl groups. This does not, however, preclude the
nitrate groups from interacting with solvent molecules
as well. Being themselves highly polar and capable of
hydrogen bonding and van der Waals interactions, it is
not unreasonable that the splitting of the asymmetric
nitrate stretch may be due to solvent interaction with
one or more of the nitrate ester groups.

A study to test this was carried out again using
the same spectrometric equipment and preparing samples
to the same concentrations. While several solvents were
explored, only two provided useful information concern-
ing the asymmetric nitrate stretching region. These
were THF and acetonitrile. Other solvents which were
tested were dimethyl sulfoxide, dimethyl formamide, and
methanol. None of these proved to have sufficient ir
throughput in the region of interest, however, and
provided no useful data. The THF data have already been
shown in Figures 16 and 19. Figure 20 shows the same

region for the same samples as Figure 19, only now in acetonitrile and at 2 cm^{-1} resolution. Note that the same splitting pattern of the asymmetric nitrate stretch is evident. Also observable is the symmetric nitrate stretching mode at 1280 cm^{-1}. Note that this absorption is not split. For samples carefully prepared to the same weight percent concentration a linear trend is observed between the absorbance at each absorption maximum, the asymmetric at 1660 cm^{-1} and the symmetric at 1280 cm^{-1}, and the degree of nitration of the respective CN (Figures 21 and 22 respectively). Such was likely the basis for several of the earlier proposed analytical methods using ir as the detector.

Another feature noted in both sets of 2 cm^{-1} data was the shift of the high energy band to higher wavenumber as the DN increased. These trends are shown in Figure 23. Note that for the 2.11 DN material the frequency of absorption is essentially the same in both solvents but that as the DN increases the absorption frequency in acetonitrile shifts to higher values than those in THF. This trend is in agreement with the observations of Panov and coworkers mentioned previously[95]. They speculated that the shift arose from the increased rigidity of the more highly nitrated materi
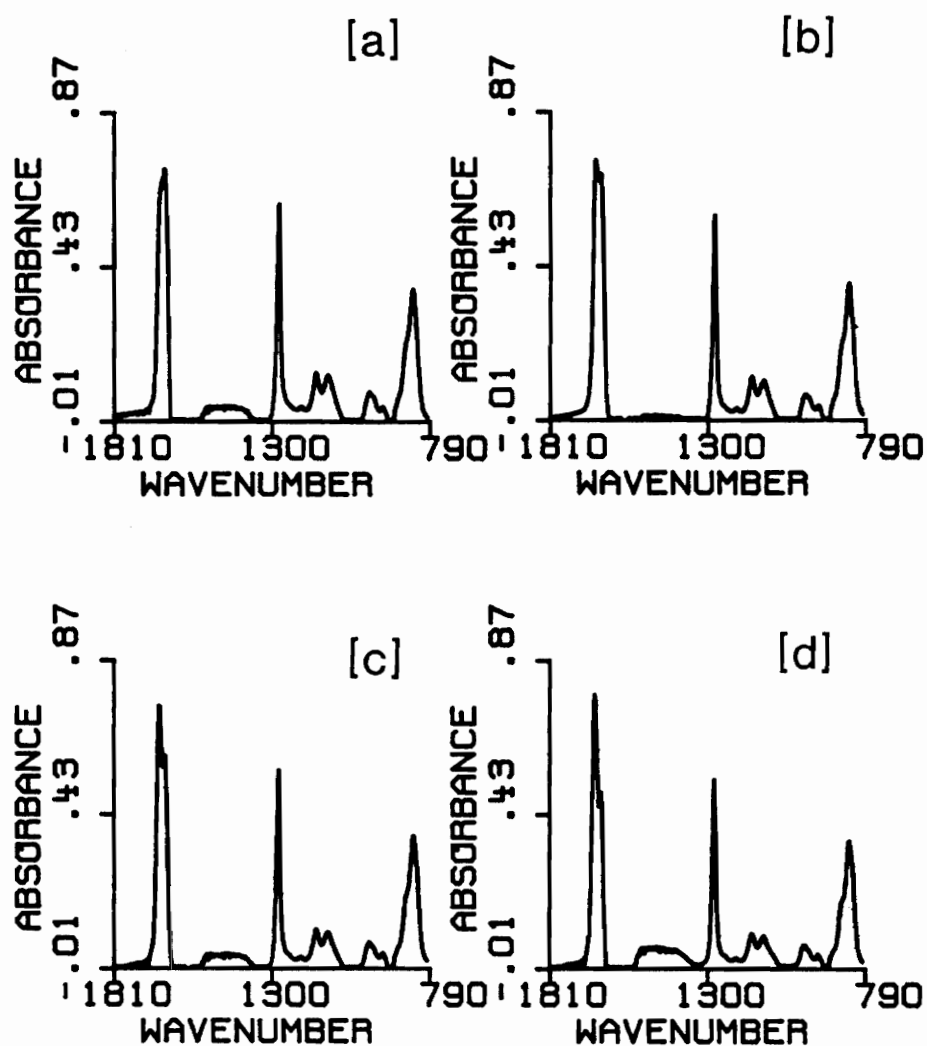
Figure 20. Spectra of [a] 2.11, [b] 2.32, [c] 2.45
and [d] 2.63 DN CNs at 2 cm^{-1}
resolution in acetonitrile

77
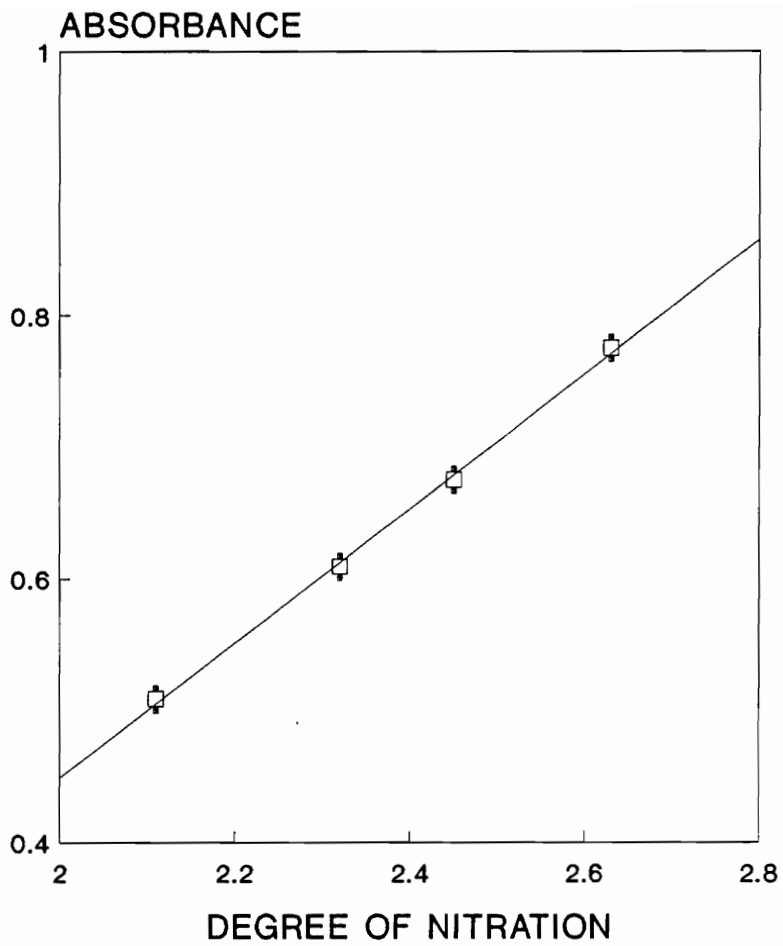
Figure 21. Correlation of the absorbance at 1660 cm^{-1} with the CN DN
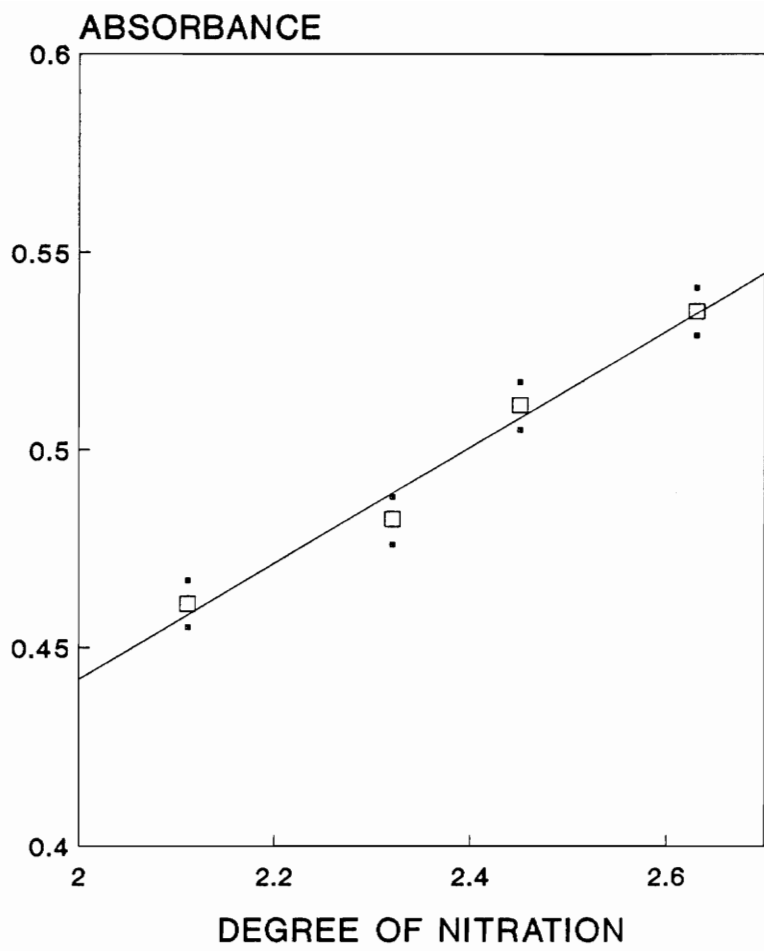
Figure 22. Correlation of the absorbance at 1280 cm^{-1} with the CN DN
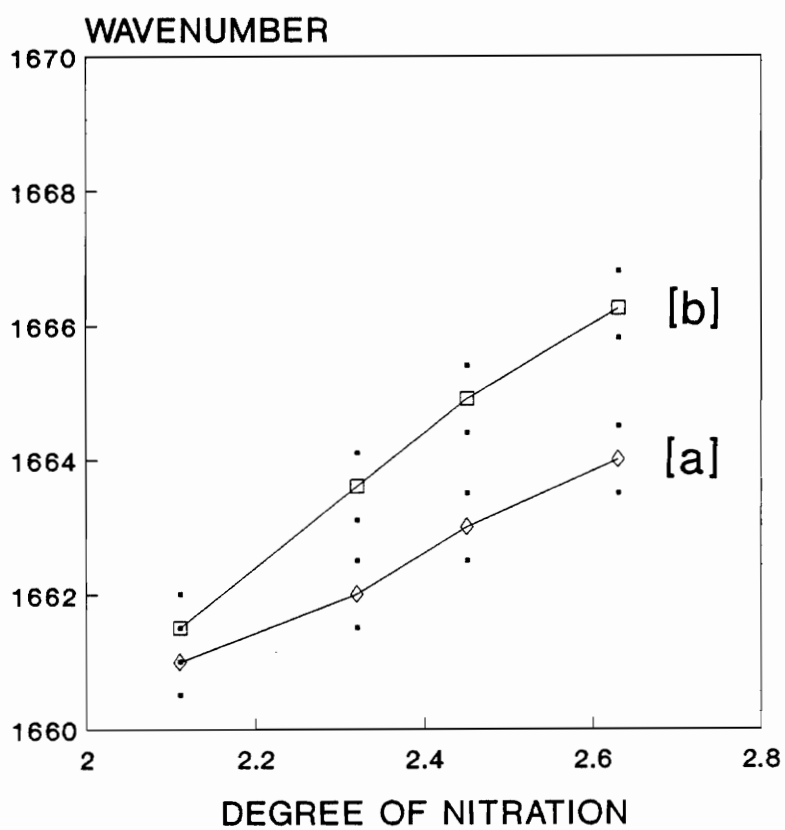
Figure 23. Asymmetric nitrate stretch as a function of
DN in [a] THF and [b] acetonitrile

al. Urbanski and Witanowski have also examined the influence of steric hindrance on nitrate esters[97,98]. They also noted that the nitrate asymmetric stretching frequency was increased when nitrate groups were situated on adjacent carbons, and where rotation about the carbon - carbon bond was possible the absorption would also be split. In order to correlate the observed trends to the molecular changes of the CN an examination of the nitration process is necessary.

Development of the Equilibrium Model

It has been recognized for some time in esterification reactions of cellulose that the rates of esterification at the three available sites were different. As far back as the 1930's Spurlin attempted to model the number of unsubstituted, mono-, di-, and tri-substituted glucose units of esterified celluloses[99]. For different ester types he approximated the relative rates of esterification to range from 10:2:1 to 4:1:1 for the positions $C_6:C_2:C_3$ respectively. In 1980 Wu took up the same task for cellulose nitrates using ^{13}C-NMR chemical shifts to experimentally determine the distribution of nitrated glucose units[85]. In his analysis he found that the equilibrium constants for the

nitration of cellulose were $K_6/K_3 = 5.8 \pm 0.6$ and $K_2/K_3 = 1.8 \pm 0.2$, where K_6, K_2, and K_3 are the constants for reaction at the C_6, C_2, and C_3 positions respectively. These values are well in line with those Spurlin estimated some forty years prior.

The equations for the equilibrium model were developed by Spurlin based on the following reaction:

$$C_6H_{10}O_5 + AB \iff C_6H_9O_5A + HB$$
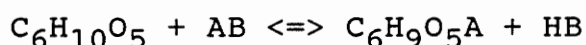
where $C_6H_{10}O_5$ represents an anhydroglucose unit and AB the esterifying medium. The equilibrium can be written as:

$$\frac{[C_6H_9O_5A]}{[C_6H_{10}O_5]} = \frac{[AB]}{[HB]} K$$

The units which contain substituents at the C_2 position (n_2) can be calculated as:

$$\frac{n_2}{(1-n_2)} = kK_2$$

or:

$$n_2 = \frac{kK_2}{(1+kK_2)}$$

where k is a parameter related to the substituting

power of the reaction medium, represented above as [AB]/[HB]. Similar equations can be written for units containing substituents at C_3 and C_6. From these a set of equations can be derived to calculate the various fractions of substituted units:

$$(2,3,6) = \frac{k^3 K_2 K_3 K_6}{[(1+kK_2)(1+kK_3)(1+kK_6)]}$$

If $d \equiv [(1+kK_2)(1+kK_3)(1+kK_6)]$

then:

$$(2,3) = k^2 K_2 K_3/d$$
$$(2,6) = k^2 K_2 K_6/d$$
$$(3,6) = k^2 K_3 K_6/d$$
$$(2) = kK_2/d$$
$$(3) = kK_3/d$$
$$(6) = kK_6/d$$

and unsubstituted units as: $1/d$

Using these equations, Wu plotted the fractions of unsubstituted, mono-, di-, and tri-substituted units for CN using values of $K_3 = 1.0$, $K_2 = 1.8$, and $K_6 = 5.8$. Figure 24 shows a reproduction of that plot. What becomes apparent by plotting the fractions in this fashion is that a CN of any nitration level between 0 and 3 is a combination of glucose units of differing substitution. This becomes of importance when trying to interpret trends in observed responses of CNs. Table II
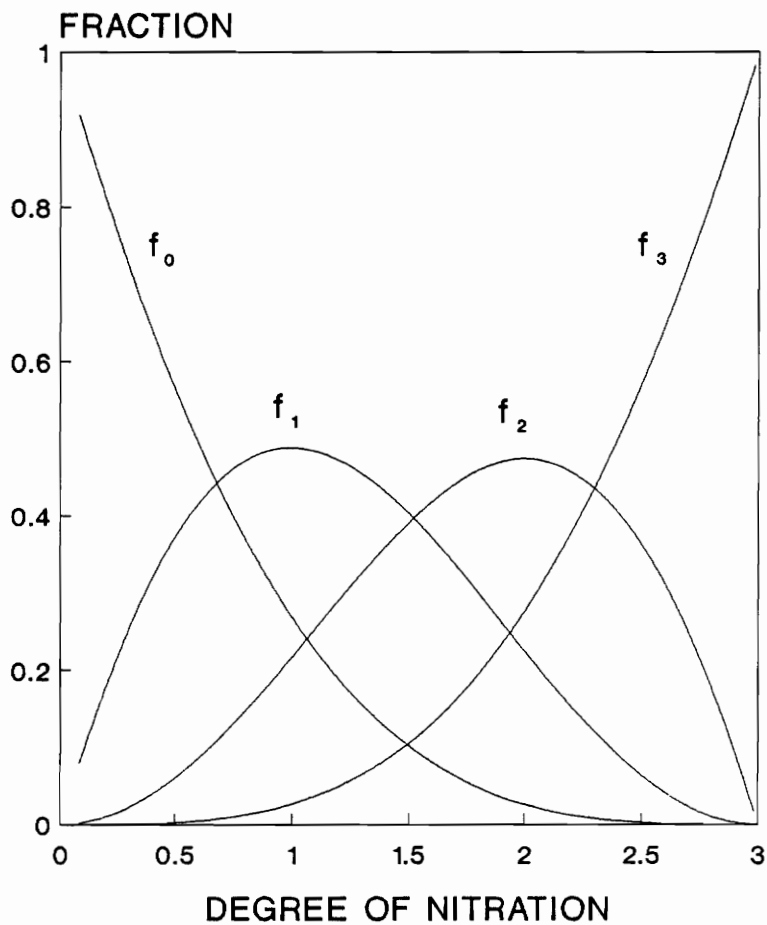
Figure 24. Fractions of unsubstituted [f_0], mononitrat-
ed [f_1], dinitrated [f_2], and trinitrated
[f_3] units for CNs.

84

lists the calculated fractions for the CNs which were examined in this study.

One means of quantifying steric, polar and other molecular interactions is through the use of the Hammett equation. This equation, in any of its many forms, correlates observed phenomena with empirical constants related to some thermodynamic property of the solute. When applied to infrared data, the form of the equation most used is:

$$v_i = v_o + p\sigma$$

for analyzing frequency data, and:

$$A^{\frac{1}{2}} = A_o^{\frac{1}{2}} + p\sigma$$

for analyzing infrared intensity data[100]. In each case p is a parameter dependent upon the solvent system and σ is a parameter dependent upon the solute. Taft has done a considerable amount of work on development of σ values for separating polar, steric, and resonance effects[101]. In the case of steric effects, the solute parameter is most often represented as E_s rather than σ. Taft reports an E_s value for the nitro group of -0.75. If for the CN system this value is assigned to

Table II

Calculated Fractions of Glucose Units for the CNs Examined

CN	c_0	c_2	c_3	c_6
2.11	0.018	0.039	0.021	0.125
2.32	0.007	0.024	0.013	0.076
2.45	0.004	0.016	0.009	0.052
2.63	0.001	0.008	0.004	0.024
2.78	0.000	0.003	0.002	0.009

CN	$c_{2,3}$	$c_{2,6}$	$c_{3,6}$	$c_{2,3,6}$
2.11	0.047	0.271	0.151	0.328
2.32	0.043	0.249	0.138	0.450
2.45	0.038	0.223	0.124	0.535
2.63	0.029	0.171	0.095	0.667
2.78	0.019	0.113	0.063	0.791

the fully substituted material (DN=3.0), and the value

for less nitrated material calculated as the fraction

of glucose units substituted at both the C_2 and C_3

positions multiplied by this value, then the Hammett

equation can be applied using the frequency data from

the 2 cm^{-1} resolution study. Assigning v_o as the fre-

quency of the 2.11 CN for convenience, the graphs of

$(v_i - v_o)$ vs E_s shown in Figure 25 are obtained. Note

that both the acetonitrile and THF plots are linear,

indicating a positive correlation of the frequency

shift with steric interaction between nitrate groups at

the C_2 and C_3 positions. Note also that the slope of

each line is different. This can also be explained in

terms of solvent-solute interactions.

That acetonitrile was the other solvent which

proved useful for this system was fortuitous. Acetoni-

trile and THF are separated by some margin in their

solvent donor/acceptor properties. Many interactions in

organic chemistry have been described by the Lewis

acid/base concept or nucleophilic/electrophilic reac-

tion scheme. Gutmann recognized that the actual chemi-

cal behavior of a molecule is highly influenced by its

molecular environment[102]. This concept proposes that a

molecule may behave as a donor, defined in a general

sense as an electron donor, Lewis base, or nucleophilic
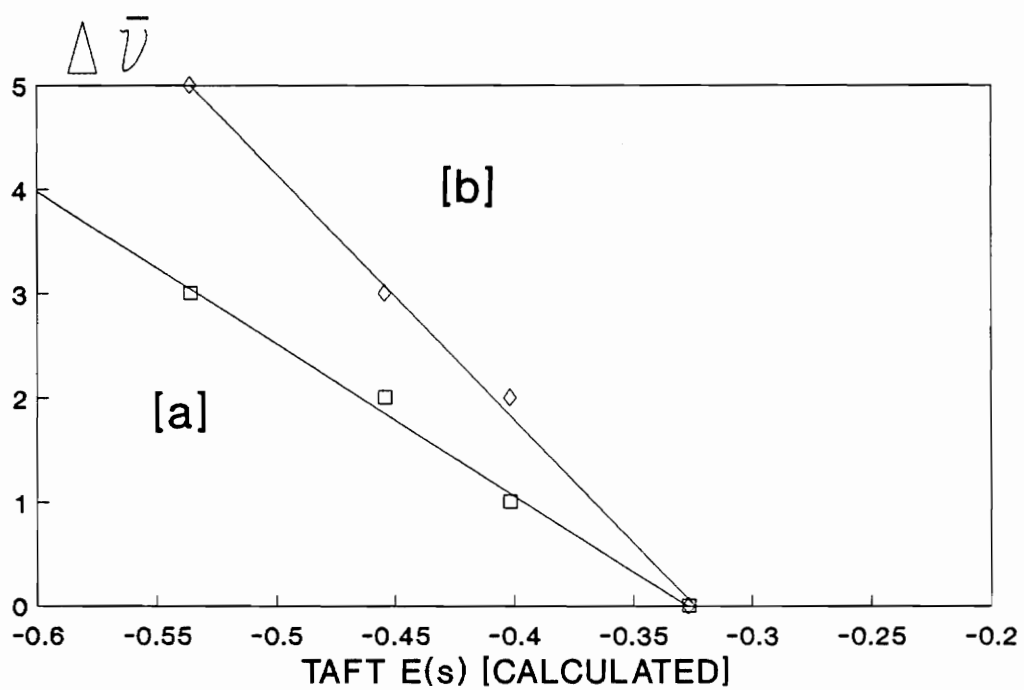
Figure 25. Hammett equation plots for 2 cm^{-1} CN data
for [a] THF and [b] acetonitrile

agent, in one chemical system, and as an acceptor, defined as an electron acceptor, Lewis acid, or electrophilic agent, in a different chemical system. The interactions of solvent-solute are described more in terms of charge density rearrangements than in charge transfers. If the solute is represented as AB and the solvent as Donor or Acceptor, the interactions can be represented as:

$$\text{Donor} \dashrightarrow A^{\delta+} \overset{\frown\!\!\!\!\!\!\longrightarrow}{-\!-\!-\!-\!-} B^{\delta-}$$
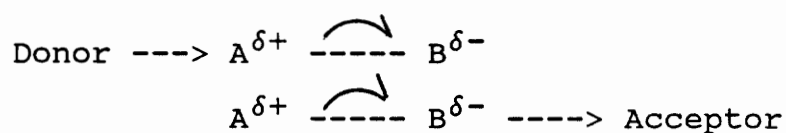
$$A^{\delta+} \overset{\frown\!\!\!\!\!\!\longrightarrow}{-\!-\!-\!-\!-} B^{\delta-} \dashrightarrow \text{Acceptor}$$

In each case the A-B bond length is increased. The relative strengths of the solvent and solute as donors and acceptors will determine the extent of the interaction, and hence the extent of the charge rearrangement and subsequent increase in A-B bond length. Table III lists Gutmann's donor and acceptor values for acetonitrile and THF.

Noting that THF is a stronger donor according to this scale a stronger interaction with an acceptor solute would be expected. This would result in a slightly longer A-B bond length for a THF solvent system than for an acetonitrile solvent system. In the infrared spectrum of the A-B solute a shift to lower

Table III

Gutmann's Donor and Acceptor Values for THF and Acetonitrile

Solvent	Donor Number	Acceptor Number
THF	20.0	8.0
Acetonitrile	14.1	19.3

energy for the THF system relative to the acetonitrile system would be expected due to the slightly longer bond. This is what is observed in the case of CN as the solute. Note that not only is the trend what would be expected but that the ratio of the slopes of the aceto-nitrile to THF Hammett plots are close to the ratio of the acetonitrile to THF donor values (0.625 and 0.714 respectively). The likely point of interaction with the nitrate group of CN is at the nitrogen atom. This is where nitro groups have been shown to be electron deficient, with the excess electron density centered on the two oxygen atoms in a fashion such as[103]:

$$- O - \overset{\delta+}{N} \underset{\underset{O\ \delta-}{\Large\diagdown}}{\overset{\overset{O\ \delta-}{\Large /\!/}}{}}$$
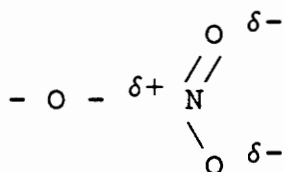
Thus it can be concluded that the observed frequency shift is a steric interaction and the difference in frequency between the solvents examined is due to the relative solvent strengths.

Second Derivative Spectroscopy

One of the limitations of condensed phase infrared studies is the bandwidth of the infrared absorptions.

It was noted earlier that even at 2 cm^{-1} resolution, the overlap of the observed absorptions was considerable, despite the fact that the bands appear to be separated by $\approx$ 16 cm^{-1}. Enhancement of FT infrared spectra can be accomplished mathematically by the application of second derivatives or what is termed Fourier self-deconvolution[8,104]. The second derivative is the rate of change of the slope of the infrared absorption band. Plotting the second derivative of a spectrum enhances narrow spectral features preferentially over broad spectral features. The result of taking the second derivative of a spectrum is the maintenance of the frequency (position) and shape of the absorption while reducing its bandwidth. In addition to decreasing bandwidth, the SNR of the spectrum is decreased by a factor of $\approx$ 4. This limits its application to spectra of intermediate or low resolution, as high resolution spectra already have a much lower SNR, and the introduction of additional noise makes interpretation of the result difficult.

Figure 26 shows the second derivative spectra for the CNs from Figure 16. Note that there appear to be three absorptions in the spectral band, not just two as would have been expected from the original spectra. Note also that the high energy band does still appear
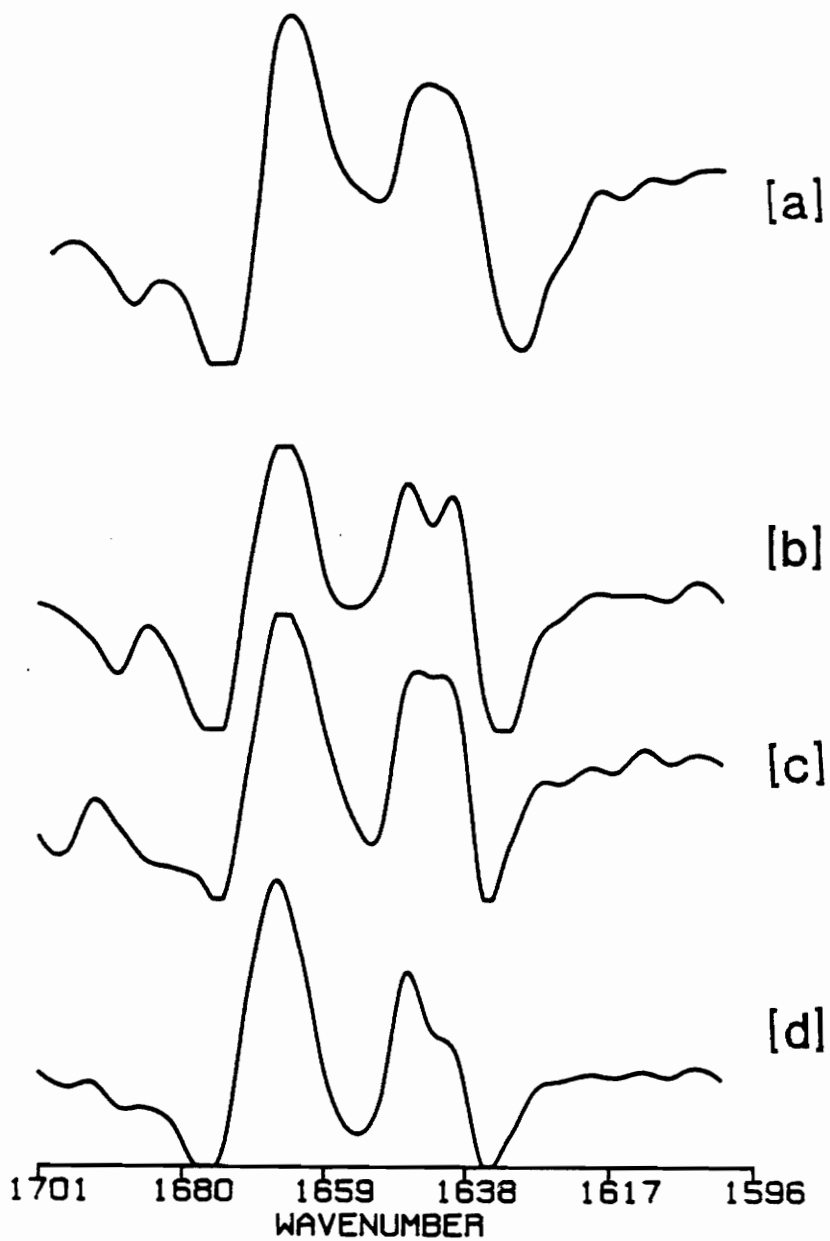
Figure 26. Second derivative spectra of [a] 2.11, [b] 2.32, [c] 2.45, and [d] 2.63 DN CNs

to increase relative to the others as the DN increases. The small shoulder absorption on the low energy band $\approx$ 1639 cm^{-1} appears to decrease as the DN increases. Since the equilibrium model predicts that for CNs of DN greater than 2 the major site of additional nitration is at the C_3 position, and since the high energy band has been assigned to steric interaction of two secondary nitrates at adjacent positions, it would be reasonable to assign this absorption (1639 cm^{-1}) to secondary nitrates which have a hydroxyl at the adjacent position. This assignment leaves the major low energy band to the primary absorption at the C_6 position. This is in agreement with previous work on alkyl nitrates. Urbanski and Witanowski found that for a series of alkyl nitrates, the order of absorption frequency decreased on going from primary to secondary to tertiary[105]. A similar trend was observed for alkyl nitro compounds[106].

Due to the overlap of the peaks observed even in the second derivative spectra there is still doubt as to the exact frequency for each of the individual bands. In order to verify specific absorptions a means was needed to remove one member of an overlapped pair so that the other absorption could be independently observed.

Selective Denitration of Cellulose Nitrates

In order to verify the frequency positions of some
of the CN infrared absorptions a selective denitration
of CN was carried out. This procedure was first de-
scribed in 1952 by Segall and Purves using pyridine
with an excess of free hydoxylamine present to hydro-
lyze the nitrate[83]. Several years later it was deter-
mined that the product of this hydrolysis was cellulose
3,6 dinitrate regardless of the DN of the starting
material[84]. This was further verified in the work by
Wu[85]. The selective removal of the secondary nitrate at
the C_2 position allows the observation of the absorp-
tion of the C_3 position with no adjacent nitrates and
the (hopefully) isolated absorption of the primary
nitrate at C_6. As described in the Experimental section
this procedure was carried out with the 2.78 and 2.11
DN material. These were selected as they were the
lowest and highest nitrated materials under study.

The chromatographic comparisons of the starting
material and denitrated material were presented in the
first part of this Chapter. Among the other tests
carried out on the products was percent nitrogen analy-
sis by an outside laboratory and ^{13}C-NMR. The results

of the percent nitrogen analysis are presented in Table IV. Note that the results indicate that the product from the 2.11 DN material was only denitrated an extent representing ≈ 50 % of what was expected. This makes interpretation of observed spectra more difficult since the relative rates of removal of a nitrate group from the variously substituted glucose units is unknown and predicting where the remaining nitrates areplaced is not possible. The product from the 2.78 DN material appears to be the expected 3,6 dinitrate.

^{13}C-NMR Analysis

In order to further verify the products of the denitration ^{13}C-NMR analysis was carried out on both the starting material and the product. Wu showed that the chemical shift of the anomeric carbon at the C_1 position is particularly sensitive to the presence or absence of a nitrate at the C_2 position[85]. In the trinitrated material the shift for this carbon is ≈ 98 ppm while in cellulose it is ≈ 103 ppm, a difference of some 5 ppm.

The C_2 and C_3 chemical shifts are also affected, moving 5 to 8 ppm as well. Here there is some disagreement as to the assignment of which observed shift is

Table IV

Percent Nitrogen Analysis of Denitrated CNs

Sample	Percent Nitrogen	DN Actual	DN Expected
2.78[*]	10.36	1.80	1.79
2.11[*]	10.06	1.72	1.40.ls1
			1.73[#]

* = Denitrated sample

\# = Expected for 50 % completion of denitration

from which carbon. Four research groups have published assignments for the observed shifts for cellulose trinitrates. To illustrate, Figure 27 shows a cellulose nitrated to DN of 2.8 (essentially trinitrate) from Reeder's work[86]. The observed shifts are numbered in sequence from high to low field. Table V lists the assignments for these shifts by the various research-ers. While all agree on the assignments of the high field for C_1 and the low field for C_5 and C_6 (coinci-dent), there are three different sets of assignments for the three middle region shifts. Only Axenrod[107] and Wu[85] agree on all assignments.

To arrive at assignments for the observed chemical shifts for CN each of the researchers applied the concept of additivity of shift parameters. This concept states that substituents one, two, and three bonds from the carbon of interest will influence the chemical shift of that carbon. If the extent of that influence for a particular substituent can be determined, and the effect of each is additive, then it should be possible to predict the spectrum of a sample from knowledge of its chemical composition.

This procedure was applied to the analysis of the starting material and denitrated products. Table VI lists the chemical resonances for the six carbons of
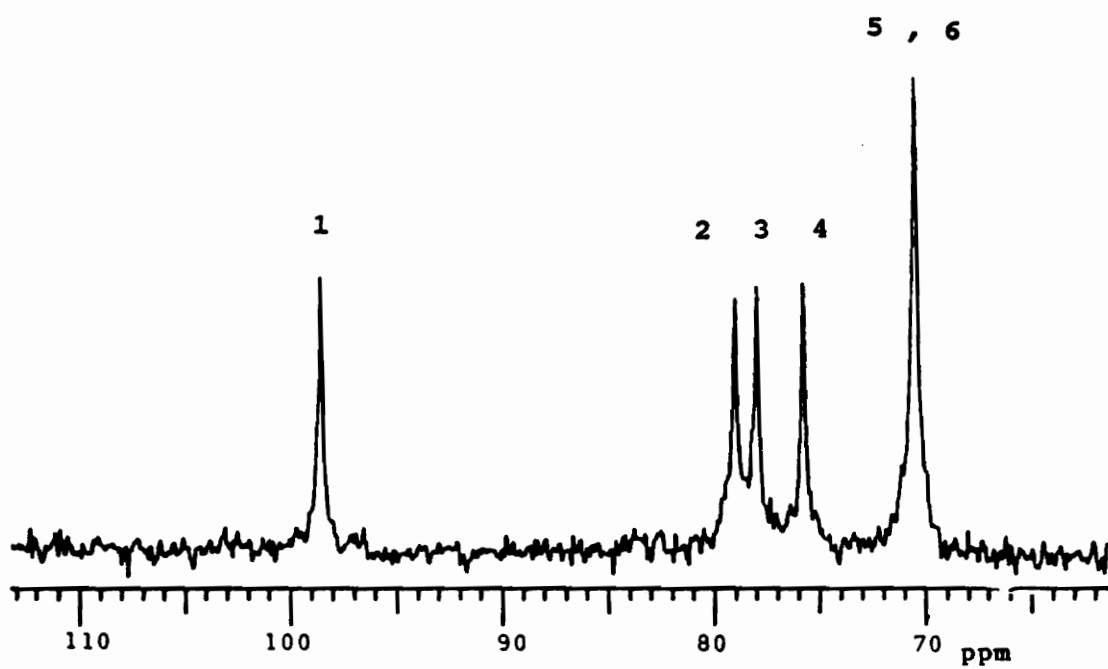
Figure 27. ^{13}C-NMR spectrum of 2.8 DN CN [86]

Table V

Assignments of CN ^{13}C-NMR Chemical Shifts

Reference	1	2	3	4	5,6
85	C_1	C_2	C_3	C_4	C_5, C_6
86	C_1	C_3	C_2	C_4	C_5, C_6
107	C_1	C_2	C_3	C_4	C_5, C_6
92	C_1	C_3	C_4	C_2	C_5, C_6

Table VI

Chemical Resonances For CN Glucose Units

Unit	c_1	c_2	c_3	c_4	c_5	c_6
Unsub	103.1	73.2	74.8	80.0	75.2	60.5
(2)	99.0	81.8	69.6	78.4	74.9	60.4
(3)	102.4	69.3	83.7	76.4	74.2	60.4
(6)	102.8	73.1	74.2	78.4	71.2	70.5
(2,3)	98.6	77.4	79.5	76.5	73.5	60.5
(2,6)	97.3	82.2	70.0	77.8	71.2	70.2
(3,6)	103.0	70.0	84.3	75.1	70.4	70.2
(2,3,6)	98.6	78.0	79.1	75.8	70.5	70.5

each of the eight possible conformations of a glucose unit in CN. These values are taken from Reeder[86] and Bell[108]. Using these data, and estimating the percent of each type of glucose unit from the equilibrium calculations (Table II), predicted spectra for the starting materials were first generated and compared to the observed spectra. Figure 28 shows the predicted and actual spectra for the 2.78 DN CN. The predicted and actual spectra appear to be match well. Table VII lists the predicted and actual chemical resonances for this material. The predicted resonances are all $\approx$ 0.5 ppm higher than the observed resonances. This provides confidence in both the shift values used and the estimated fractions of glucose units.

The same procedure was carried out for the 2.11 DN material. Figure 29 shows the predicted and actual spectra for this sample. While the match appears reasonable the much poorer SNR in the actual spectrum as compared to that for the 2.78 DN material and the many more peaks predicted makes one to one comparisons of the peaks difficult. For comparison, however, Table VIII lists the **major** peaks predicted based upon the near equal presence of 2,3,6-trinitrated, 2,6-dinitrated, 3,6-dinitrated, and 6-mono nitrated glucose units and the **major** peaks observed. There is question as to
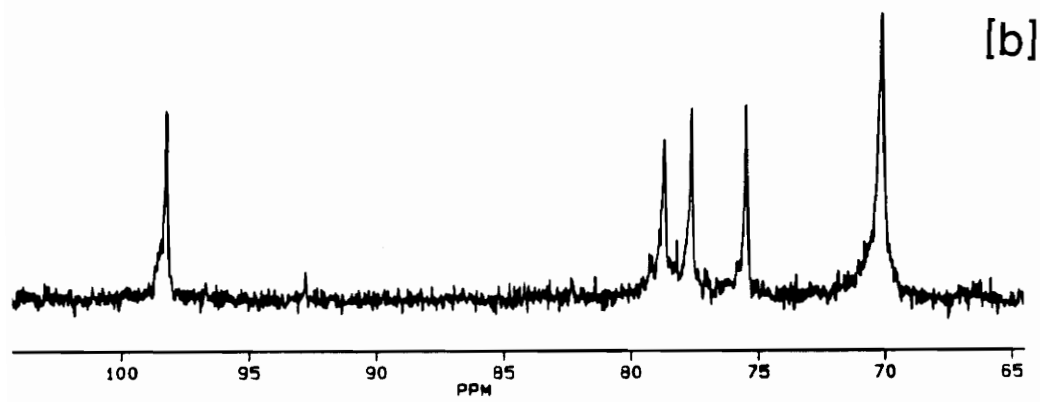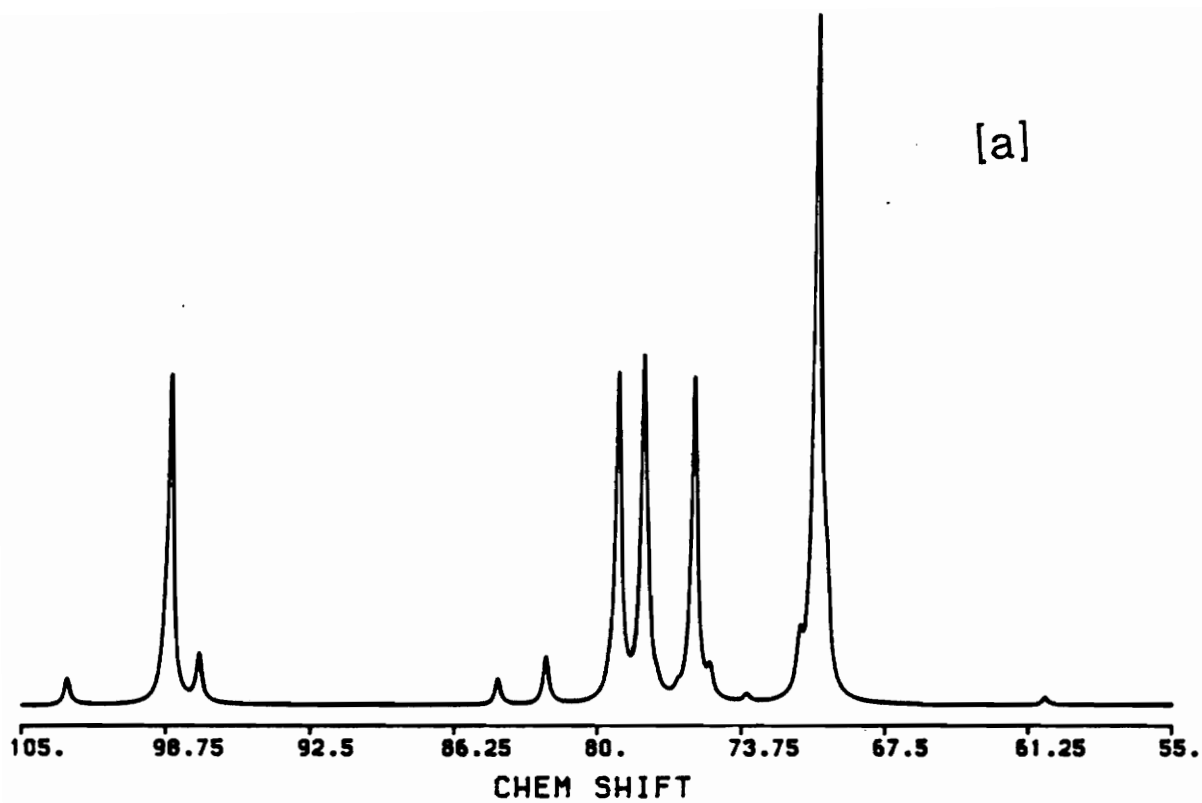
Figure 28. Predicted [a] and observed [b] ^{13}C-NMR

spectra of CN of 2.78 DN

Table VII

Predicted versus Observed ^{13}C-NMR Resonances for 2.78 DN CN

Carbon	Predicted	Observed
C_1	98.6	98.2
C_2	78.0	77.6
C_3	79.1	78.6
C_4	75.8	75.4
C_5, C_6	70.5	70.0
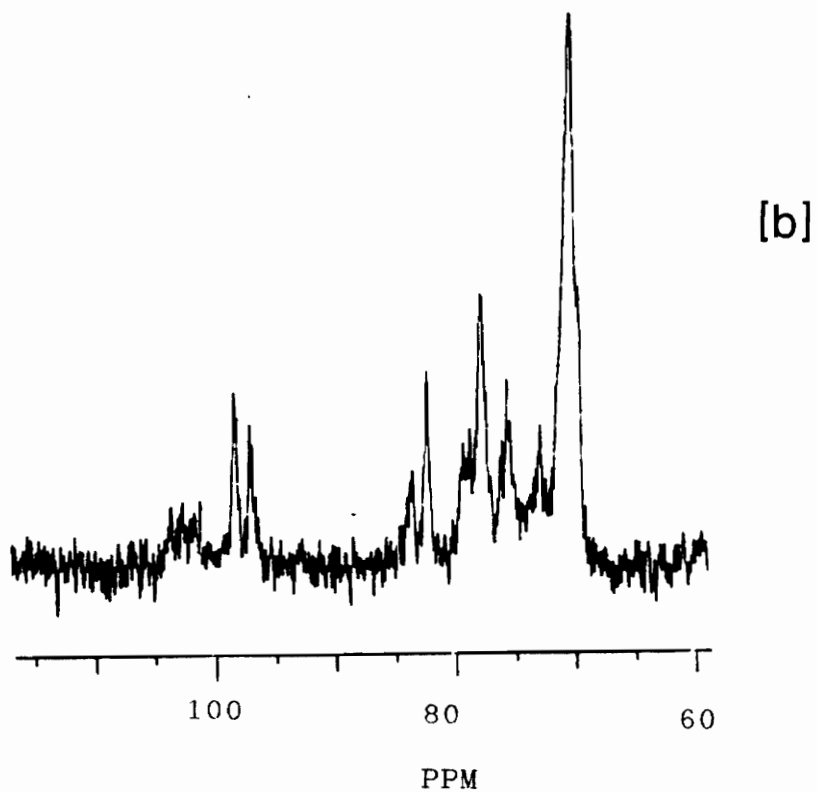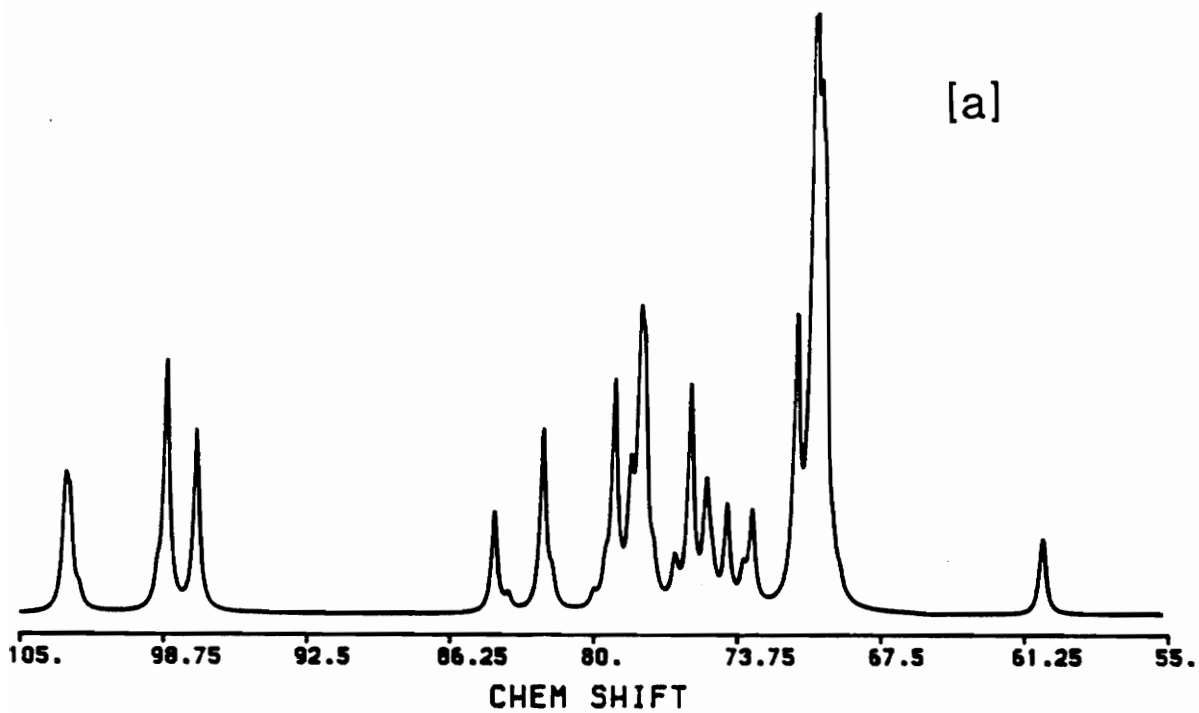
Figure 29. Predicted [a] and observed [b] ^{13}C-NMR
spectra of 2.11 DN CN

Table VIII

Predicted and Observed ^{13}C-NMR Resonances for 2.11 DN CN

Carbon	Predicted*	Observed
C_1	98.6, 97.3 102.8, 103.0	97.0, 98.3 (102-104)
C_2	70.0, 73.1 82.2, 78.0	82.3, 72.8
C_3	70.0, 74.2 79.1, 84.3	≈84, (78-80)
C_4	75.1, 75.8 77.8, 78.4	75.6 77.7
C_5	70.4, 70.5 70.5, 71.2	70.4
C_6	70.2, 70.2 70.5, 70.5	70.4

* For the presence of four differently nitrated glucose units

the absolute assignments of the observed peaks, however the utility of the prediction program is evident for determining the approximate structure of the CNs.

The principle objective in carrying out the ^{13}C-NMR analyses was to verify the products of the denitration procedure. Wu performed a similar denitration in 1980[85]. He found that indeed the procedure of Segall and Purves yielded almost exclusively the 3,6 dinitrate. The prediction procedure described above was applied to the denitrated products of this study. Figure 30 shows the predicted and observed spectra for the denitrated product of the 2.78 DN material. The tabulation of predicted and observed chemical resonances is given in Table IX. While there is a little more variation between the predicted and observed values than was observed for the starting material predicted resonances are still within 1 ppm of the observed values. This provides confidence in assigning this material as cellulose 3,6 dinitrate.

The same procedure was followed for the denitrated product of the 2.11 DN material. Recall that percent nitrogen analysis indicated that this reaction proceeded to only 50 % completion and that the product is not a 3,6 dinitrate but something in between the starting material and 3,6 dinitrate. In fact, the predicted
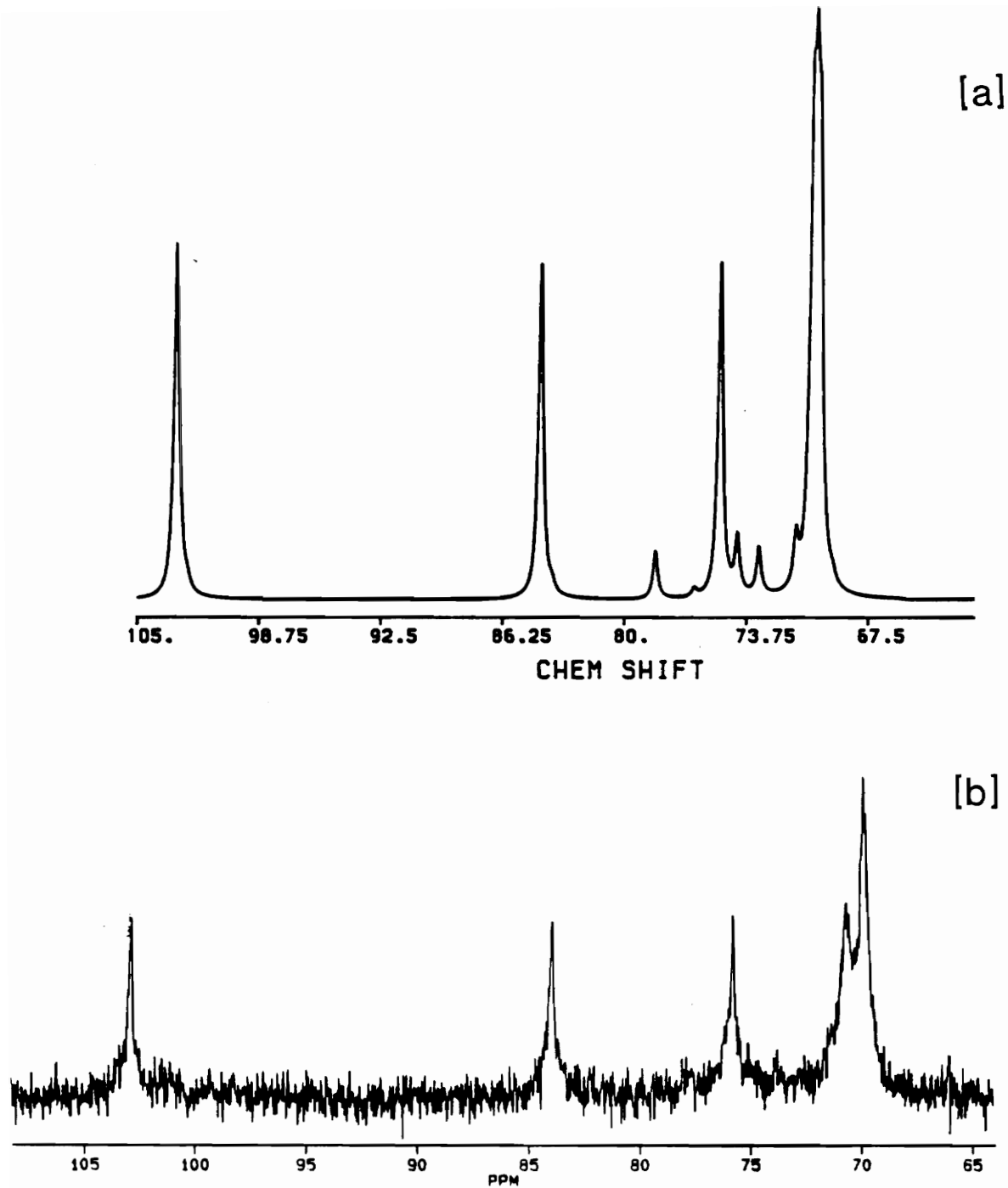
Figure 30. Predicted [a] and observed [b] ^{13}C-NMR
spectra of denitrated 2.78 DN material

Table IX

Predicted and Observed ^{13}C-NMR Resonances for

Denitrated 2.78 DN CN

Carbon	Predicted	Observed
C_1	103.0	102.8
C_2	70.0	70.7
C_3	84.3	83.9
C_4	75.1	75.8
C_5	70.4	69.9
C_6	70.2	69.9

peaks for the material assuming 50 % reaction are the same as for the starting material but with the relative intensities different. Figure 31 shows the comparison of the predicted and observed spectra assuming 50 % reaction. For reference, the predicted spectrum for 100 % reaction is shown in Figure 32. It is readily apparent that the 50 % prediction provides a spectrum much closer in appearance to the observed spectrum than the 100 % prediction. This is in agreement with the percent nitrogen data. Since only relative intensities have changed, assignments are the same as in Table VIII.

Infrared Analysis

With confidence that at least one of the denitrated materials is indeed a cellulose 3,6 dinitrate infrared characterization was conducted to address the issue of the infrared absorption frequency of the primary nitrate at C_6 and a secondary nitrate at C_3. Figure 33 shows the asymmetric nitrate stretching region for the 2.78 DN material and its denitrated counterpart. The most obvious difference is the complete loss of absorption at the higher energy side in the denitrated material. This is in agreement with the assignment of that absorption arising from steric interaction between
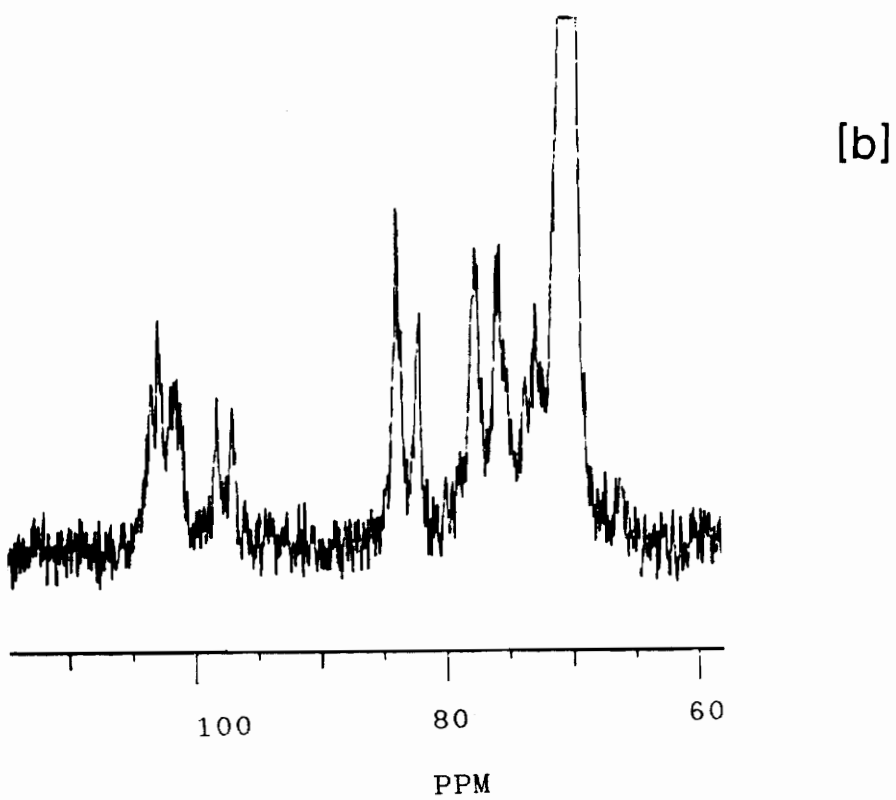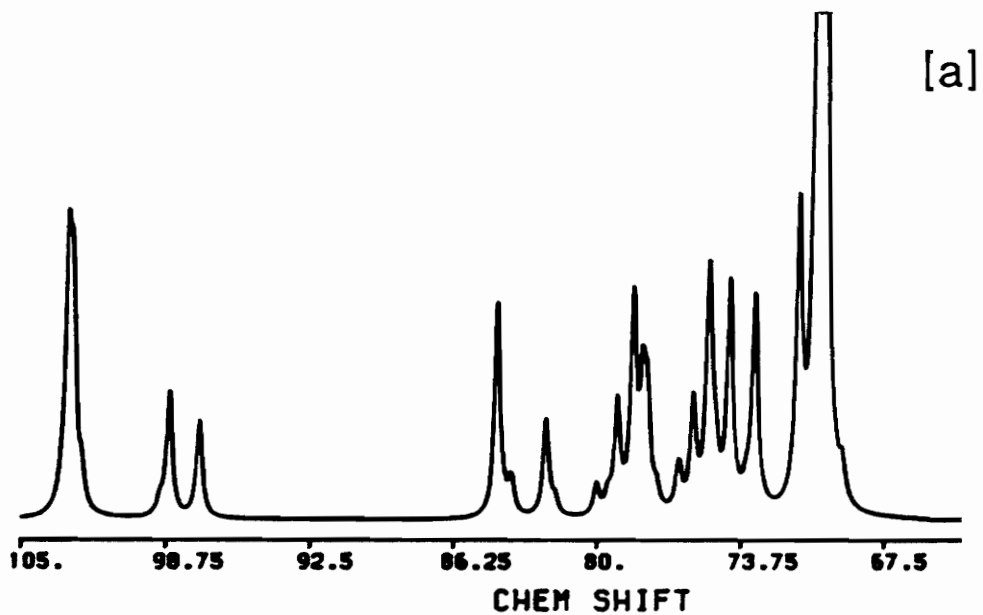
Figure 31. Predicted [a] and [b] observed ^{13}C-NMR
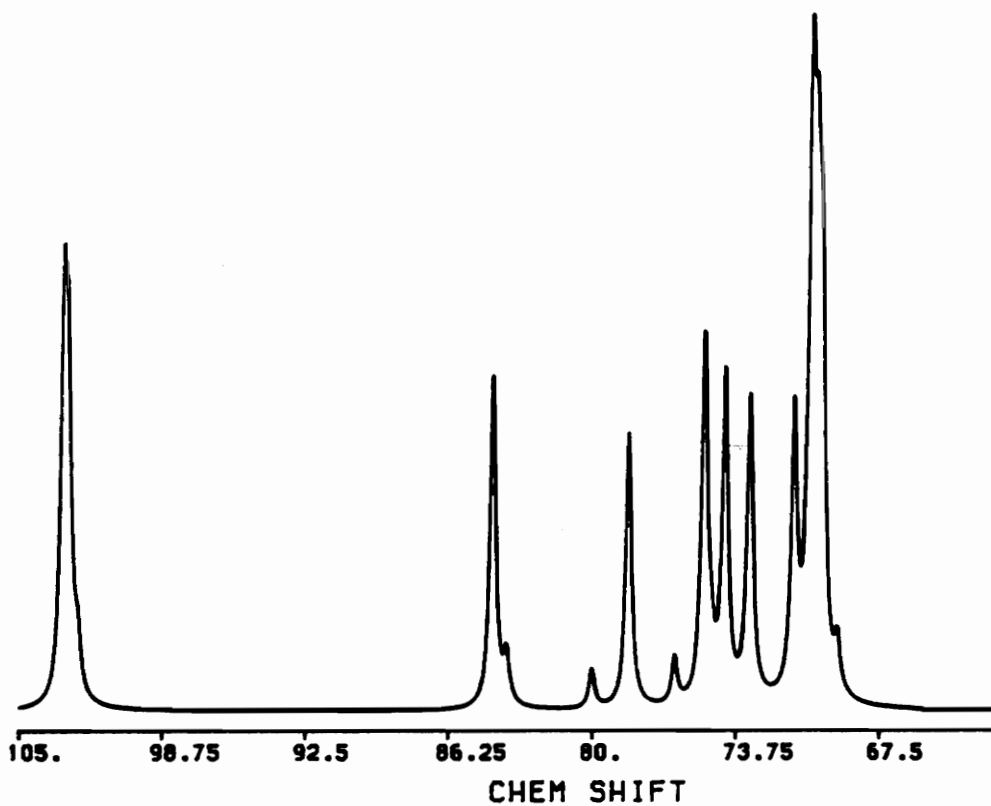
spectra of denitrated 2.11 DN CN

Figure 32. Predicted ^{13}C-NMR spectrum of denitrated
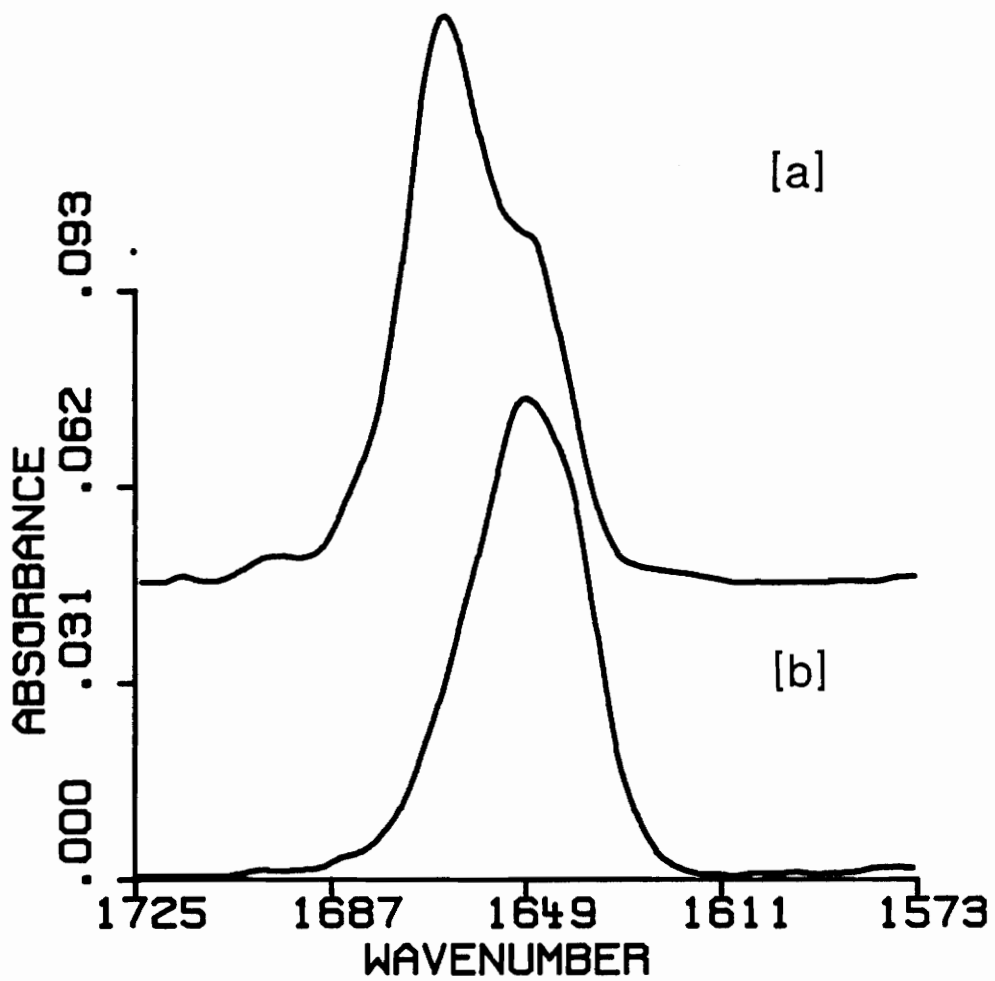
2.11 DN CN assuming 100 % reaction

Figure 33. Infrared spectra of [a] 2.78 DN CN and [b]
its denitrated counterpart

113

neighboring nitrate groups. The 3,6 dinitrate does not contain any glucose units with such a substitution. There does appear to be a slight asymmetry to the denitrated material's absorption, however, indicating the possible presence of two absorptions with extensive spectral overlap. To evaluate this possibility further second derivative analysis was applied to each spectrum. The resulting spectra are shown in Figure 34. Note that the 2.78 second derivative spectrum is very similar to the 2.63 spectrum in Figure 26. The denitrated second derivative spectrum only shows two absorption bands. This is consistent with there being separate, noninteracting absorptions for the C_6 primary and C_3 secondary nitrate groups. What is of most interest is that one of the absorption maxima occurs at a completely different frequency than any of the bands observed in the CN samples. The lower energy band of the denitrated sample appears at about the same frequency as the shoulder observed in the lower energy components of the CN samples. The absorption maxima of the second derivative peaks for the denitrated material are 1651 cm^{-1} and 1639 cm^{-1}. The observed absorption maximum in the lower energy region of the original spectrum occurs at 1647 cm^{-1}. This would indicate a somewhat greater contribution to the observed absorption
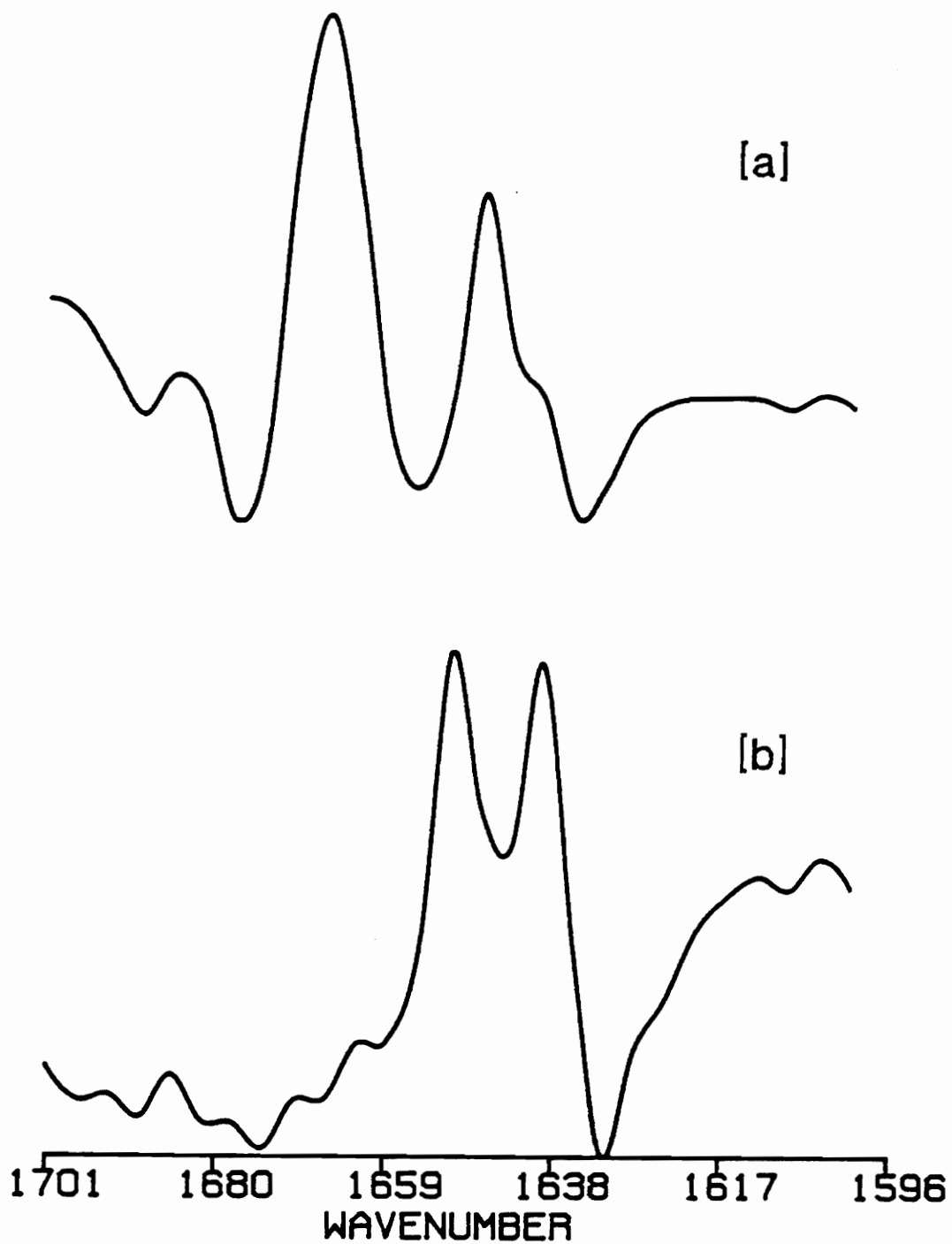
Figure 34. Second derivative spectra of [a] 2.78 DN CN
and [b] its denitrated counterpart

by the 1651 cm^{-1} band. Indeed, the relative absorption
of this band in the second derivative spectrum is
greater by $\approx$ 24 % (1.24:1). This is in agreement with
the expected relative amounts of $C_6:C_3$ for this materi-
al (1.12:1) based upon the equilibrium model. This
would indicate an assignment of the 1651 cm^{-1} absorp-
tion to the C_6 primary nitrate and the 1639 cm^{-1} ab-
sorption to the C_3 secondary nitrate. This is in agree-
ment with the observations made earlier for the second
derivative spectra of the CN samples and with the
observations of previous workers as to the relative
frequencies of absorption for primary and secondary
nitrates.

Development of the Infrared Model

Spectral curve fitting techniques for infrared
spectroscopy have been of increasing interest in an
effort to improve on current deconvolution
methods[104,109-112]. Most of these employ a Lorentzian
band profile to approximate the infrared band or a
combination Lorentzian-Gaussian profile. A simple
Lorentzian equation can approximate most of the ob-
served infrared bands[8]. The equation for such a profile

can be written as[110]:

$$F(v_1) = \frac{\sigma/\pi}{\sigma^2 + (v_1 - v_o)^2}$$

where σ is the half band width at half height, v_o is the peak frequency maximum, and v_1 the frequency variable in wavenumbers. For the situation where more than one absorption is present the equation is simply expanded and each band summed over the range of interest.

To model the observed CN infrared spectra, the experimentally determined values of 1651 cm^{-1} for the C_6 absorption and 1639 cm^{-1} for the C_3 absorption may be used, but the question of what values to assign to the C_2 absorption when there is no nitrate adjacent to it and the high energy absorption for the glucose units with both a C_3 and C_2 nitrate remains. Considering that only three absorptions were observed in the second derivative spectra of the CNs examined, and only two in the region where the noninteracting nitrates absorb, the 1639 cm^{-1} absorption may also be assigned to the C_2 nitrate as well. That is to say that there is no evidence that a secondary nitrate at C_2 should absorb at a different frequency than one at C_3. To assign a value to the combined C_2 and C_3 frequency a reexamination of the 2 cm^{-1} resolution data is needed. Note that while the frequency trends are not quite linear the Hammett

plots are (Figures 23 and 25). If the Hammett plot is
extrapolated to DN = 3.0 we find that its frequency
would be 1667 cm^{-1} in THF. Using these frequency values
and the equilibrium data from Table II it is possible
to model the expected appearance of the CN infrared
absorptions.

The selection of a value for σ for this system is
more difficult to address. The overlap is so extensive
in all spectra examined that exact values for the
individual bandwidths is not possible. Noting that the
assigned frequencies are 16 and 12 cm^{-1} apart, and
recalling that for overlapped bands the half width of
the bands is greater than the separation, σ values
greater than 8 are required to approximate the actual
situation. In the model σ values were allowed to vary
until the resultant peaks resembled the actual spectra
throughout the range of CNs examined. Final values were
$\sigma = 9$ for the 1667 cm^{-1} frequency and $\sigma = 16$ for the
1651 cm^{-1} and 1639 cm^{-1} frequencies.

Figures 35, 36, and 37 show the model results for
the 2.11, 2.32, and 2.63 DN CNs respectively. While not
a perfect match the trends observed in the actual
spectra are seen in the model as well. On the high
energy side of the spectra a band due to those glucose
units containing a nitrate group at both C_2 and C_3 can
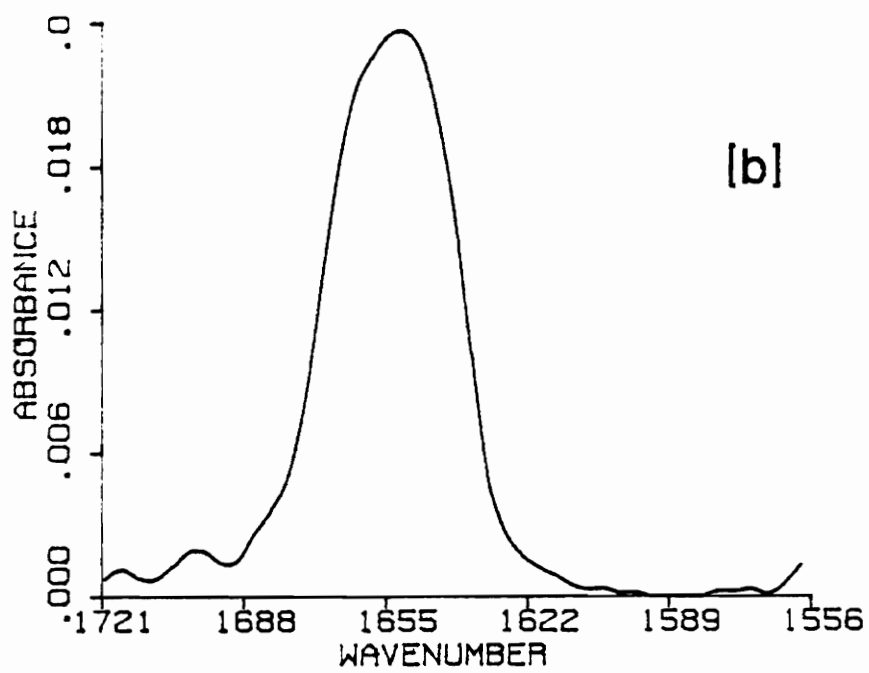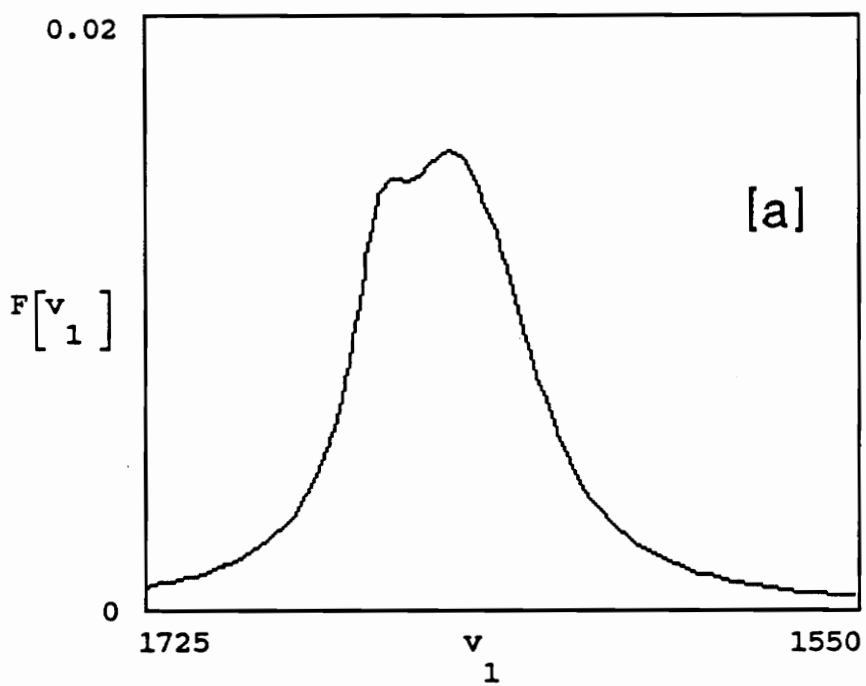
Figure 35. Predicted [a] and observed [b] infrared
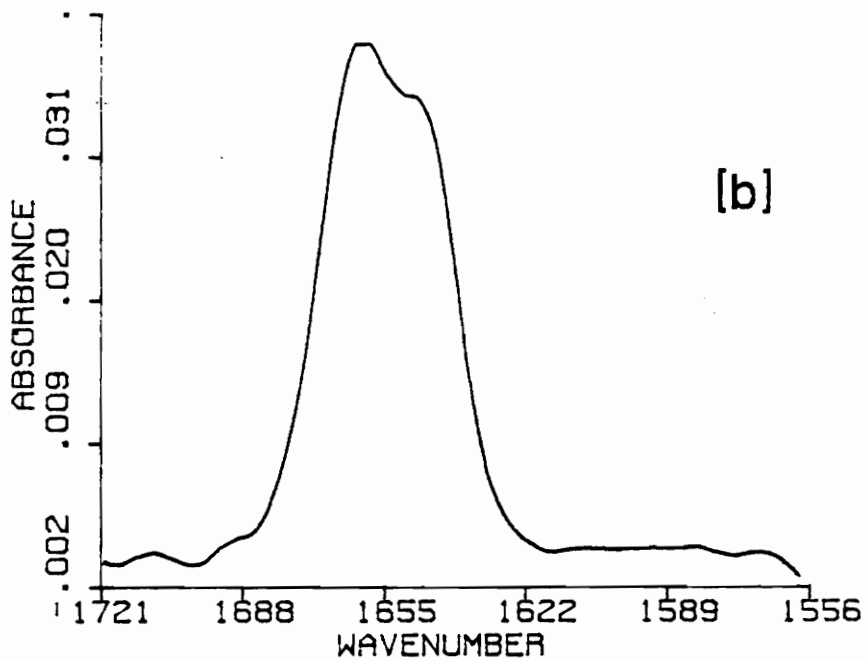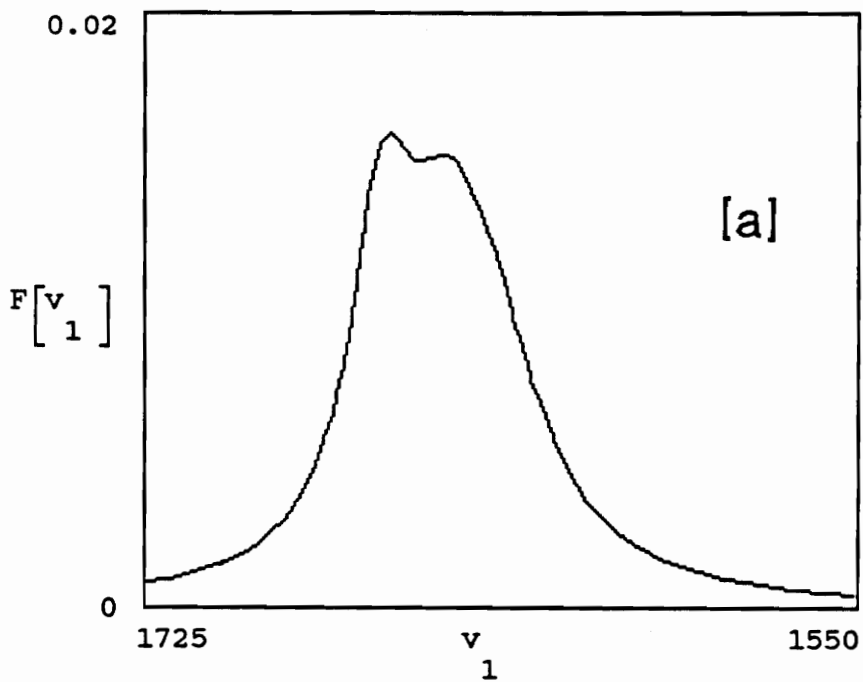spectra of 2.11 DN CN

119

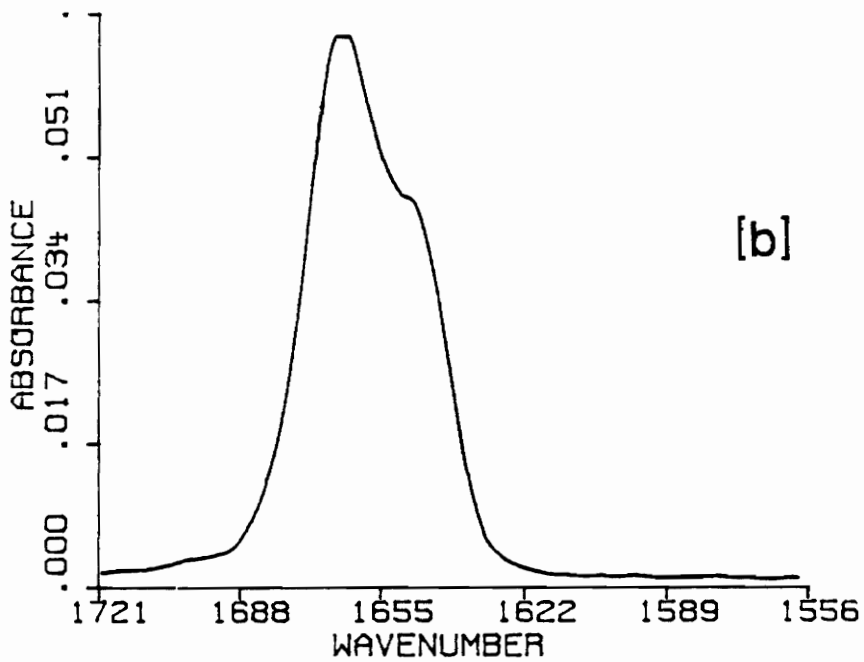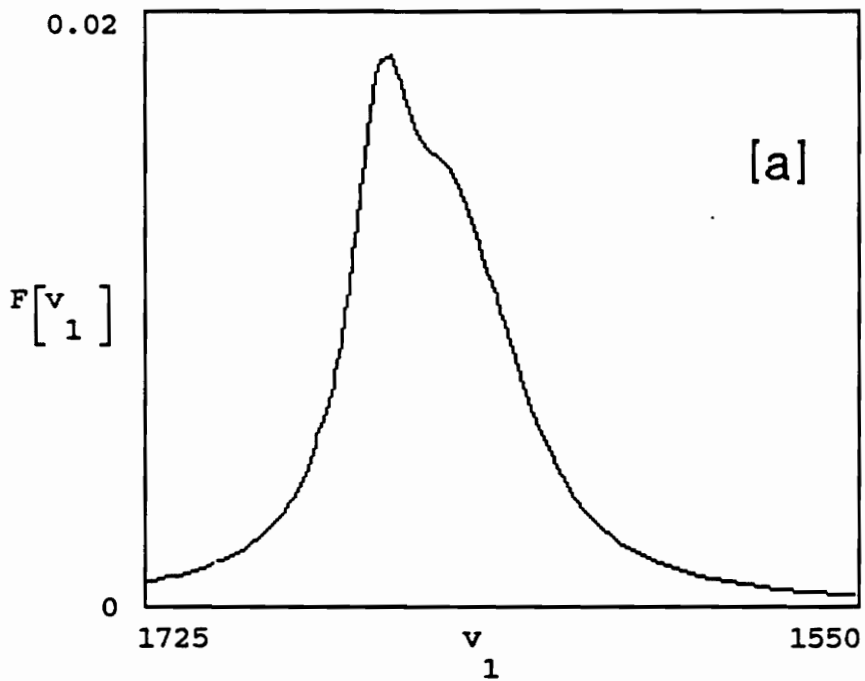Figure 36. Predicted [a] and observed [b] infrared
spectra of 2.32 DN CN

Figure 37. Predicted [a] and observed [b] infrared
spectra of 2.63 DN CN

be seen to increase as the DN increases. The low energy band is due to overlap of the primary C_6 band at 1651 cm^{-1} and the secondary band at 1639 cm^{-1}. This secondary band arises from those glucose units which contain a nitrate group at either C_2 or C_3 but not both.

Improvements to the model could be made if it were possible to have the computer use the digitized data of the actual spectra and calculate the best fit for the parameters. Recent research has shown that an overall improvement in the modeling of spectral features is realized when residual differences between the model spectrum and the actual spectrum are minimized in this fashion[109,111]. In addition, Figure 38 shows the model spectrum of the denitrated 2.78 material along with its observed spectrum. The model also accurately predicts the observation of a nearly symmetrical band with a maximum in the range of the low energy shoulder of the CN spectra.

In conclusion, these studies have shown that the GPC of cellulose nitrates is not influenced by the degree of nitration when the integrity of the column used is not in question. In addition, the infrared absorptions of cellulose nitrates are different when taken in solution as opposed to the solid state and are further influenced by the choice of solvent. The solu-

122
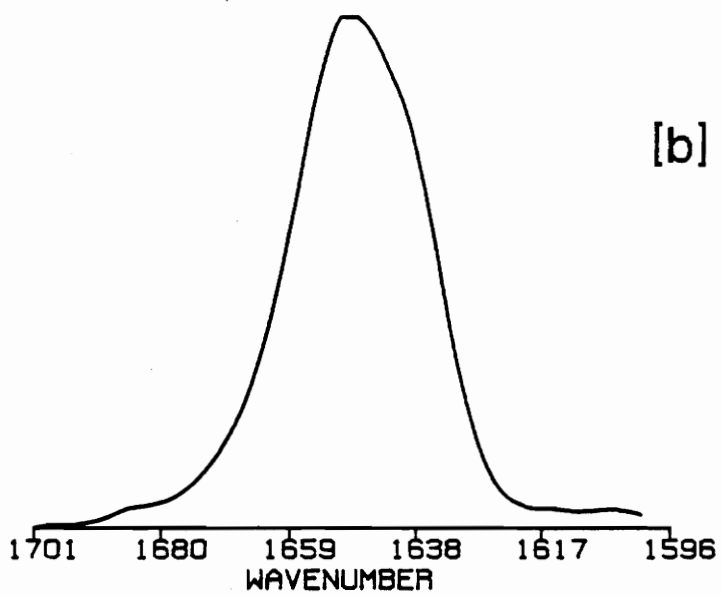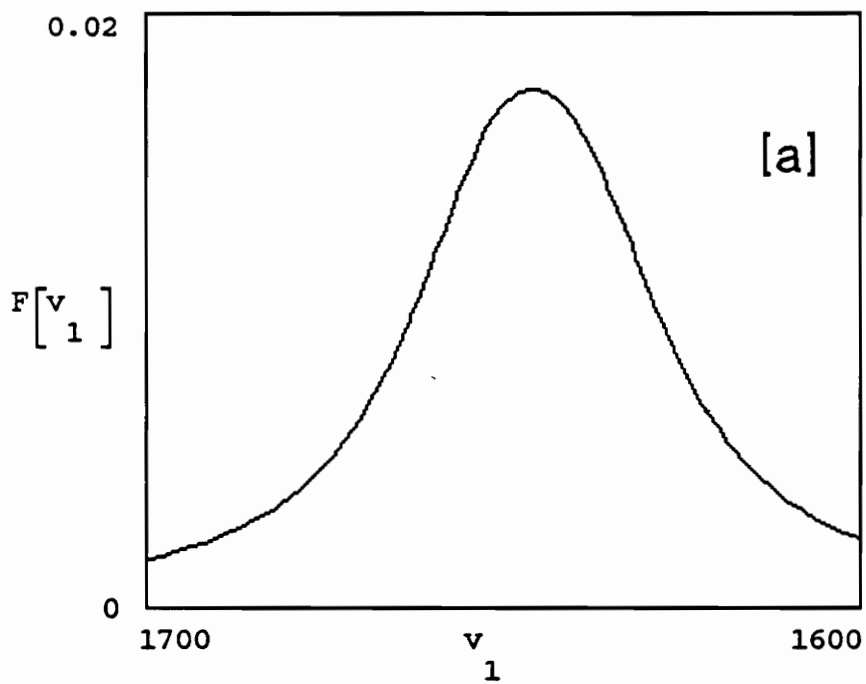
Figure 38. Predicted [a] and observed [b] infrared
spectra of denitrated 2.78 DN CN

tion infrared spectra are dependent upon the position of the nitrate group (primary or secondary) and whether or not the adjacent position contains a nitrate or hydroxyl group in the case of the secondary nitrates. Three infrared absorption bands have been identified. The high energy band seen to increase with increasing DN is due to the steric interaction of nitrate groups at the secondary sites in those glucose units containing nitrates at both the C_2 and C_3 positions. The secondary nitrates in those glucose units substituted at either C_2 or C_3, but not both, absorb at 1639 cm^{-1}. The primary nitrate at C_6 absorbs at 1651 cm^{-1}.

Chapter 4

Characterization of Cellulose Acetate

Butyrates Via GPC/FT-IR

Introduction

Cellulose acetate butyrates (CABs) are organic esters of cellulose used in moldings and extrusion materials[4]. They can be found in a wide variety of products such as buttons, knobs, toothbrushes, and screwdriver handles. The production of the mixed esters is carried out using a mix of acetic and butyric acids together with acetic anhydride. The acetyl to butyryl ratio of the final product is controlled by the ratio of acetic to butyric acid used.

As with cellulose nitrate there are three possible sites for substitution on the cellulose unit. But because there are now two different ester types possible as well as the unreacted hydroxyl, there are 27 possible substitution patterns for an anhydroglucose unit with CAB. Figure 39 shows an anhydroglucose unit together with the possible substituents. While the relative rates of reaction at the three positions parallels that in the nitration of cellulose, it is not known whether there is a preferred site for the incorporation of a specific ester type. Thus it is not known for example, if the butyryl group might preferentially react with the primary site at C_6.
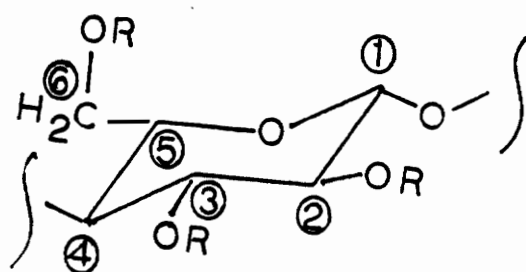
Figure 39. Anhydroglucose unit of cellulose acetate butyrate, where R = H, C(=O)CH$_3$, or C(=O)C$_3$H$_7$

This Chapter explores the infrared characterization of CABs with the goals of identifying those elements specific to each ester type and use them in an effort to identify substitution patterns.

Experimental

For the chromatographic work a single PL-gel styrene divinylbenzene column of either 50 Å pore size or mixed pore bed was used (Perkin Elmer, Norwalk, CT). The 50 Å column was needed to separate the lower molecular weight CABs from the solvent. All chromatographic work was carried out using HPLC grade acetonitrile as the solvent (Fisher Scientific, Raleigh, N.C.). Due to acetonitriles' high solubility parameter (11.5), the columns were first conditioned by passing 3 - 4 column volumes of acetone through and then 3 - 4 column volumes of acetonitrile. After use, columns were again flushed with acetone and then THF and stored in stabilized THF.

The infrared detector used was a Nicolet 5SXC FT-IR fitted with a multipath liquid flowcell (Nicolet Instruments, Madison WI.). Chromatographic data were collected using the available instrument software, collecting 4 scans to a data file at 8 cm^{-1} resolution.

A data file was collected each second of the chromato-graphic run. For the independent spectral analysis the samples were injected directly into the flowcell and spectra collected at 2 cm^{-1} resolution and ratioed against a solvent background. For the solvent study, additional solvents used were HPLC grades THF and methylene chloride (Fisher Scientific, Raleigh, N.C.). Where applied, spectral deconvolution was performed by the second derivative technique.

The CAB samples provided had varying acetyl to butyryl contents (Eastman Chemicals, Kingsport, TN.). These are listed in Table X. The three digit CAB type identification is that used by the supplier, where the first two digits refer to the approximate percent butyryl content and the third digit to the number of unesterified hydroxyls per four anhydroglucose units. The number following the dash is the viscosity of the CAB in seconds by the falling ball method. Samples with higher viscosities are higher in molecular weight. Samples were prepared at $\approx$ 0.2 % wt./wt. except for the lower molecular weight CABs chromatographed on the 50 Å column. These were prepared at $\approx$ 0.6 % wt./wt.

Table X

CAB Samples Examined

CAB Type	$DS_{acetate}$	$DS_{butyrate}$
171-15s	2.04	0.71
381-20	0.99	1.78
381-2	0.98	1.86
500-1	0.30	2.69
531-1	0.22	2.63
551-0.2	0.16	2.53
553-0.4	0.15	2.03

Results and Discussion

Some preliminary work indicated that acetonitrile offered more spectral windows for CAB than THF, as was the case for CN described in Chapter 2. For this reason, all chromatographic work and much of the spectrometric work was performed in acetonitrile.

Chromatography of CABs

The GPC of CABs is very much like that of cellulose acetate, but the problems encountered with CN have not been observed for CABs. Figure 40 shows the GSRs of CABs 171 and 381 separated on the mixed bed column. The 381 CAB has a somewhat broader distribution, and both samples possess a small high molecular weight peak which elutes prior to the main peak. Since the lower viscosity (molecular weight) samples could not be separated from the solvent on this column, all samples were chromatographed on the 50 Å column. These are shown in Figures 41 and 42. Since all the polymers were excluded to about the same extent from the small pores, all elute at about the same elution time, which is normal for GPC. Since this study was more concerned with the spectral characterization of CABs, no further
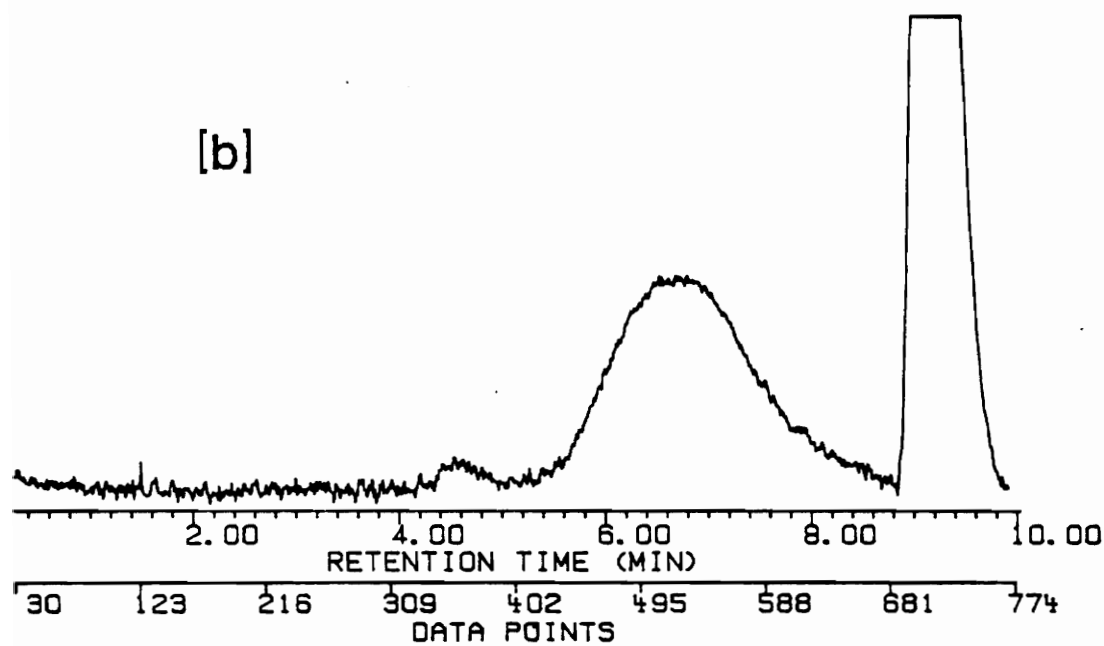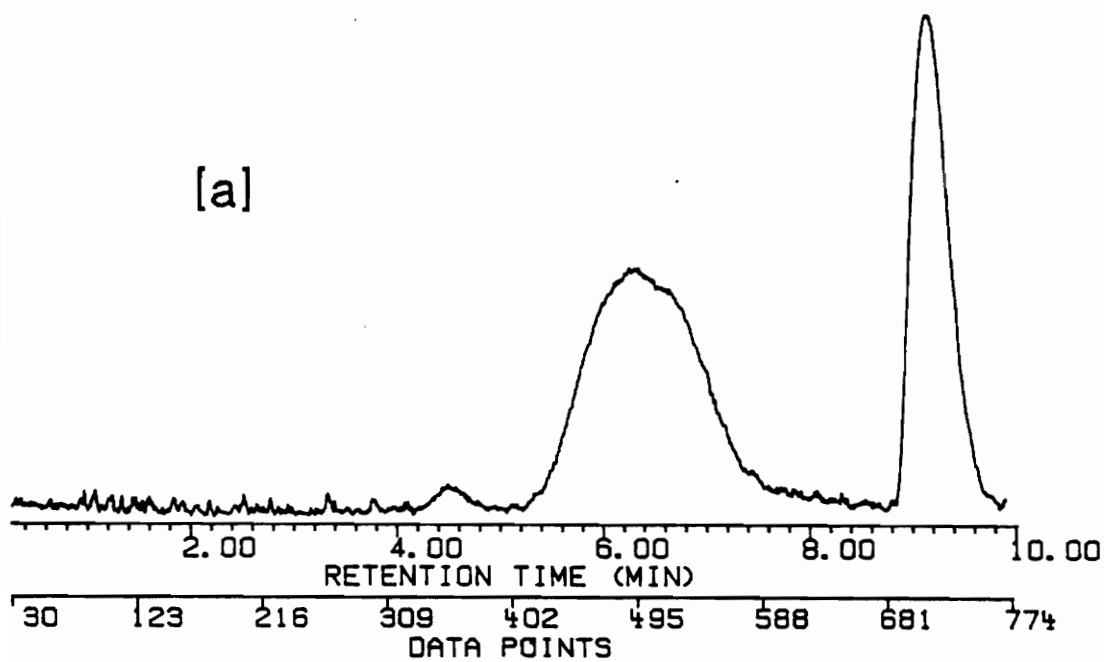
Figure 40. GSRs of CABs 171 [a] and 381 [b] in acetoni-
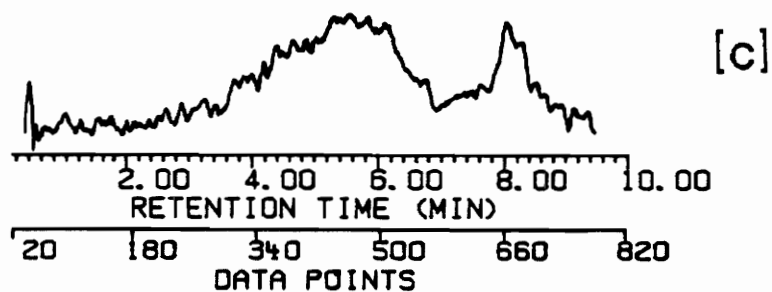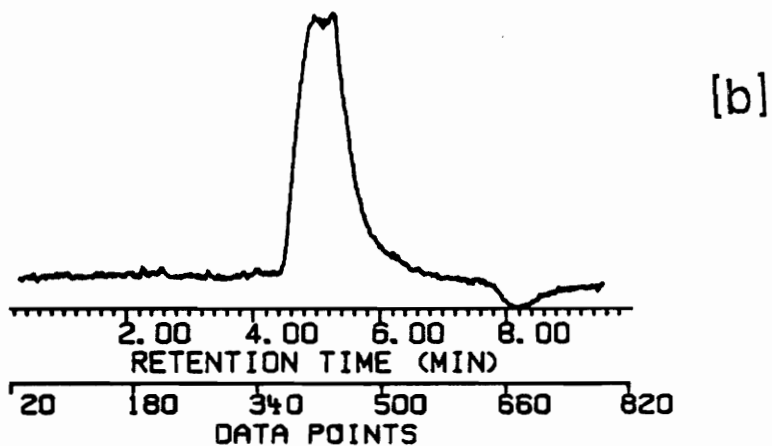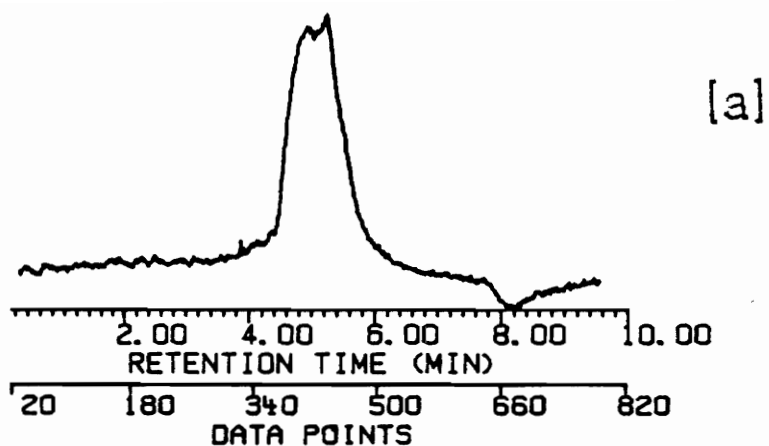trile on the mixed bed GPC column

132

Figure 41. Reconstructed chromatograms of CABs 171 [a], 381 [b], and 500 [c] on the 50 Å GPC column
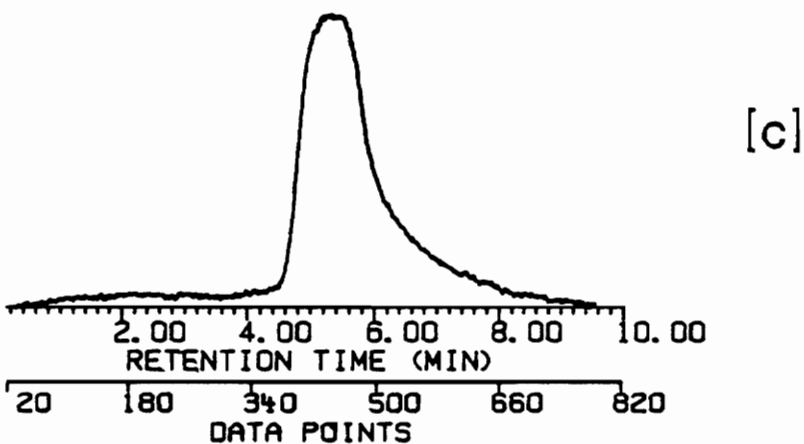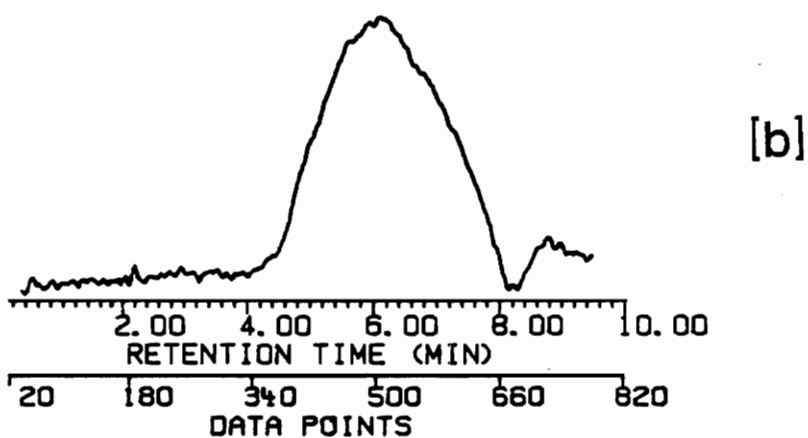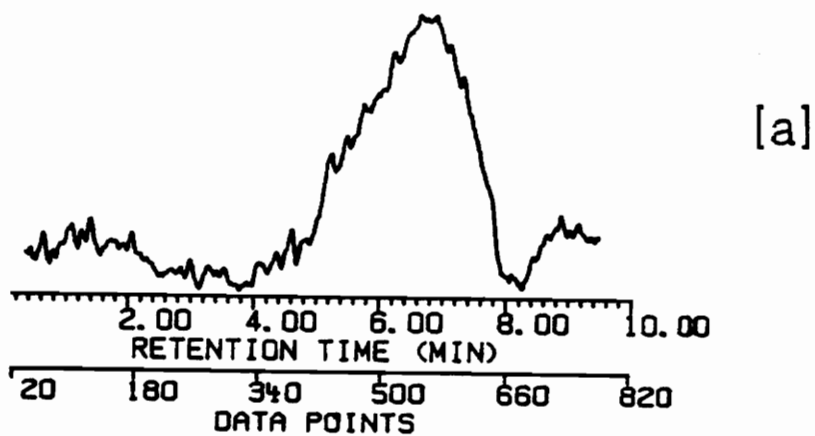
Figure 42. Reconstructed chromatograms of CABs 531 [a], 551 [b], and 553 [c] on the 50 Å GPC column

GPC work was carried out.

Spectroscopic Characterization of CABs

Three solvents were examined for the CAB charac-
terization: THF, acetonitrile, and methylene chloride.
A comparison of the appearance of CAB 381-20 in each of
these solvents is shown in Figure 43. Note that in THF
only the carbonyl stretching mode is observed. In
acetonitrile two additional absorption bands are ob-
served between 1100 cm^{-1} and 1300 cm^{-1}. It will be
shown that these arise from the asymmetric stretch of
the C - O - C bond of the ester groups. In methylene
chloride only one of these additional bands is observed
$\approx$ 1180 cm^{-1}, but the other is obscured by solvent
absorption. In addition, another band appears in meth-
ylene chloride below 1100 cm^{-1}. This absorption arises
from the C_1 - O - C_4 bond of the cellulose linkages.

To identify the bands observed between 1100 cm^{-1}
and 1300 cm^{-1} the various CABs were all run in acetoni-
trile. These spectra are shown in Figures 44 and 45.
Note that as the acetyl content of the CAB increases so
does the absorbance at the 1235 cm^{-1} band. A similar
trend is observed for the 1176 cm^{-1} band with the
butyryl content. Figures 46 and 47 show the trends in
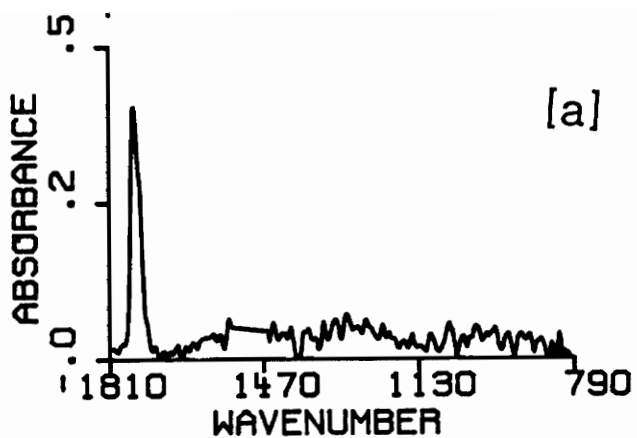
Figure 43. Infrared spectra of CAB 381-20 in THF [a],
acetonitrile [b], and methylene chloride [c]

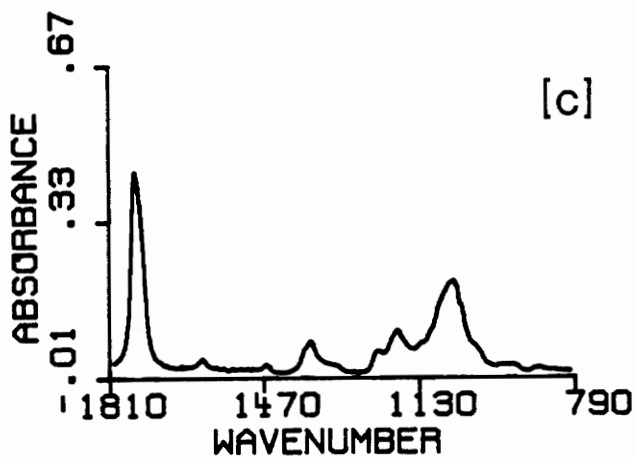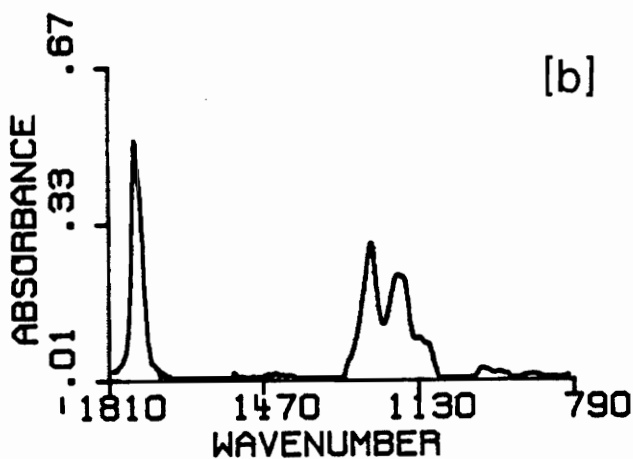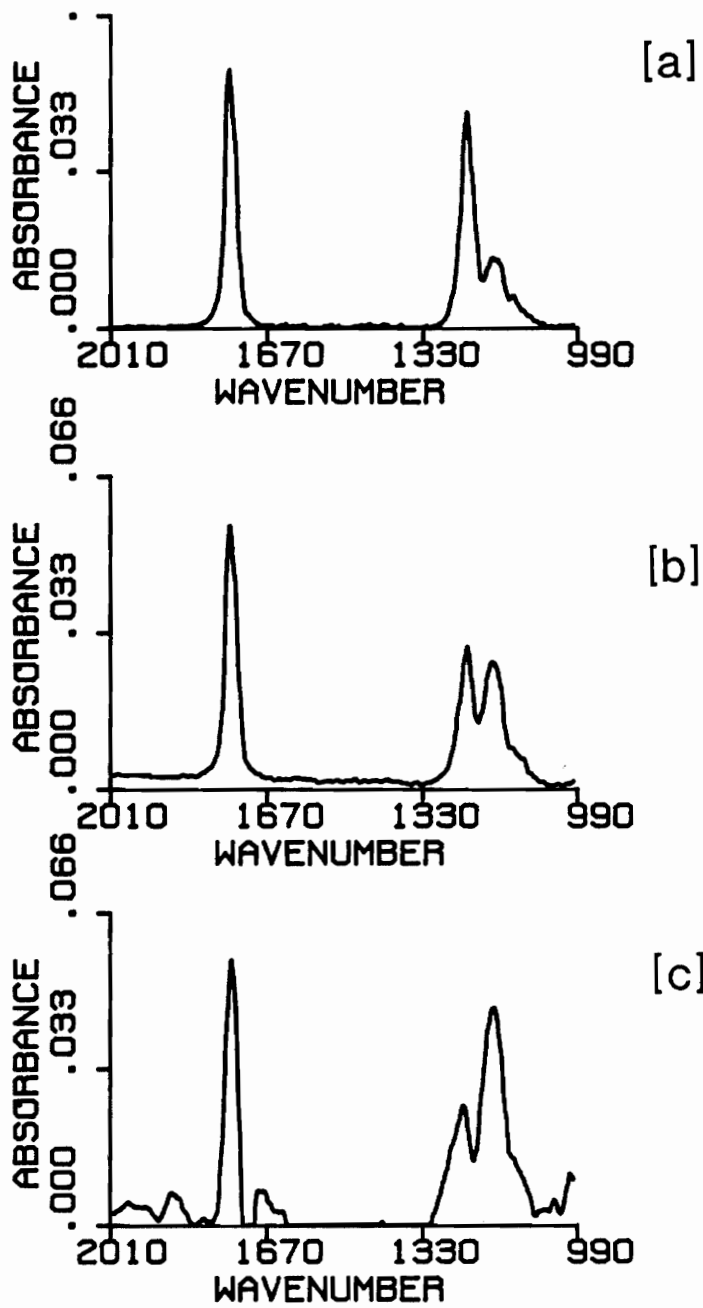Figure 44. Infrared spectra of CABs 171 [a], 381 [b], and 500 [c] in acetonitrile
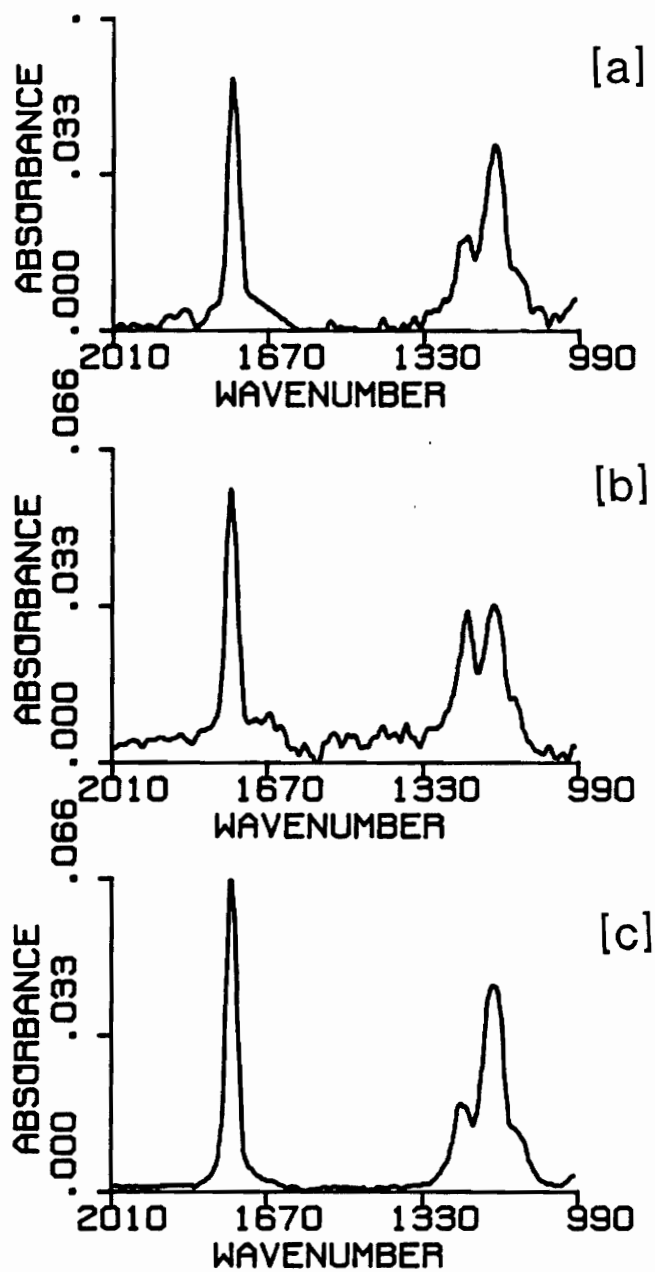
Figure 45. Infrared spectra of CABs 531 [a], 551 [b], and 553 [c] in acetonitrile

absorbance for the 1235 cm^{-1} and 1176 cm^{-1} bands with the acetyl and butyryl substitution respectively.

To further verify the assignments of the observed absorption frequencies in the 1100 cm^{-1} to 1300 cm^{-1} region a pair of cellulose acetate propionates were run. They too possessed the absorption at 1235 cm^{-1}, but the propionate C - O - C absorption was found at 1186 cm^{-1}. This suggests a clear trend in the frequency of this absorption dependent upon the length of the ester side chain. Figure 48 shows this trend as a function of the number of carbons contained in the ester side chain. This trend is common with esters and in fact can be used to identify the ester type[113].

Note that while separate absorption bands are observed for the ester types for the C - O - C bond, only one absorption is observed for the carbonyl stretching mode. This band appears in the 1750 cm^{-1} region. Figure 49 shows an expansion of this region for the CAB 171. Note that similar to the asymmetric nitrate stretch discussed in Chapter 2, this peak appears to consist of two or more overlapping bands. Applying the second derivative technique for spectral deconvolution, shown in Figures 50 and 51, we see that indeed there are two absorptions contained within this peak. Note that the amount of separation of the two bands is
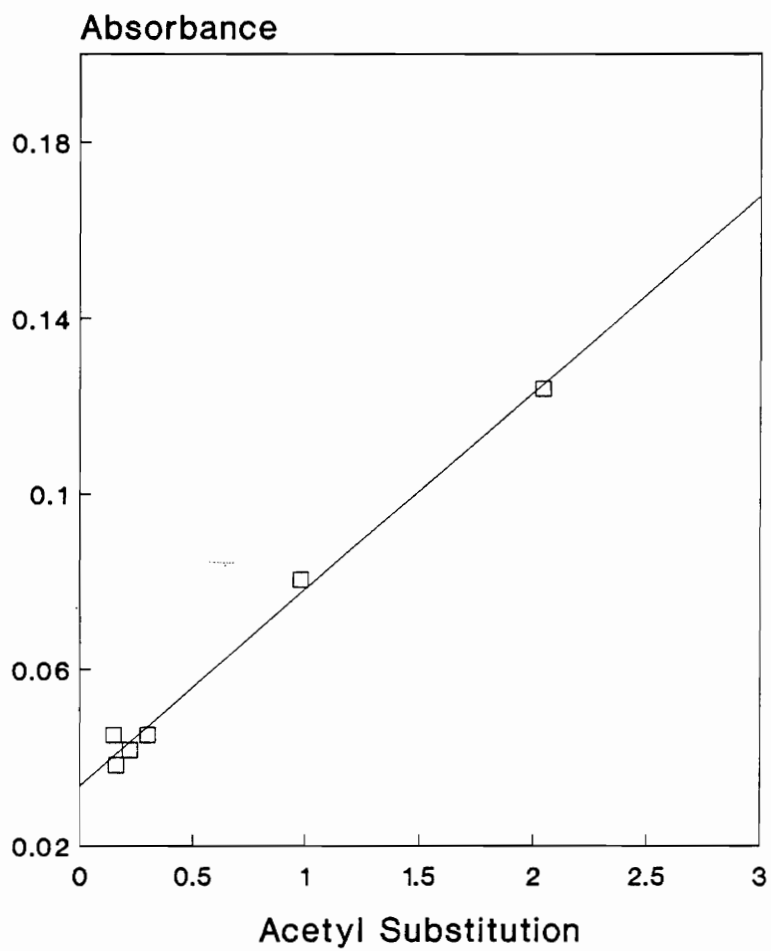
Figure 46. Infrared absorbance at 1235 cm^{-1} versus
degree of acetyl substitution
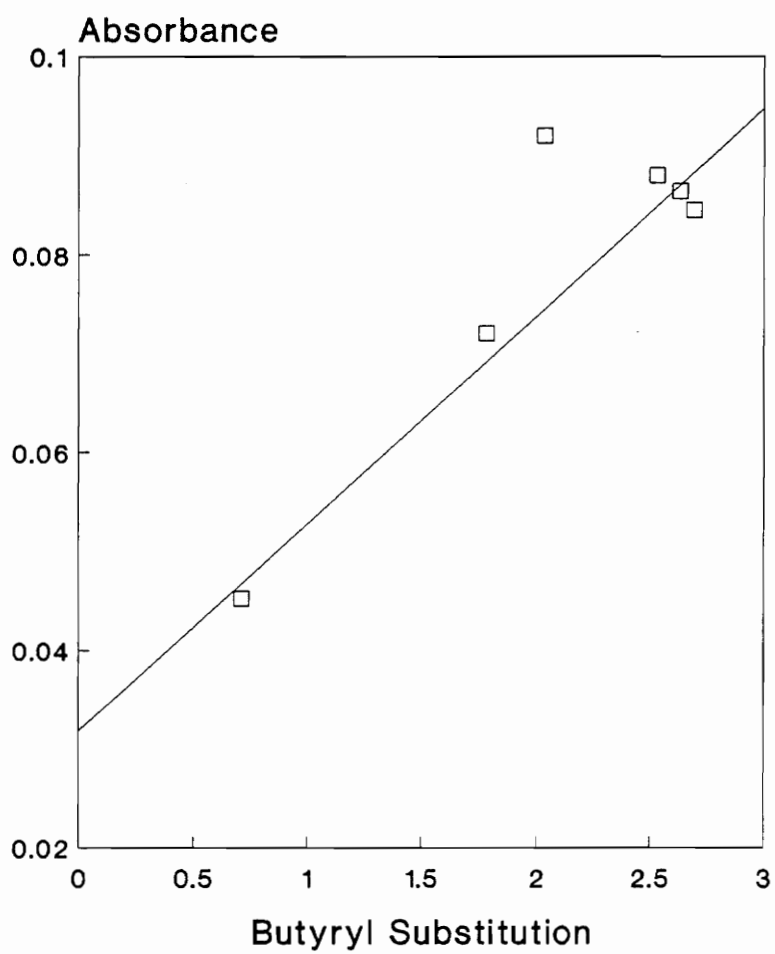
Figure 47. Infrared absorbance at 1176 cm^{-1} versus
degree of butyryl substitution

FREQUENCY, cm-1 x 10-3

Carbons in Side Chain
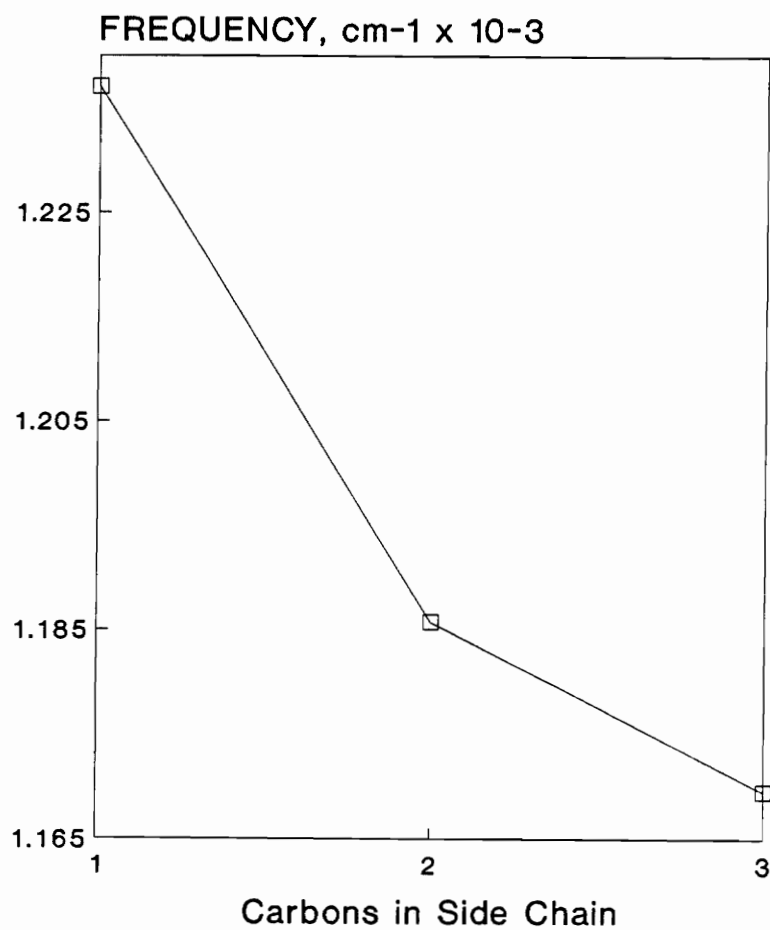
Figure 48. Trend in C - O - C absorption frequency
as a function of the ester group side chain
length, expressed in carbon atoms
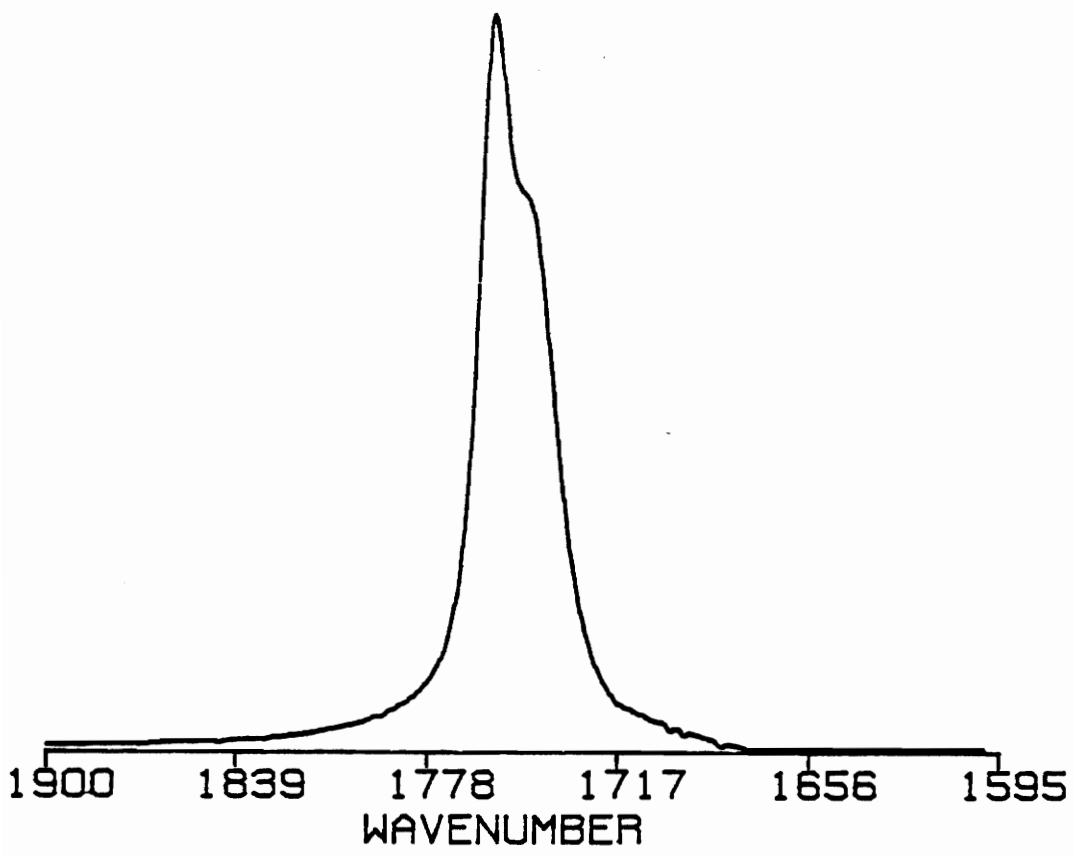
Figure 49. Infrared spectrum in the carbonyl region of
CAB 171 in acetonitrile
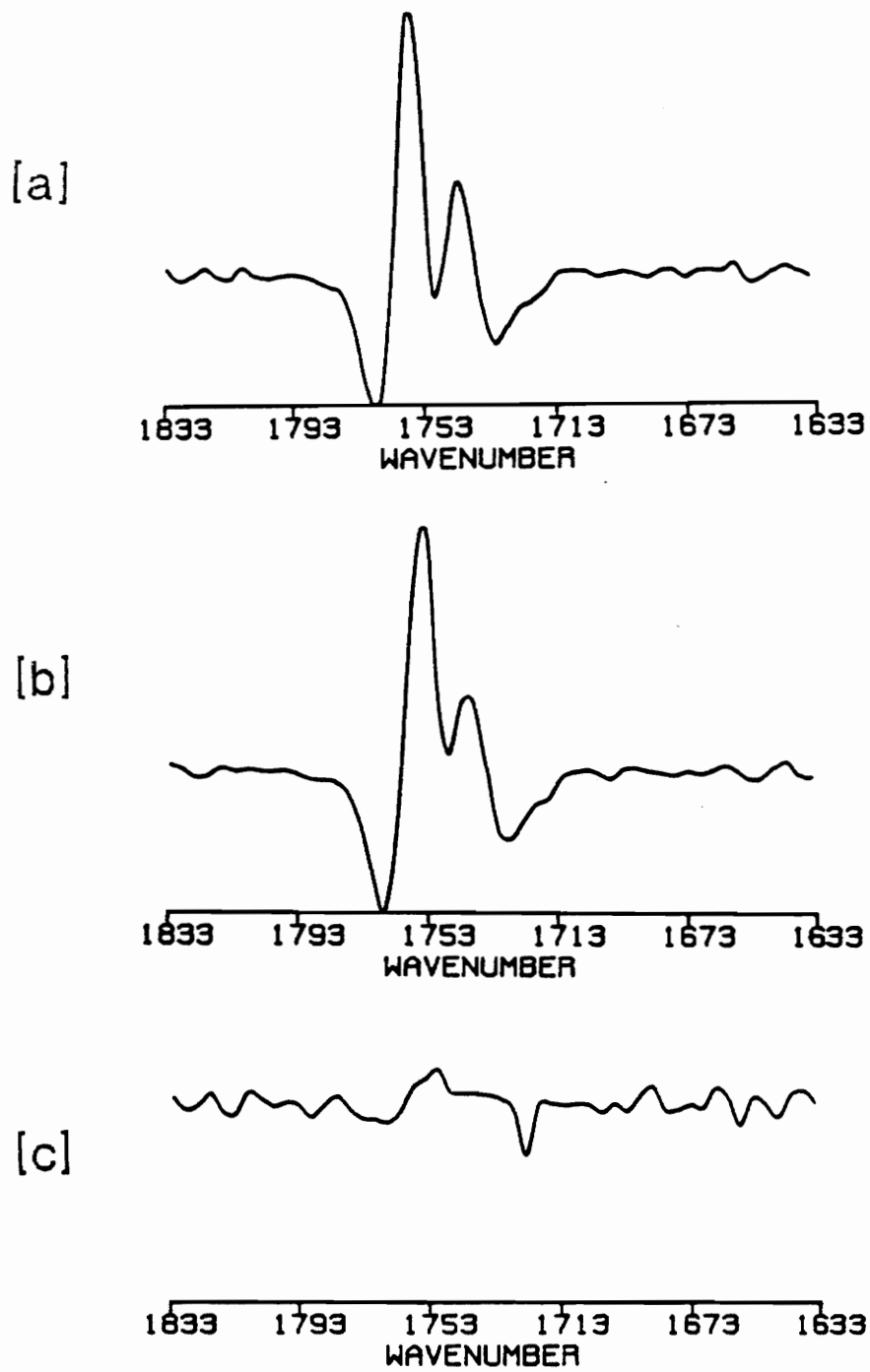
Figure 50. Second derivative spectra of CABs 171 [a], 381 [b], and 500 [c]
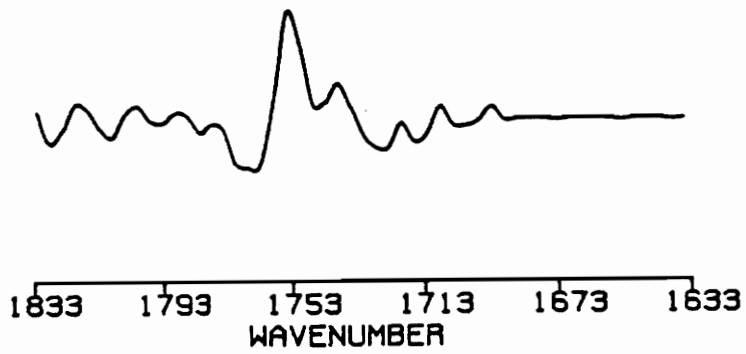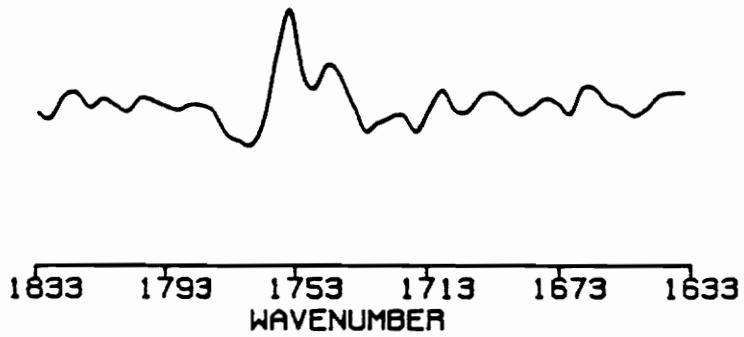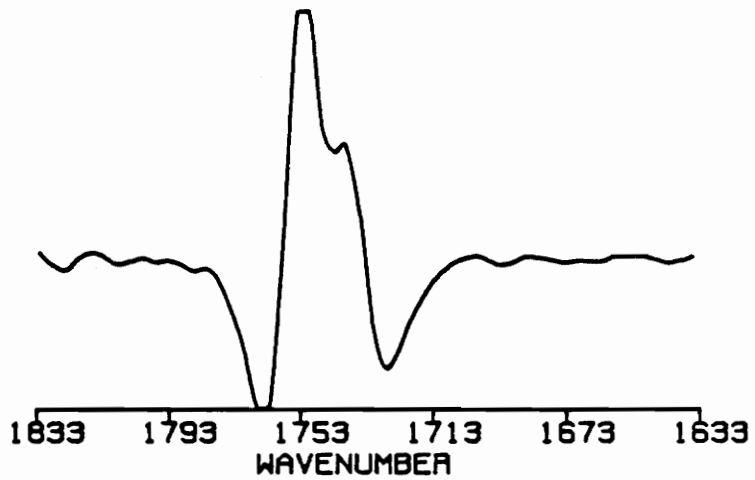
Figure 51. Second derivative spectra of CABs 531 [a],
551 [b], and 553 [c]

dependent upon the CAB substitution. The CAB 553 shows
little additional resolution while the 171, 381, 531,
and 551 show two distinct bands. The CAB 500 has such
poor SNR in the second derivative that no assessment
can be made. An evaluation of the relative amounts of
the two peaks may give some indication as to the nature
of each absorption. Measuring the peak heights on
baseline corrected spectra, and peak areas by also
measuring the peak width where possible (at 70 % of
peak height for those examined), the results shown in
Table XI were found. They are inconclusive, as there is
no trend or relationship to the degree of each ester
substitution, total substitution, or even positional
substitution (one primary versus two secondaries). From
visual observation of the second derivative spectra,
the only trend noted is that the hydroxyl content
influences the amount of resolution.

Solvent Influence

Following these observations, a further study was
designed to determine if the solvent of choice was
influencing the infrared spectra. These studies were
carried out by direct injection of the sample solutions
into the flowcell and collecting the spectra at 2 cm^{-1}

Table XI

Peak Height and Peak Area Ratios For The Carbonyl

Bands From The Second Derivative Spectra

Cab Type	Height Ratio	Area Ratio
171	2.04	1.57
381	2.10	1.89
531	2.07	2.07
551	1.79	1.57
553	1.59	

resolution. The solvents compared were THF, acetonitrile, and methylene chloride. Recall from Chapter 2 that THF and acetonitrile have different donor and acceptor properties. Methylene chloride has similar acceptor properties as acetonitrile, but its donor capability is unknown[102].

Figure 52 shows the trend of the principal carbonyl frequency as a function of the acetyl substitution for all three solvents. In THF there appears to be no correlation with substitution, either acetyl or otherwise. In acetonitrile and methylene chloride, however, there does appear to be a correlation of the carbonyl position and the acetyl substitution of the CAB, and the position in these solvents is different than that in THF.

This sort of solvent influence has been observed previously for carbonyl containing compounds. Wohar and coworkers examined the solvent influence on the shift of the carbonyl band frequency in tetramethylurea[114]. They found a linear correlation between the shift of the frequency with the acceptor number of the solvent. Nyquist and coworkers found a discontinuous relationship when they compared the carbonyl shift of acetone with solvent acceptor number[115]. Studying additional ketones, they came to the conclusion that bulk dielec
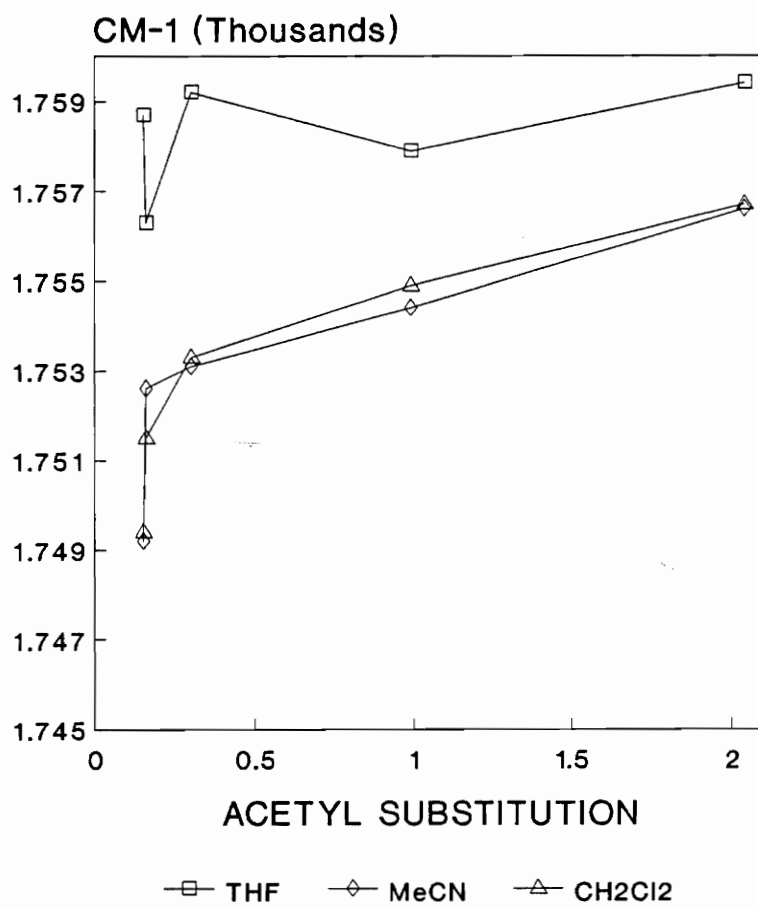
Figure 52. Carbonyl absorption frequency as a function
of acetyl substitution

tric properties of the solvent system are responsible for the observed shifts[116,117]. In addition, they found concentration differences of less than 10 weight percent of solute also influenced the observed shifts[118].

To examine the nature of the interactions occurring we can again turn to Gutmann's concept of the donor/acceptor system and Hammett's and Taft's interaction parameters. Recalling the donor concept from Chapter 2, we can examine the solvent influence on the carbonyl absorption frequency. In this system though, the CAB ester groups are the better donor. The carbonyl moiety is in general a good donor, hence the observed linear relationship of Wohar, et al. of the carbonyl shift with solvent acceptor numbers[114]. From Table III, the acceptor number of THF is much lower than that of acetonitrile, and methylene chloride has an acceptor number very close to that of acetonitrile (20.4). This would suggest that with a good donor solute such as CAB, there would be greater interaction with the solvents acetonitrile and methylene chloride than with THF. This is in fact what is observed. Because there is less interaction with THF as the solvent, the carbonyl C=O bond is not lengthened as much as with the other two solvents, and the carbonyl absorption frequency is

higher. With the greater interaction between the CAB and a better acceptor solvent the C=O bond length is increased and the carbonyl absorption frequency is lowered.

The nonlinear trend of absorption frequency versus acetyl content in acetonitrile and methylene chloride is even more interesting. Recall that the C-O-C absorption frequency of esters is influenced by the type of ester present. It appears that in the presence of a good acceptor solvent, with its greater interaction with the CAB, that the ester type also influences the C=O absorption frequency. To confirm this we can apply the Hammett equation using Taft's σ^* parameter, since it is a measure of a compounds electron donating capability. For the CAB system the Hammett equation would be written as:

$$v_i - v_o = p(\alpha\sigma^*_{acetate} + \beta\sigma^*_{butyrate})$$

since the solvent parameter p is independent of the solute. The parameters α and β are the mole fractions of acetyl and butyryl groups, taken as the percent of total substitution. Since it is the influence of the side chain length which is under study, σ^* values for a methyl group (acetate) and propyl group (butyrate) are

needed. Shorter gives values for these as 0.00 for methyl and -0.115 for propyl[101]. Since the methyl influence is the reference value for the series, it is appropriate to assign the frequency of the greatest acetyl containing CAB as v_o, which is the 171-15s. Since this CAB has the highest absorption frequency, all values for $(v_i - v_o)$ are negative. The graph of this equation is shown in Figure 53. Note there is one point which falls well below the others. This point is for the CAB 553, the one which contains 3 hydroxyls per 4 glucose units, where the others contain only 1 or no (CAB 500) hydroxyls per 4 glucose units. This would suggest that there is more intramolecular hydrogen bonding between the additional hydroxyls and the CAB ester groups, since the C=O frequency is lowered to a greater extent than would be predicted.

In conclusion, these studies have shown the observance of individual C-O-C IR bands for the ester types contained within a CAB, while only one C=O IR band. This band was also shown to be a combination of two overlapping frequencies, in a manner similar to the asymmetric nitrate stretch of CN. The overlapped bands are probably the result of steric interactions of bulky acyl groups on adjacent secondary sites in the same manner as the nitrate groups from Chapter 2, and also
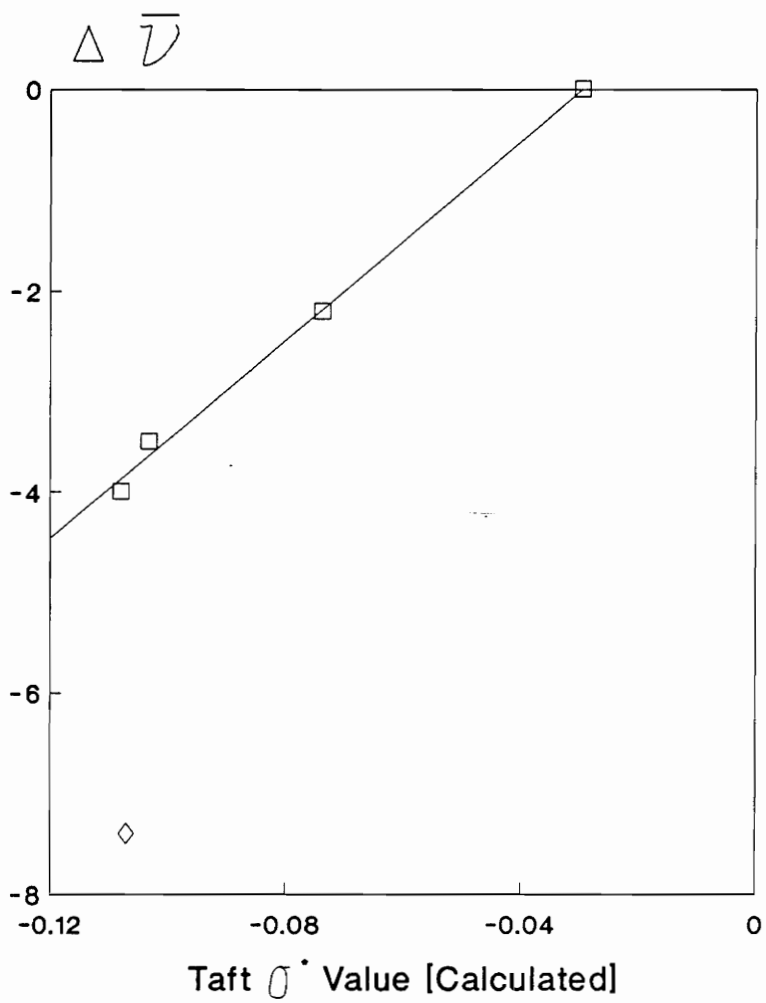
Figure 53. Hammett plot for CABs in acetonitrile

from more extensive solvent interaction, as was learned in this Chapter. The extent of solvent interaction with a CAB has been shown to be dependent upon the donor/acceptor properties of the solvent. In addition, in a good acceptor solvent, the influence of the ester type and intramolecular hydrogen bonding can be observed and measured.

Chapter 5

Applications of GPC/FT-IR

To Cellulosics

Introduction

Several applications where infrared detection was coupled to GPC were described in Chapter 1. These included using discrete infrared absorptions to spectrally identify eluting components[73,77], measurement of specific functional groups contained within a polymer as a function of the MWD[74], and determination of the MWD of CN by monitoring the 1660 cm^{-1} absorption of the nitrate group[33].

This Chapter focuses upon the development of methods to quantify the substitution of cellulose esters as a function of the MWD. The objective is to develop methods which might profile the homogeneity of commercial polymers. Typically only the average degree of substitution for a whole polymer is determined and homogeneity is assumed.

The first part deals with the degree of nitration in several commercial CNs. These fall into two categories of commercial propellant formulations: single and double base. Single base propellants are those which contain only cellulose nitrate, while double base propellants contain both cellulose nitrate (CN) and nitroglycerine (NG) as major ingredients.

The second part deals with the degrees of acetyl
and butyryl substitution of several commercial CABs. In
the one case the issue of the origin of the cellulose
raw material is examined. Cellulose is obtained commer-
cially from both cotton linters and wood pulp. Cotton
linters are the "fuzz" left on the cotton seed after
the cotton fibers have been removed. The major differ-
ences between the two sources is the amount of alpha,
or "pure", cellulose and the degree of polymerization.
The second example of a CAB application is the determi-
nation of the DS in a CAB contained in a LOVA propel-
lant. LOVA stands for low vulnerability ammunition, and
the propellant is designed to reduce spontaneous igni-
tions.

Experimental

The chromatographic system for all studies con-
ducted here consists of a Perkin Elmer LC-10 HPLC pump
and a single Perkin Elmer PL-gel mixed bed GPC column
(Perkin Elmer Corp., Norwalk, CT.). The mobile phase
for the CN work was HPLC grade THF and for the CAB work
HPLC grade acetonitrile (Fisher Sci., Raleigh, N.C.).
All chromatography was performed with a 1 mL/min.
flowrate.

The infrared spectra were collected on-line using a Nicolet 5SXC FT-IR fitted with an in-line multipath-length flowcell (Nicolet Instr., Madison, WI.). Acquisitions were performed with the standard GC/IR software, yielding 8 cm^{-1} resolution and collecting 4 scans per data file. One data file was collected each second of the chromatographic run. Where applied, spectral deconvolution was accomplished by the second derivative technique. Peak heights were measured on baseline corrected absorbance spectra.

The CN samples were obtained from two sources. The double base propellants were obtained from the Naval Surface Warfare Center (NSWC), Indian Head, MD. The single base propellants were obtained from the Naval Ordnance Station (NOS), also located in Indian Head, MD. The CABs prepared from different celluloses were obtained from NSWC and the LOVA propellant from NOS. All samples for GPC were prepared to a polymer concentration of 0.2 % wt./wt., allowed to stand for two days at room temperature, and filtered prior to analysis.

Results and Discussion

Applications of Quantitative GPC/FT-IR to Propellants

Propellant formulations incorporate CN in varying
amounts as the principal binding agent. Single base
propellants are $\approx$ 90 % CN, while double base material
is $\approx$ 45 % CN and $\approx$ 45 % NG. The studies conducted here
focus solely upon the CN contained in the propellants.

In the production of double base propellants, the
NOS began having problems extruding newer material.
This problem coincided in time with a change in the
manufacturing process for CN. The manufacturers of CN
had switched from a batch nitration process to a con-
tinuous one. Though the average DN and MWD of the CN
met specifications, the CN was still thought to be the
source of the problem. Thus a program was designed to
develope methods which identify changes which might
exist in the CN contained in extrudable and non-
extrudable propellants.

Devlopment of the Method

In Chapter 2 it was shown that the asymmetric
nitrate absorption at 1663 cm^{-1} increased linearly with

increasing DN. This served as the basis for several early proposed methods for quantifying CN, but suffers in that polymer concentrations must be carefully controlled. During a chromatographic run the polymer concentration in the flowcell is constantly changing. Any useful method for GPC/FT-IR thus must remove this concentration dependance. This can be accomplished by taking advantage of the improved resolution acheived by spectral deconvolution. With the second derivative technique sufficient resolution between the high and low energy components of the asymmetric stretch is acheived to allow integration of the peak areas by triangulation. This is illustrated in Figure 54 for a 2.32 DN CN. The peak height in absorbance is multiplied by the peak width at half height for each component of the spectral band. The ratio of the high energy component to the low energy component is then calculated for a range of CNs of differing DN. A plot of these ratios as a function of the DN is shown in Figure 55. Since only CNs of DN greater than 2 were available, the standard curve generated by this technique has no applicability below this value.

During a chromatographic run spectra are being collected and stored each second. The SNR of the spectra can be improved by the co-addition of 10 files and
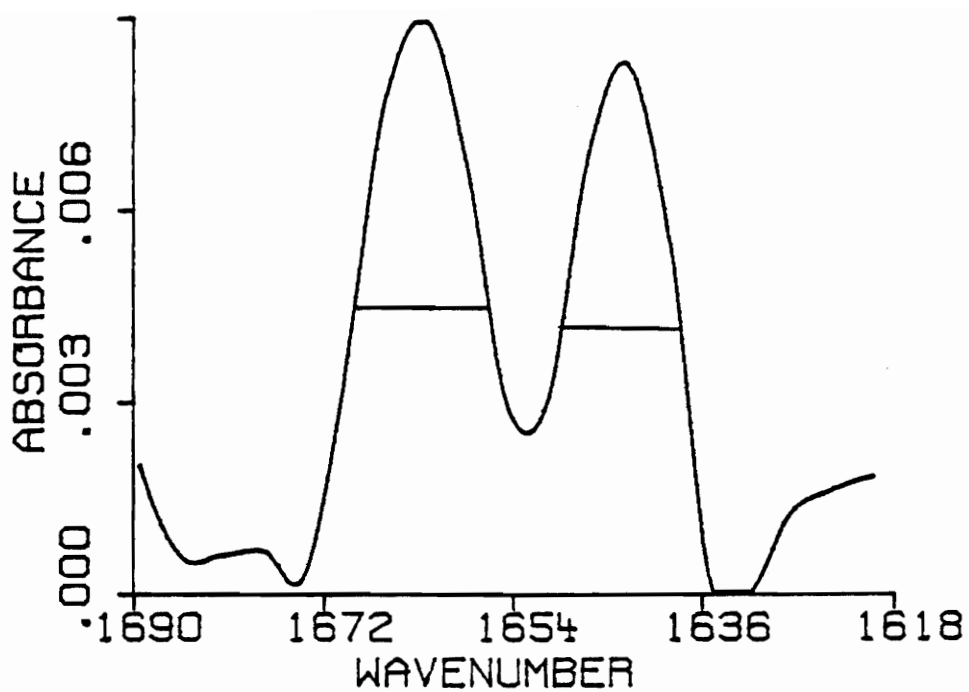
Figure 54. Illustration of integration of a second
derivative spectrum
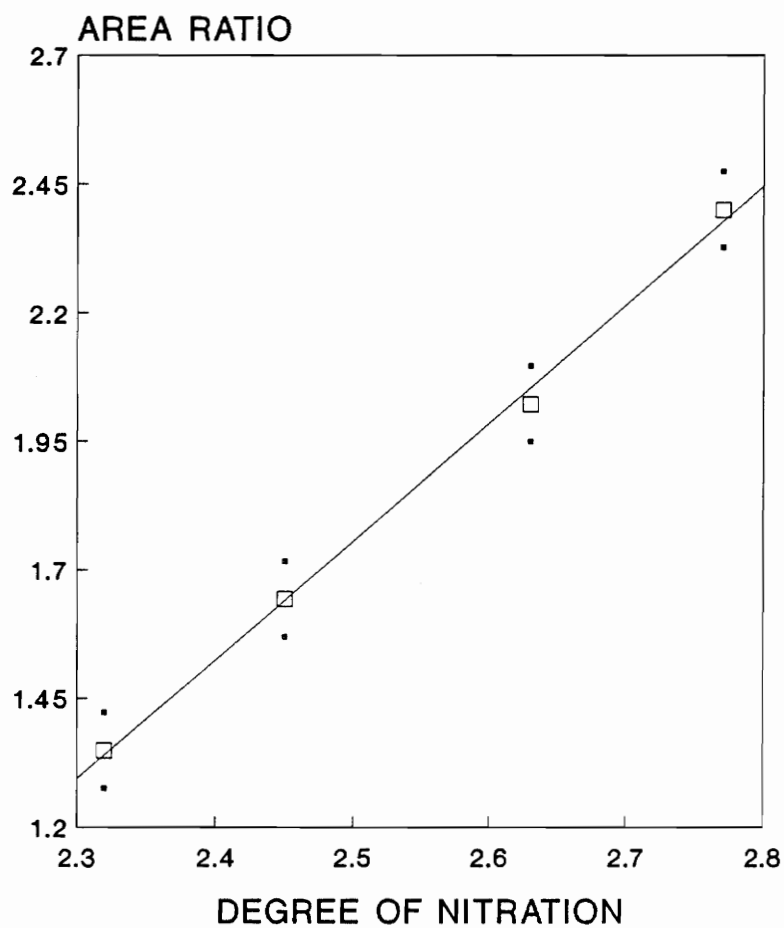
Figure 55. Area ratios of second derivative spectra of
1663 cm^{-1} to 1647 cm^{-1} versus CN DN

storing this result. In a typical GPC peak, which is often over two minutes wide in this system, this still affords the selection of several regions within the chromatographic peak for analysis. By calculating the area ratios from different data files within the peak and comparing to the standard curve, the DN through the GPC peak can be evaluated.

Double Base Propellants

With the method established, the DN within a GPC peak of the extrudable and non-extrudable propellants can be determined and compared. Table XII lists the set of double base propellants examined. They consist of two sets of material of two levels of nitration. Figure 56 shows the GPC traces of the AA-2 propellants, which were prepared with 2.32 DN CN. No real difference appears to be present in the chromatography. Figure 57 shows the calculated DN of several data files through the chromatographic peak. The dots above and below the points plotted represent the 95 % confidence interval using t statistics. Note that there is no difference here either. In fact these two propellants appear to be homogenous throughout the MWD, and the DN is what was expected.

Table XII

Double Base Propellants Examined

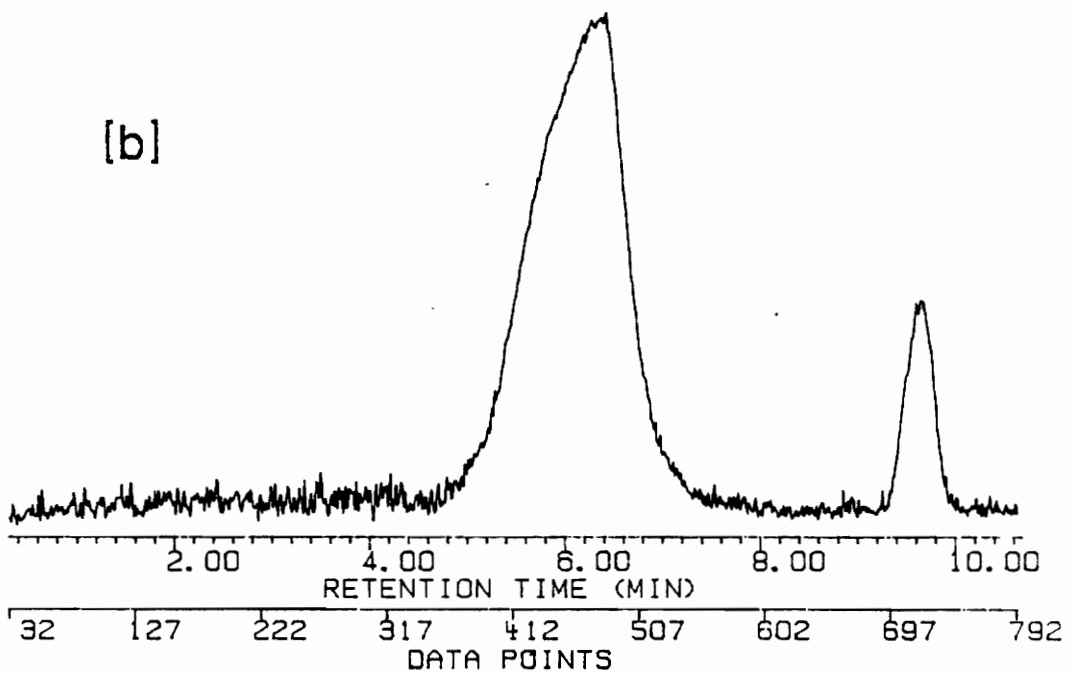| Type	Identification	DN	Extrubability
AA-2	RAD 87	2.32	extrudable
AA-2	RAD 84	2.32	nonextrudable
AA-6	RAD 87	2.37	extrudable
AA-6	RAD 84	2.37	nonextrudable

Figure 56. GPC chromatograms of AA-2 propellants RAD 87 [a] and RAD 84 [b]
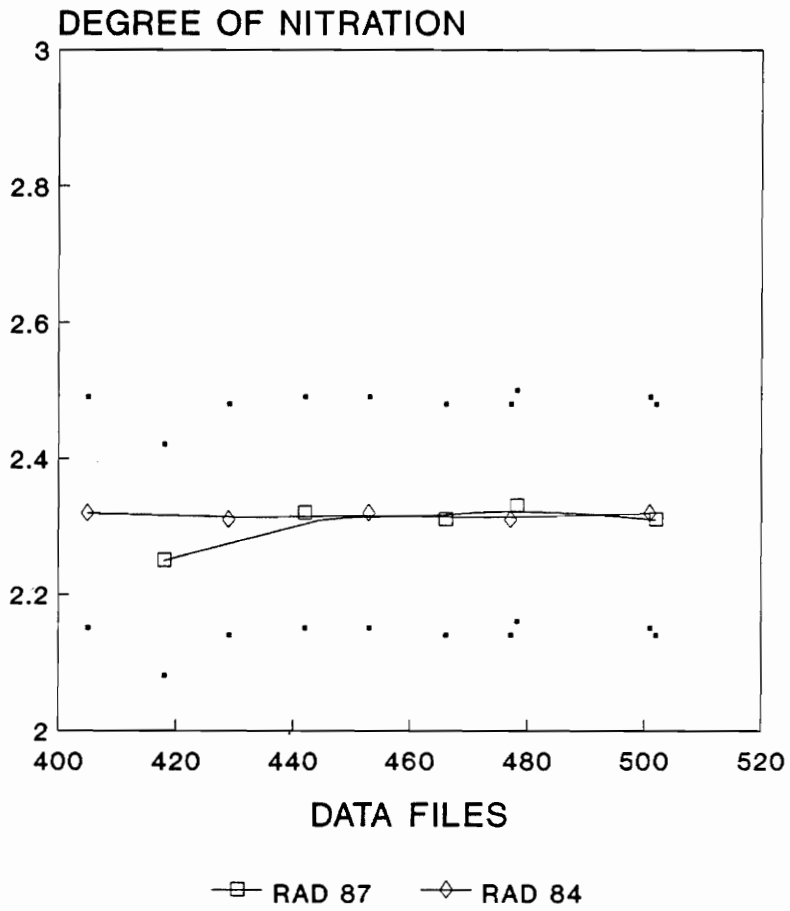
Figure 57. Degree of nitration within the GPC peaks of AA-2 propellants

Figure 58 shows the GPC traces for of the AA-6 propellants, which were prepared with 2.37 DN CN. There is a slight difference in the shapes of the two peaks, indicating a small difference in the MWD. Whether this difference affects processibility is uncertain, since the propellants were processed three years apart, and this may only reflect the age difference. Figure 59 shows the calculated DN through these peaks. Note that while the extrudable, RAD 87, sample averages consistently lower than the nonextrudable sample, the difference is not statistically significant.

Single Base Propellants

The single base propellants examined were part of a long term study on the stability of propellants as determined by accelerated aging. Accelerated aging of propellants is accomplished by heating the propellant to 65.5 $^{\circ}$C for periods of days, which can be used to estimate stability of the material in years. The particular materials examined have shown unusually long term stability and it was of interest to determine why so that future formulations might include this stabilizing feature.
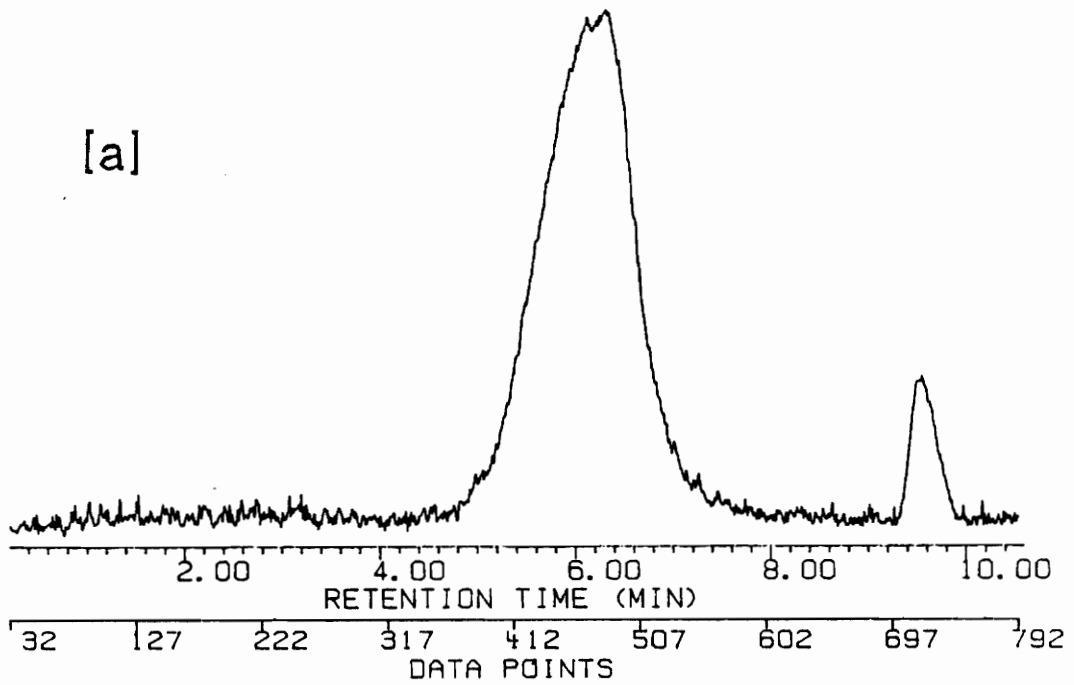
Table XIII lists the single base propellants

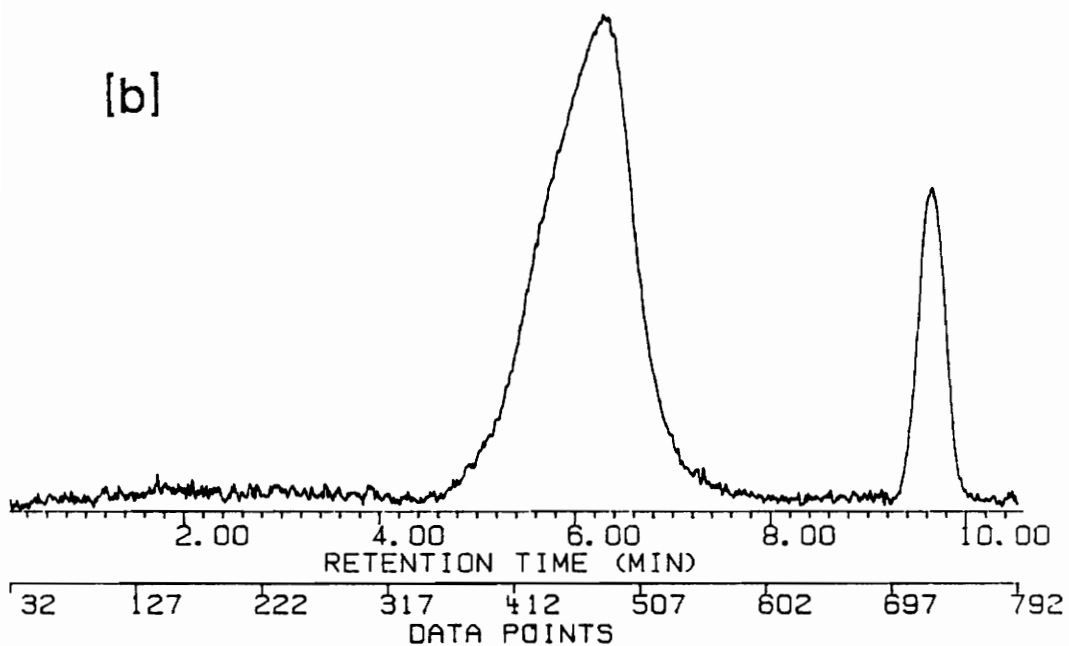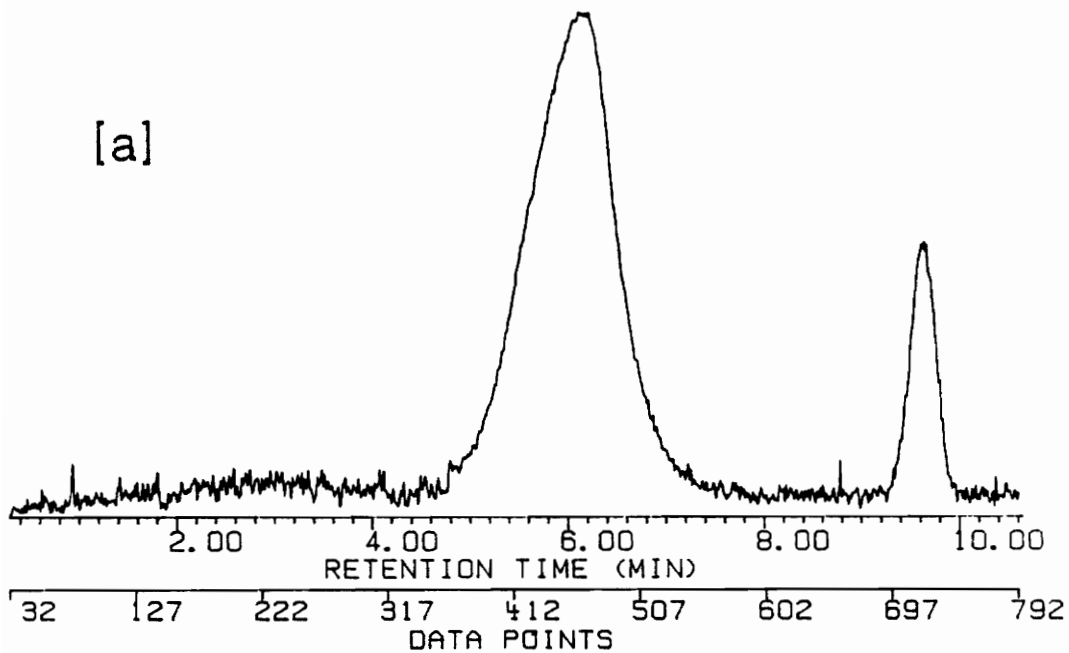Figure 58. GPC chromatograms of AA-6 propellants RAD 87

[a] and RAD 84 [b]

168
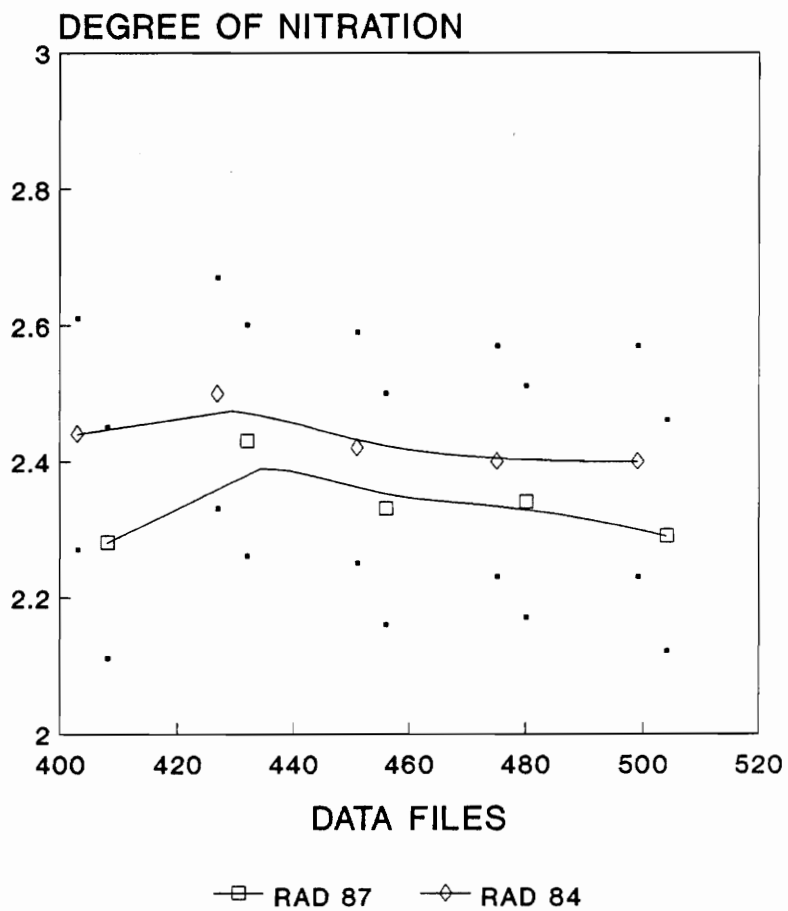
Figure 59. Degree of nitration within the GPC peaks of
the AA-6 propellants

Table XIII

Single Base Propellants Examined

Identification	CN Base	Days Heated
3582	cotton linter	310
4022	wood pulp	615
4021	wood pulp	915
4147	cotton linter	1230
4260	cotton linter	1500

examined. Due to the age of these materials (all were produced ≈ 1943), samples of the starting materials were unavailable, so an unheated sample of each was used as a control sample. Also included in the Table is a column designating the base material used in the production of the CN incorporated in the propellant. The source of cellulose used to produce CN has been shown to influence its processibility[119,120]. This is due in large part to the nitration process itself. In nitration, the cellulose never dissolves in the acid reaction mixture. Any differences in crystalline morphology are retained in the nitrated product.

Chromatographic Analysis

Figures 60 to 64 show the GPC traces of the control and heated samples for each single base propellant. They are in sequence according to heating days. Note that in each case the heated sample appears to be shifted to lower molecular weight and to be slightly broadened. This would be expected of a polymer subjected to extended elevated temperature.Since the flowrate was maintained a constant 1 mL/min., the shift in elution time in minutes is equivalent to the change in elution volume in mL. Table XIV lists the shifts for
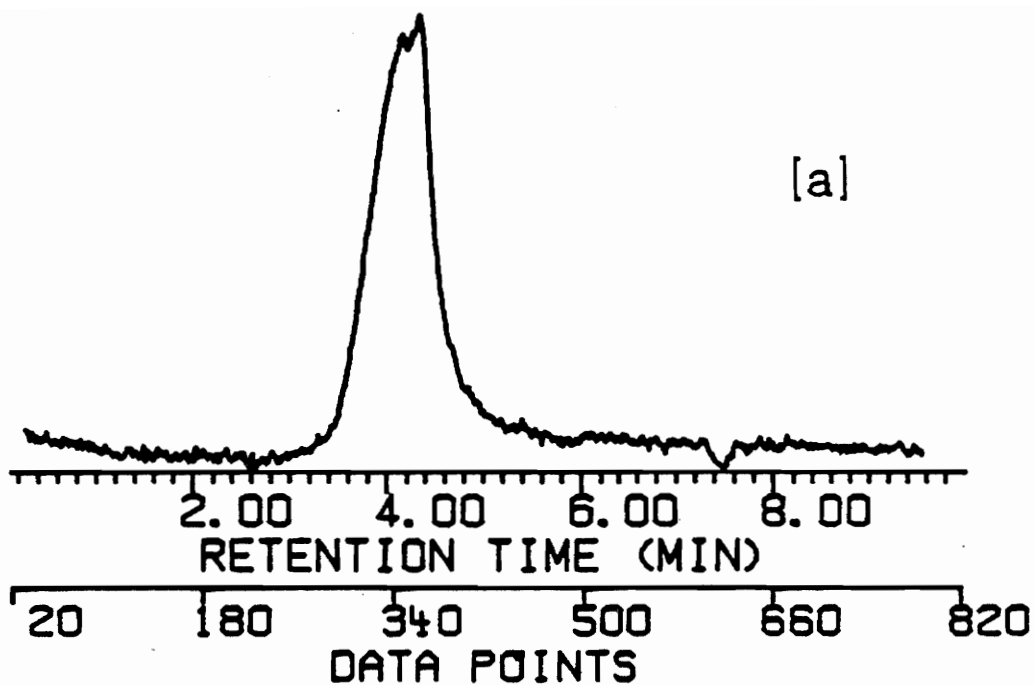
Figure 60. GPC chromatograms of sample 3582 control [a]
and heated 310 days [b]
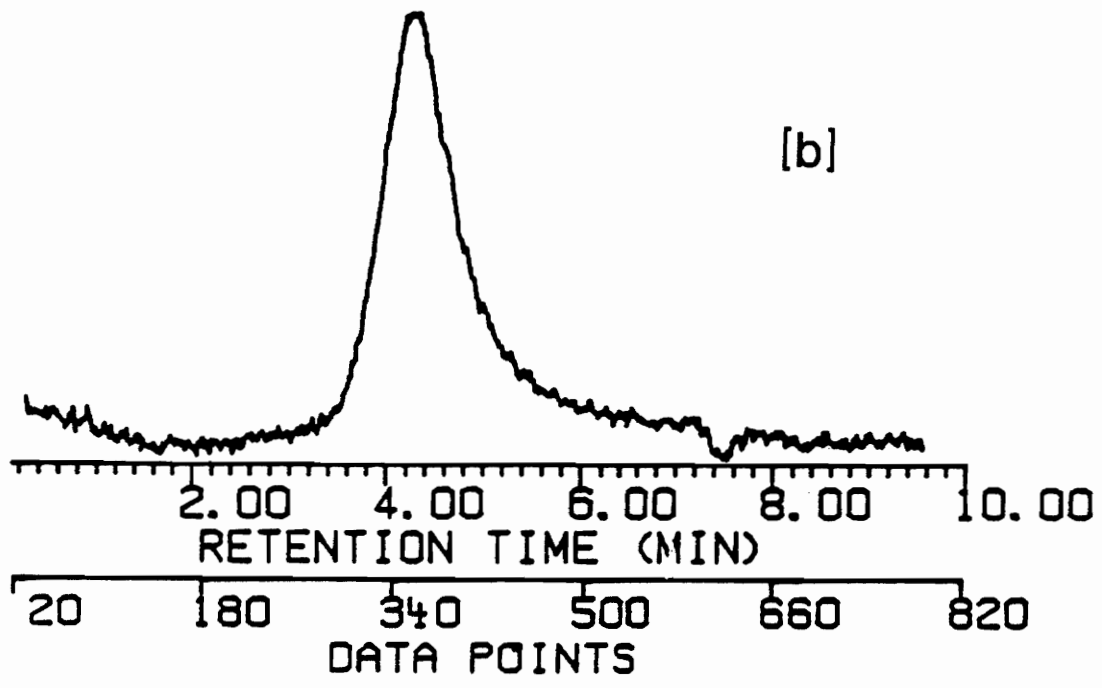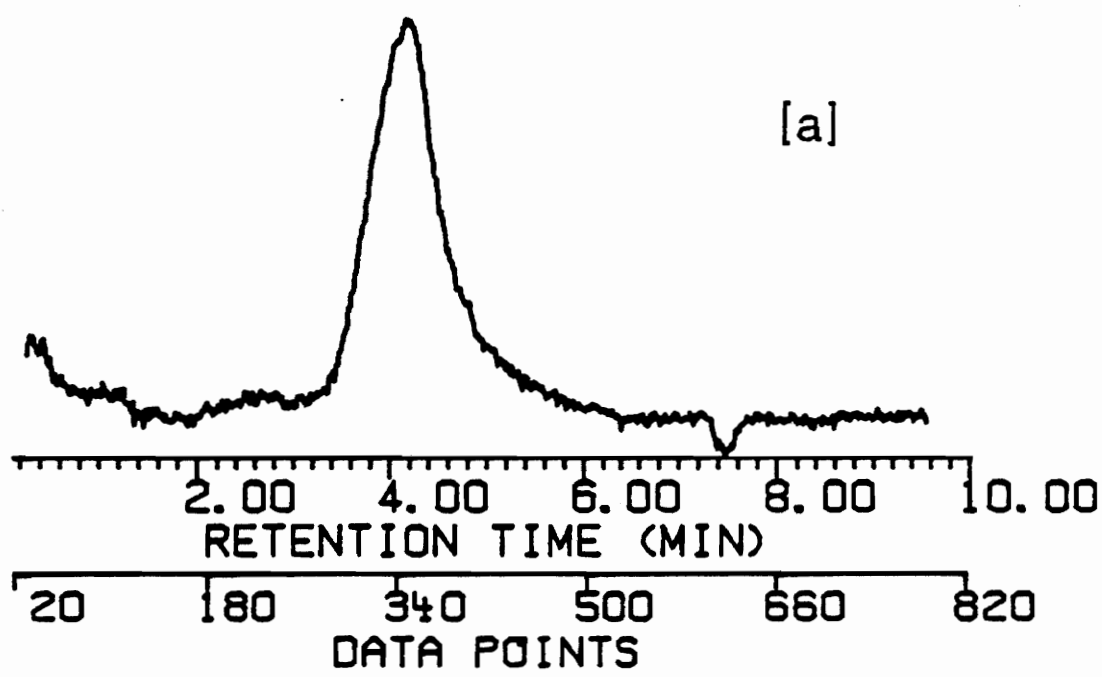
Figure 61. GPC chromatograms of sample 4022 control [a]
and heated 615 days [b]
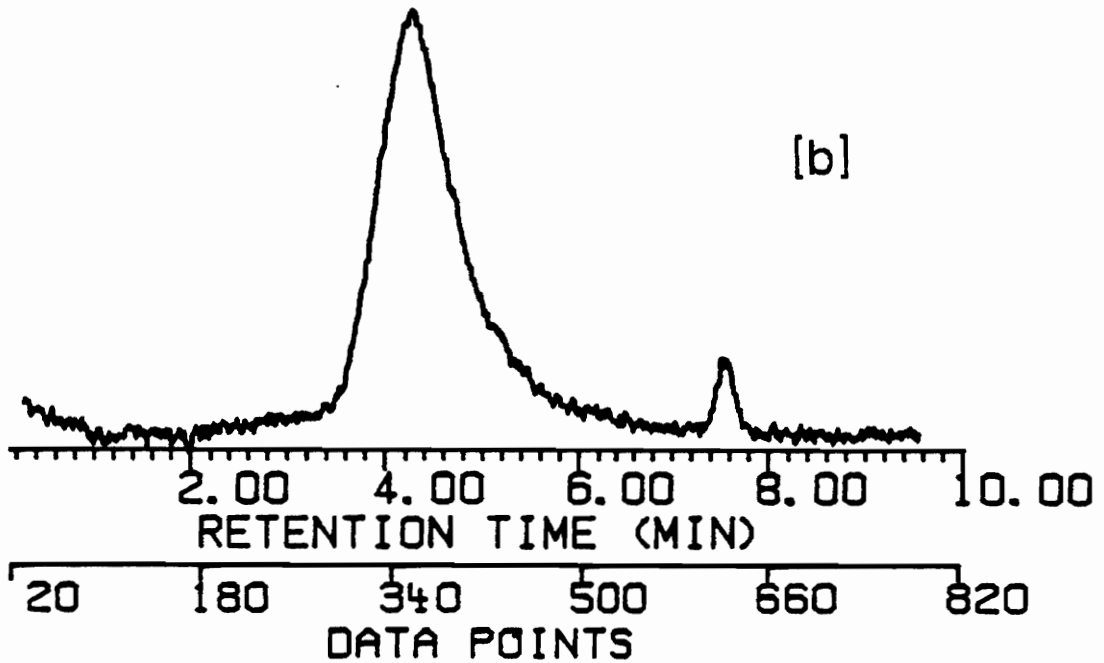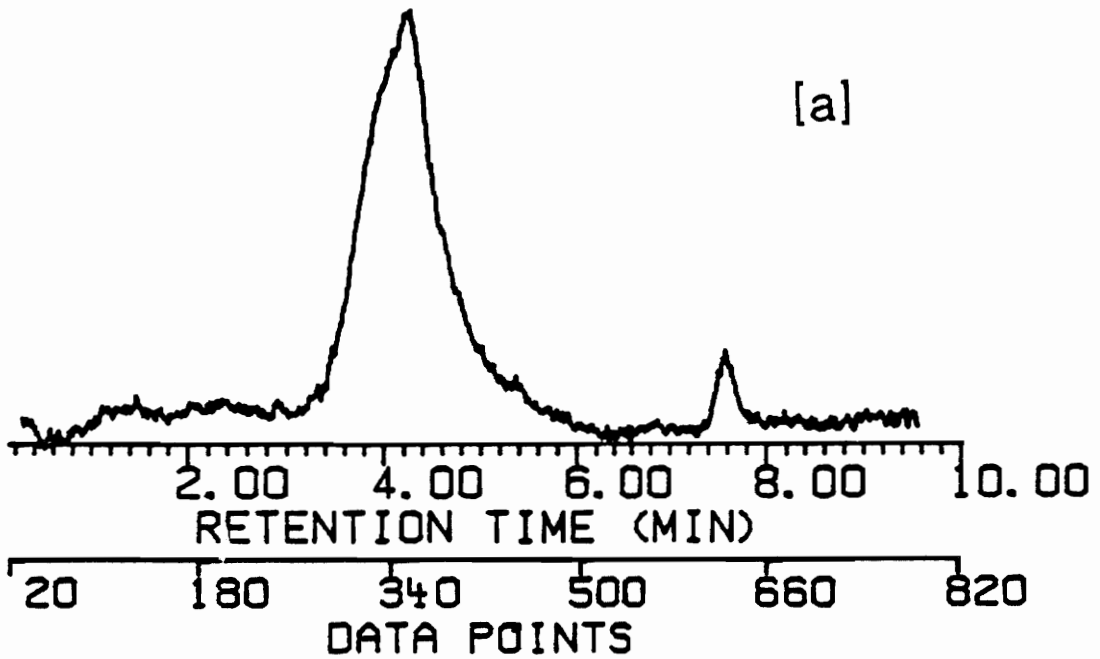
Figure 62. GPC chromatograms of sample 4021 control [a]
and heated 915 days [b]
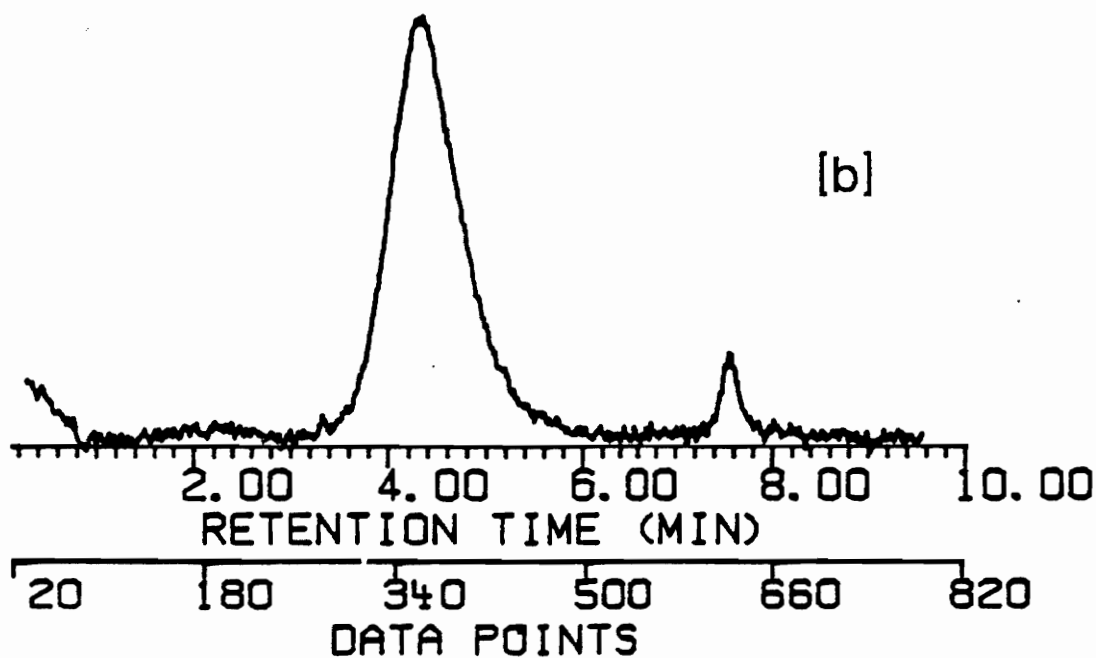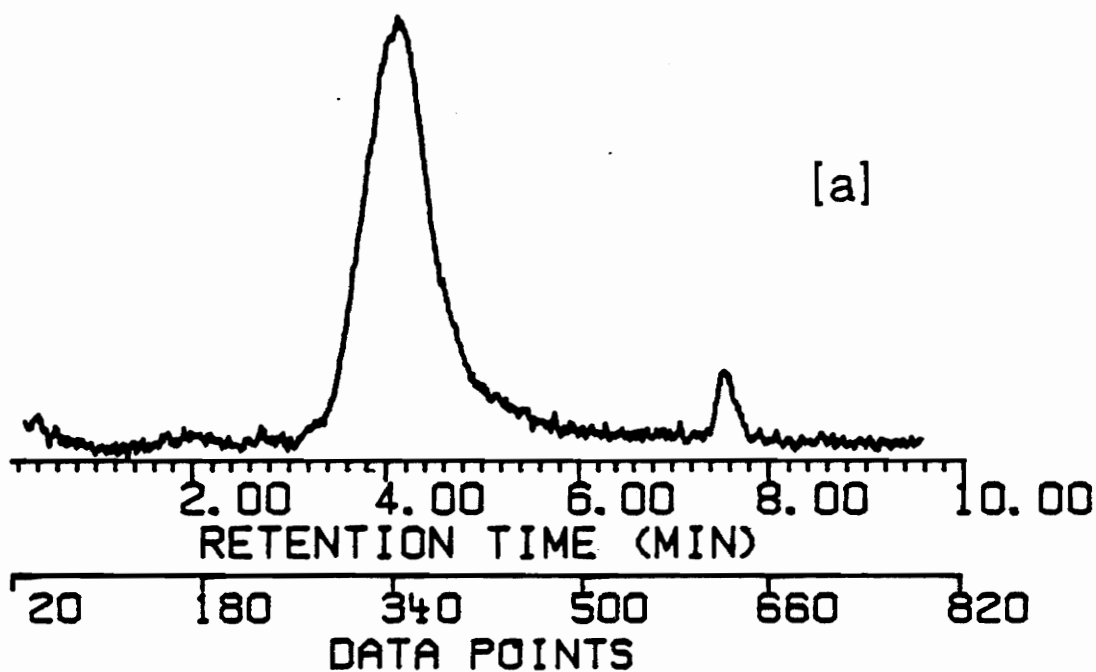
Figure 63. GPC chromatograms of sample 4147 control [a]

and heated 1230 days [b]
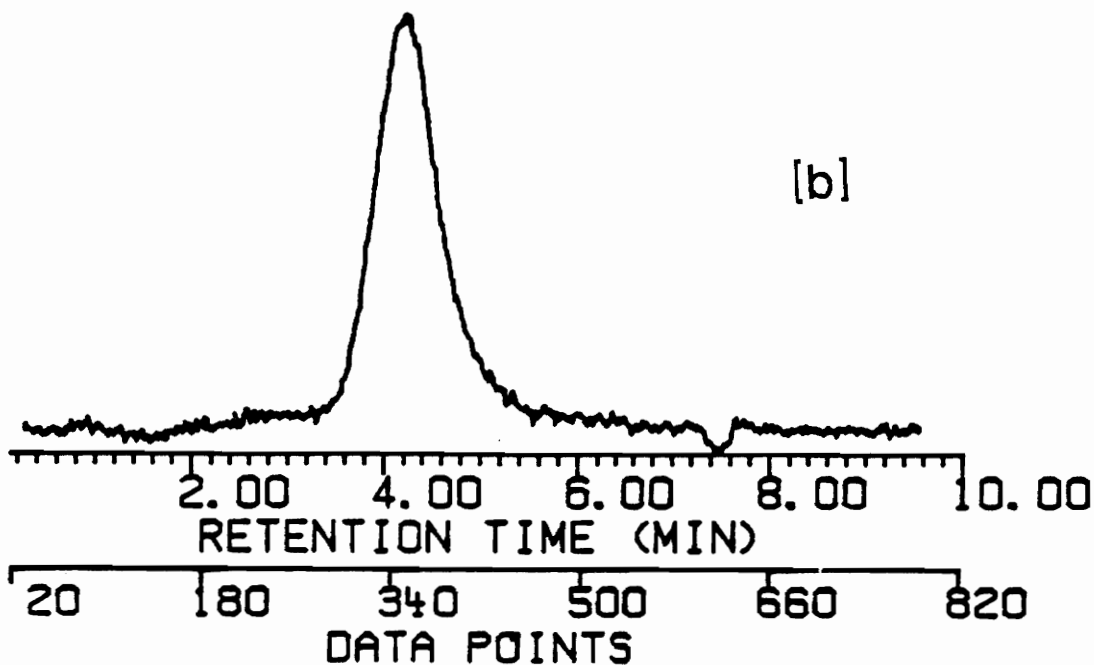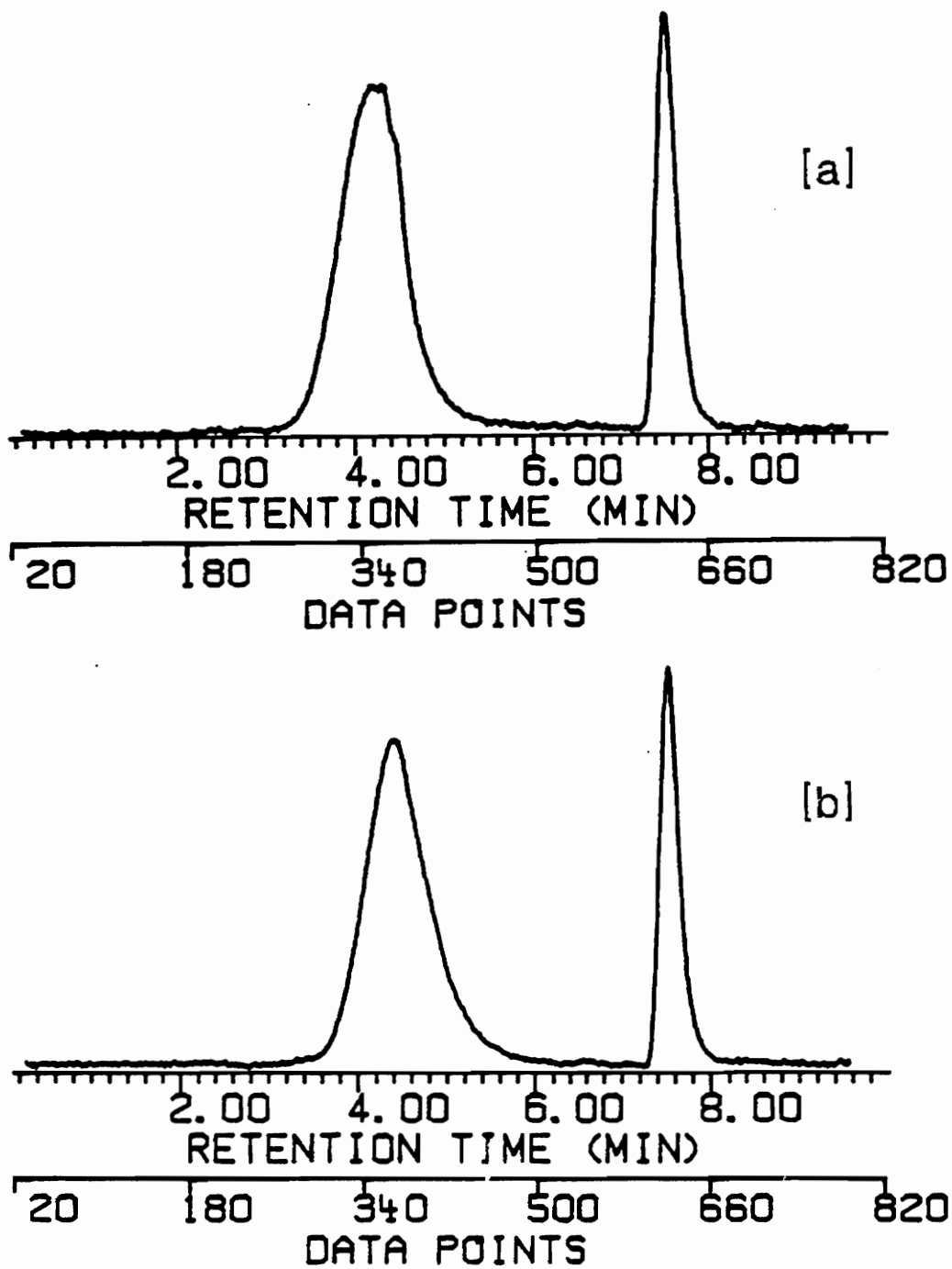
Figure 64. GPC chromatograms of sample 4260 control [a]
and heated 1500 days

Table XIV

Elution Volume Change For Heated vs. Control Samples

Sample	Elution Change, mL.
3582	0
4022	0.08
4021	0.02
4147	0.14
4260	0.14

the peak maxima of each sample. Note that the trend is one of increased elution volume change for samples heated for longer periods.

Spectral Analysis

Following comparisons of the chromatographic traces, a determination of the degree of nitration through each GPC peak was conducted to evaluate any differences which might have occurred. Figures 65 to 69 show the comparisons for the samples in the same sequence as described previously. The dots representing the 95 % confidence intervals have been left out of these Figures for clarity. For sample 3582, heated 310 days, no difference is observed between the control and heated sample. Sample 4022, heated 615 days, shows a drop in nitration for the low molecular weight tail not present in the control. This would indicate that not only is the MWD of the polymer being broadened and lowered, some nitrate groups are being removed at the same time. This trend is even more extensive in sample 4021, heated for 915 days. Here the DN in the central region of the peak is also lower than the control. Sample 4147 shows an even larger difference between control and heated, but the point from the lowest

178
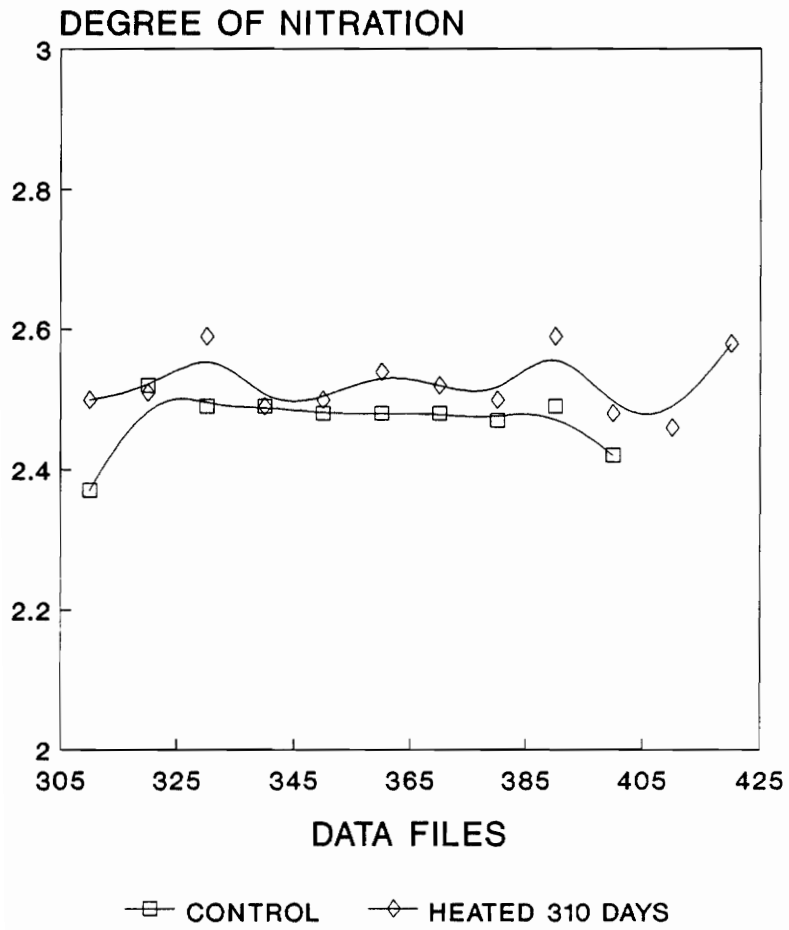
Figure 65. Calculated DN for sample 3582
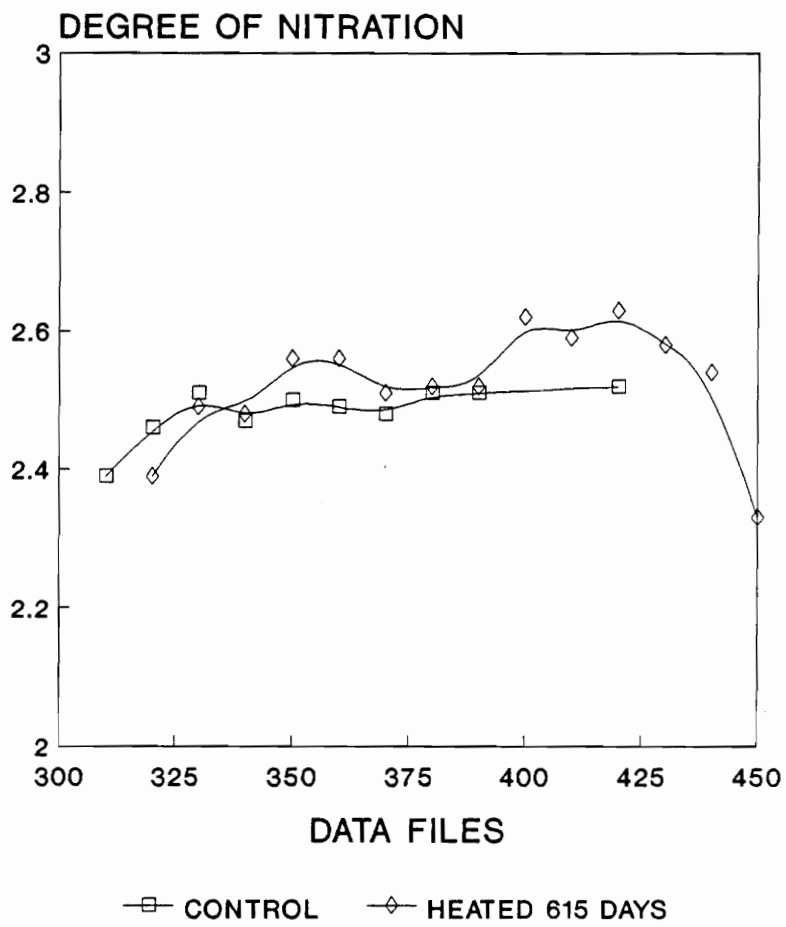
Figure 66. Calculated DN for sample 4022
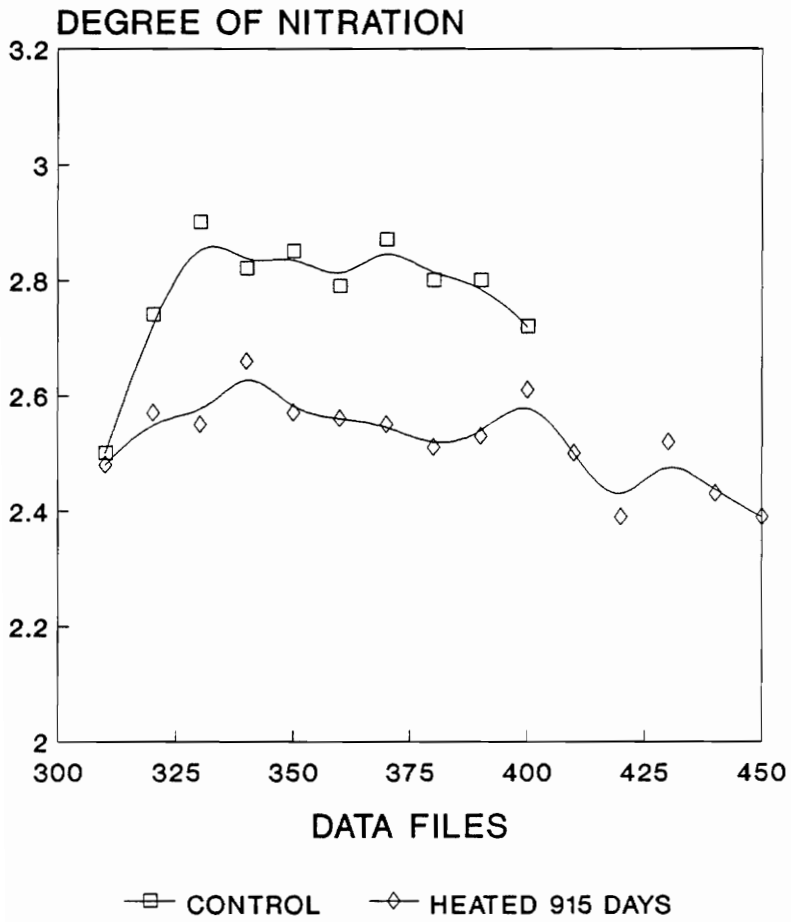
Figure 67. Calculated DN for sample 4021
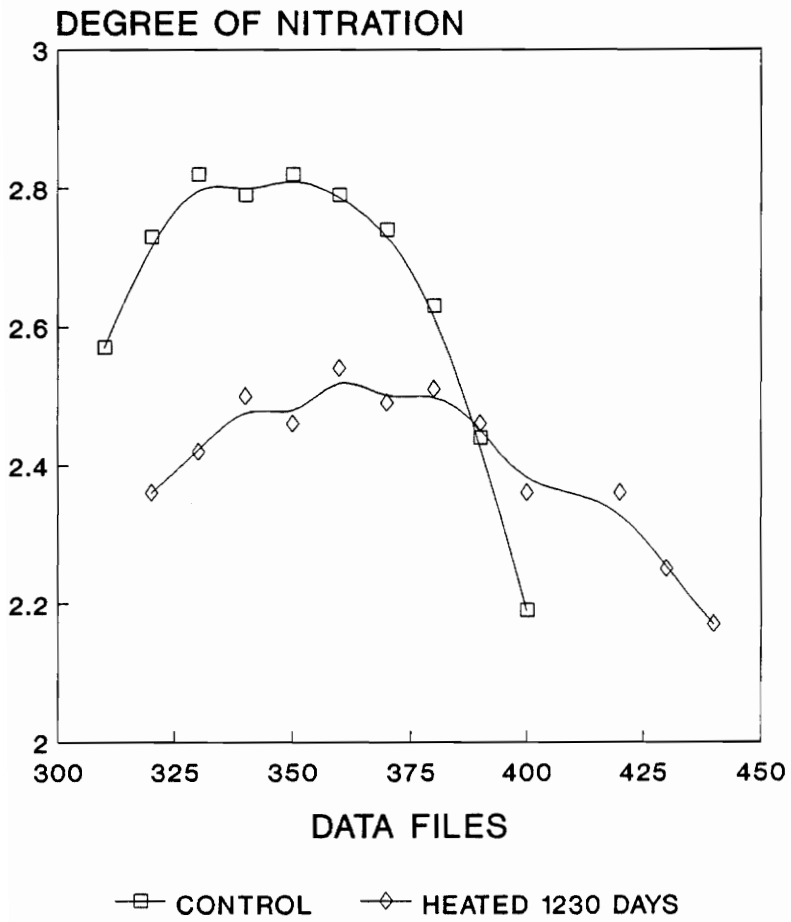
Figure 68. Calculated DN for sample 4147
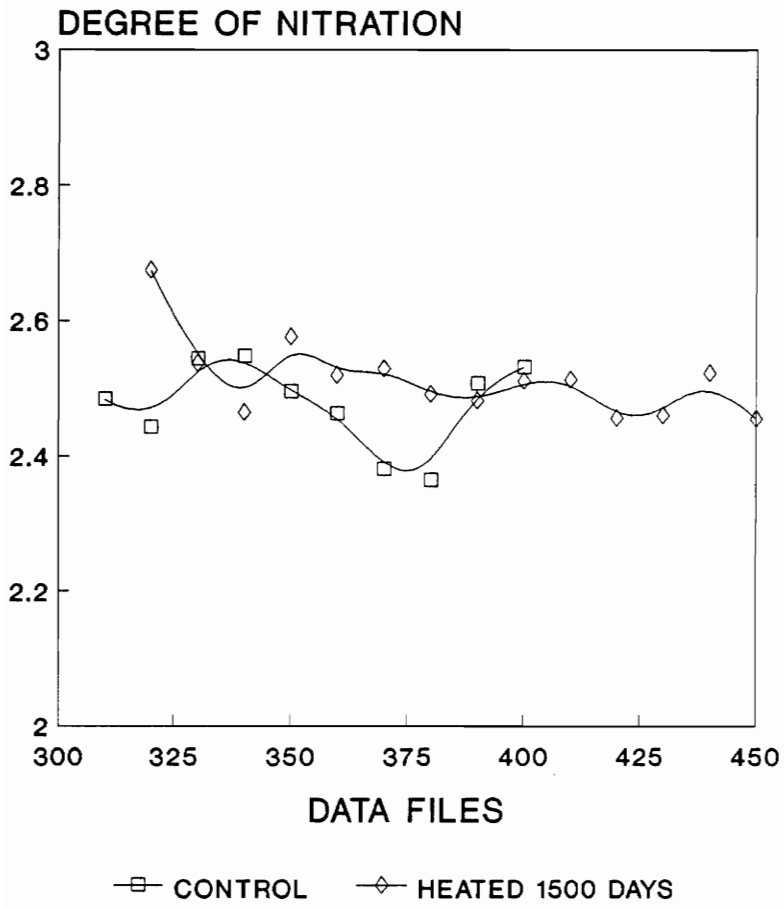
Figure 69. Calculated DN for sample 4260

molecular weight region of the control also dips to a much lower DN. This may have been inherent in the original material, since generally only the overall average DN is determined. Curiously, sample 4260, which had been heated the longest at 1500 days, shows no difference between control and heated. No explanation for this can be made without additional information.

Quantitative GPC/FT-IR Applied To CABs

The observations of processing differences for CNs prepared from wood pulp versus from cotton linters prompted some to question if there was a difference in the CABs prepared from cellulose from different sources. A major difference exists in the esterification, however, since with CABs the cellulose actually dissolves in the reaction mixture as the reaction proceeds. It is felt that any differences in morphology between types of cellulose are lost at this stage and the precipitated product will be the same.

Development of the Method

The situation for the CABs is different from the

CN described in the first part of this Chapter in that rather than one absorption band there are three to work with. In Chapter 3 it was shown that the absorbance at 1235 cm^{-1} was proportional to the acetyl substitution and the absorbance at 1176 cm^{-1} was proportional to the butyryl substitution. Again though, a means of eliminating the concentration dependance is needed. The application of the second derivative technique does not work here due to the excessive noise introduced for CABs with low acetyl or butyryl content, where the absorbance at the respective band is low. Peak areas are the preferred technique when possible, since the area is a more accurate measure of the amount of material present. However, examining the spectra in Figures 44 and 45, it is apparent that selecting the appropriate endpoints for the peak widths is difficult. This was examined, and it was found that reproducible areas by this method could not be obtained. This leaves peak heights as the best approach to developing a method.

In order to remove the concentration dependance, the peak heights of the 1235 and 1176 cm^{-1} bands were ratioed against the peak height of the 1753 cm^{-1} band. The logic for this is that the 1235 and 1176 cm^{-1} bands are due to only one ester type, while both esters give rise to some portion of the 1753 cm^{-1} band. The re-

sults, together with 95 % confidence limits are shown in Figures 70 and 71. Note that the butyryl calibration, again due to the spectral overlap, has a larger associated error. Both curves give correlation coefficients of 0.99.

Comparison of CAB From Wood Pulp and Cotton Linter

Using the ratio technique, the substitution within the GPC peaks of CABs prepared from wood pulp and cotton linters can be determined and compared. Figure 72 shows the comparison of the chromatograms of CAB 381-20 made from wood pulp and cotton linters. Both demonstrate a small high molecular weight peak eluting prior to the main GPC peak. The distributions appear to be very much the same, though. Calculating the respective degrees of substitution as described above, the data in Figures 73 to 76 result. Figures 73 and 74 show the acetyl substitution of the wood pulp and cotton linter samples respectively. In these Figures a solid line has been drawn across the data to indicate the expected substitution level. The differences noted here are that the cotton linter sample appears to be low in acetyl content in the small high molecular weight peak (first three points) and in the tailing region of the
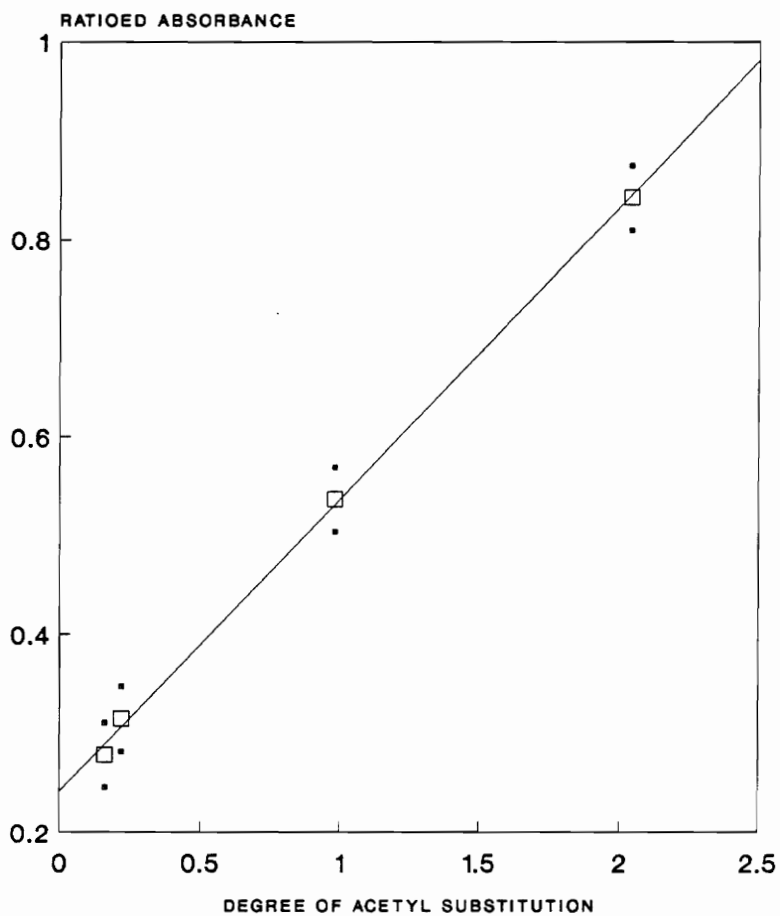
Figure 70. Calibration plot for acetyl substitution using 1235 cm^{-1} to 1753 cm^{-1} ratioed absorbances

RATIOED ABSORBANCES

DEGREE OF BUTYRYL SUBSTITUTION
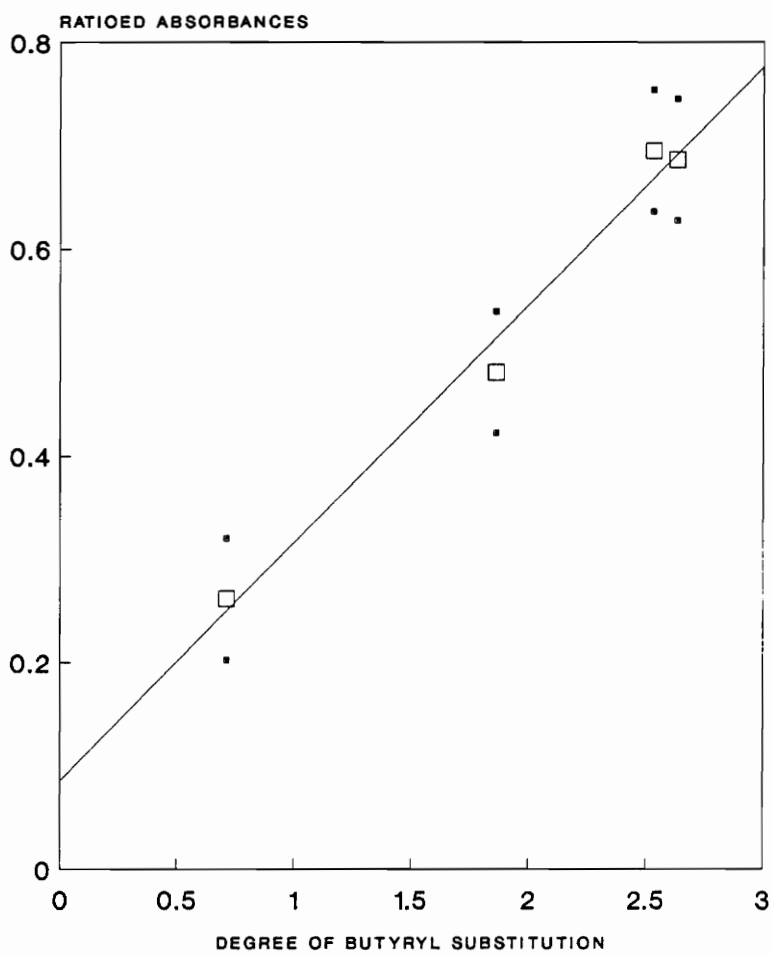
Figure 71. Calibration plot for butyryl substitution using 1176 cm^{-1} to 1753 cm^{-1} ratioed absorbances
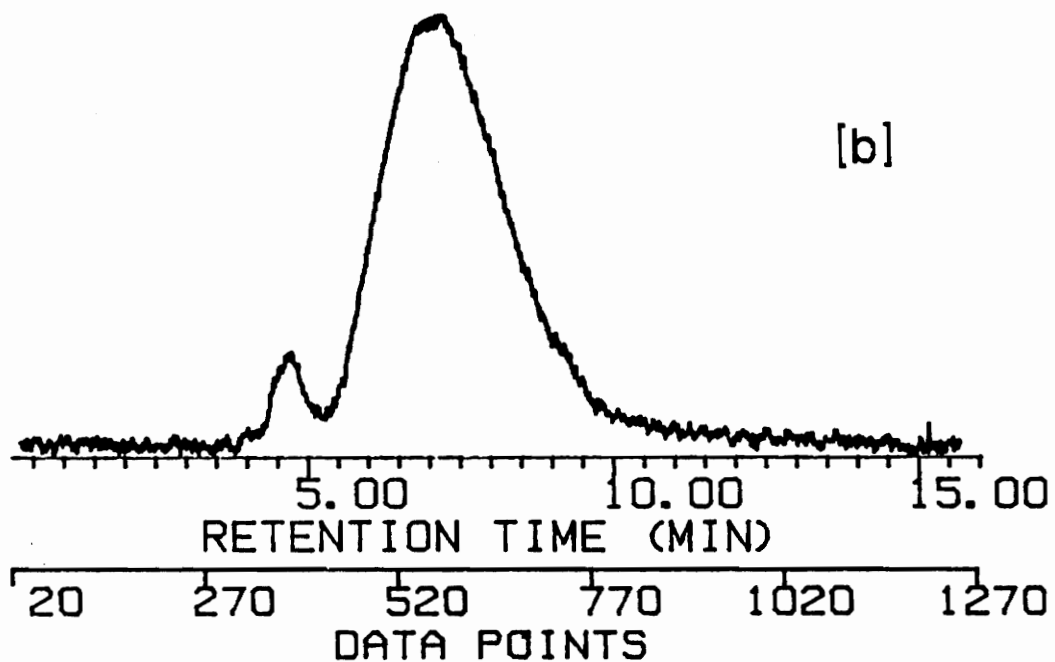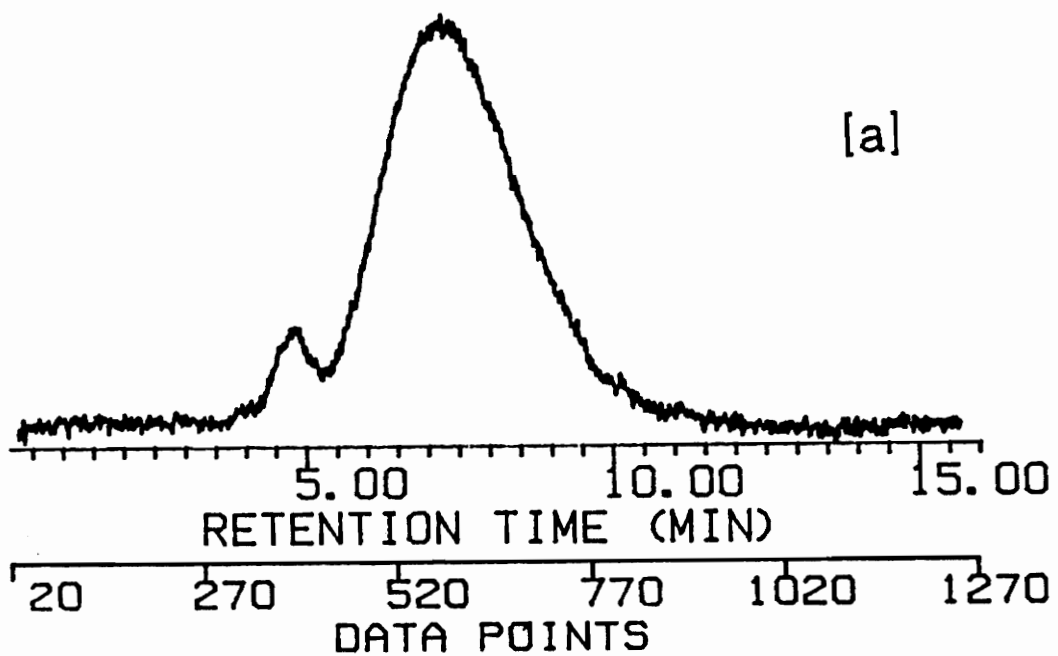
Figure 72. GPC chromatograms of CAB 381-20 from wood
pulp [a] and cotton linters [b]
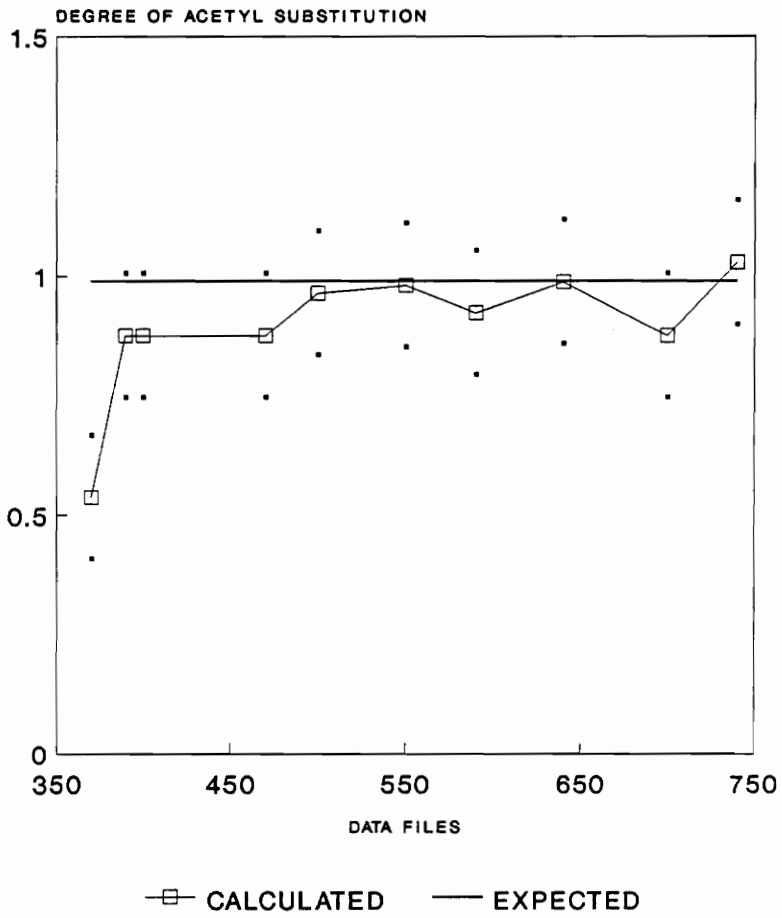
Figure 73. Calculated acetyl substitution for CAB
made from wood pulp
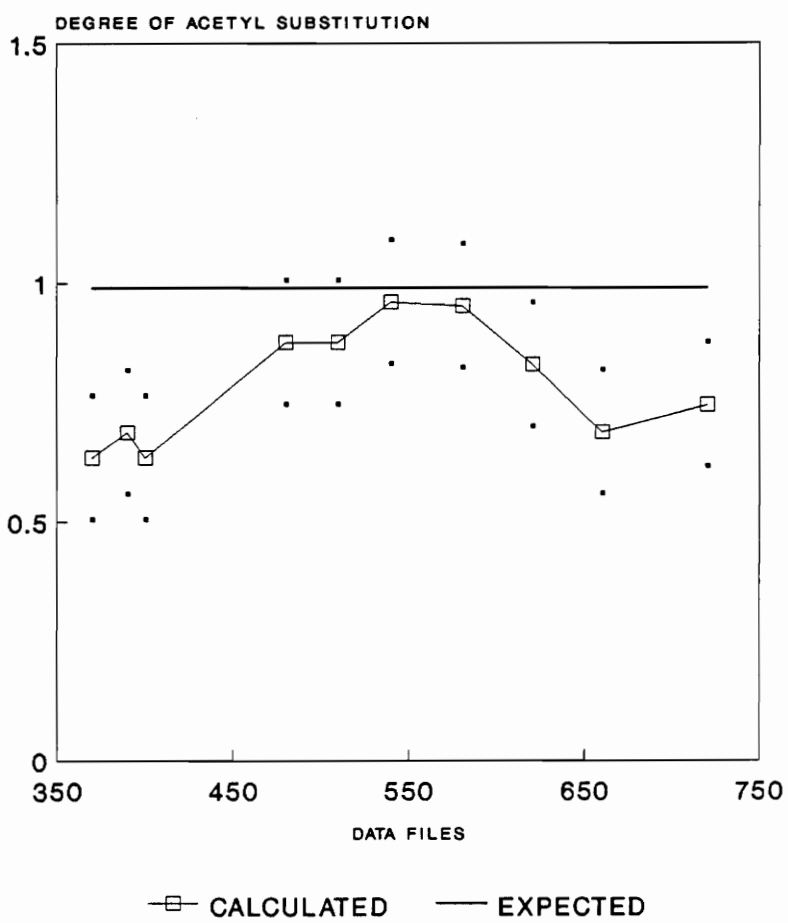
Figure 74. Calculated acetyl substitution for CAB
made from cotton linters

DEGREE OF BUTYRYL SUBSTITUTION
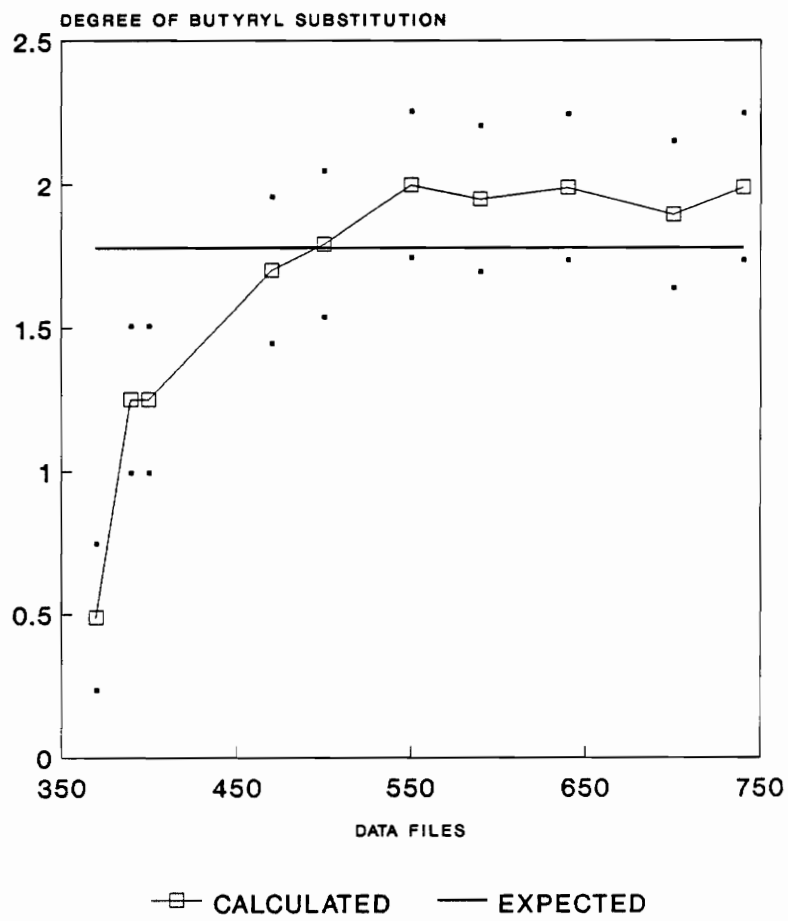
Figure 75. Calculated butyryl substitution for CAB
made from wood pulp
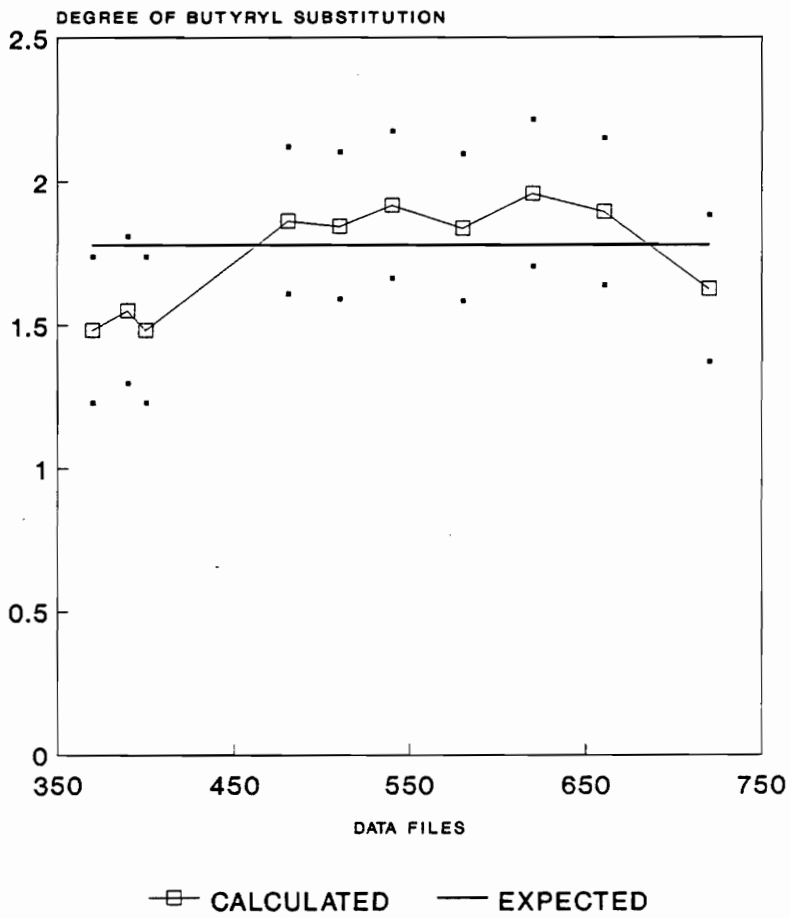
Figure 76. Calculated butyryl substitution for CAB
made from cotton linters

peak. Figures 75 and 76 show the same data for the butyryl substitutions. Here only the small high molecular weight peak of the wood pulp sample appears low, with the remainder of both samples about the same. While this does show some difference between the two samples, the differences are not large and may have arisen from factors other than just the source of cellulose.

Applications to LOVA Propellants

LOVA propellants are being investigated to reduce the spontaneous ignition hazard present in materials containing nitroglycerin. CAB is incorporated into these propellants to add an inert polymeric binder. The NOS has selected CAB 381-20 for this purpose. Figure 77a shows the GPC trace of a LOVA propellant. Note that the peaks are not fully resolved on this chromatographic system. This is not a problem when identification is needed and an infrared detector has been used. Figure 77b shows the integrated absorbance over the 1759-1747 cm^{-1} region, where CAB and only CAB in this sample absorbs. The two chromatograms are scaled the same to allow comparison. Note that the CAB peak tails into the region where the additional components elute, but it is

[a]

Cab

RETENTION TIME (MIN)

DATA POINTS

[b]

RETENTION TIME (MIN)

DATA POINTS
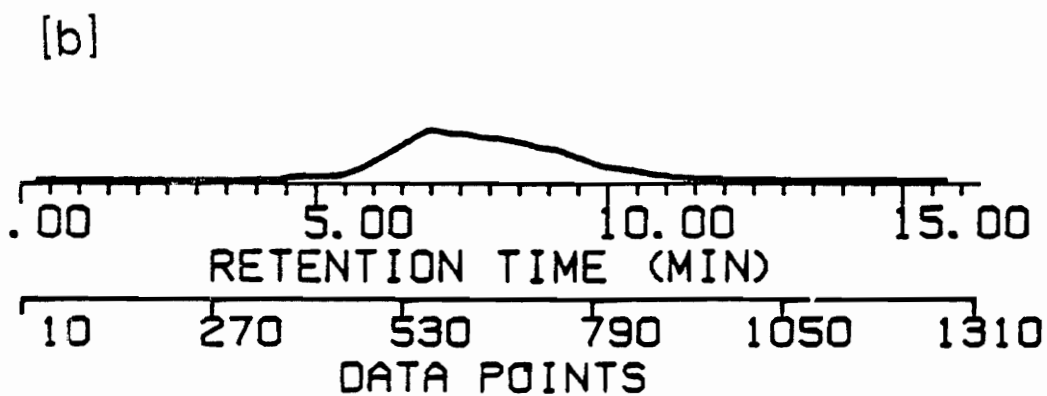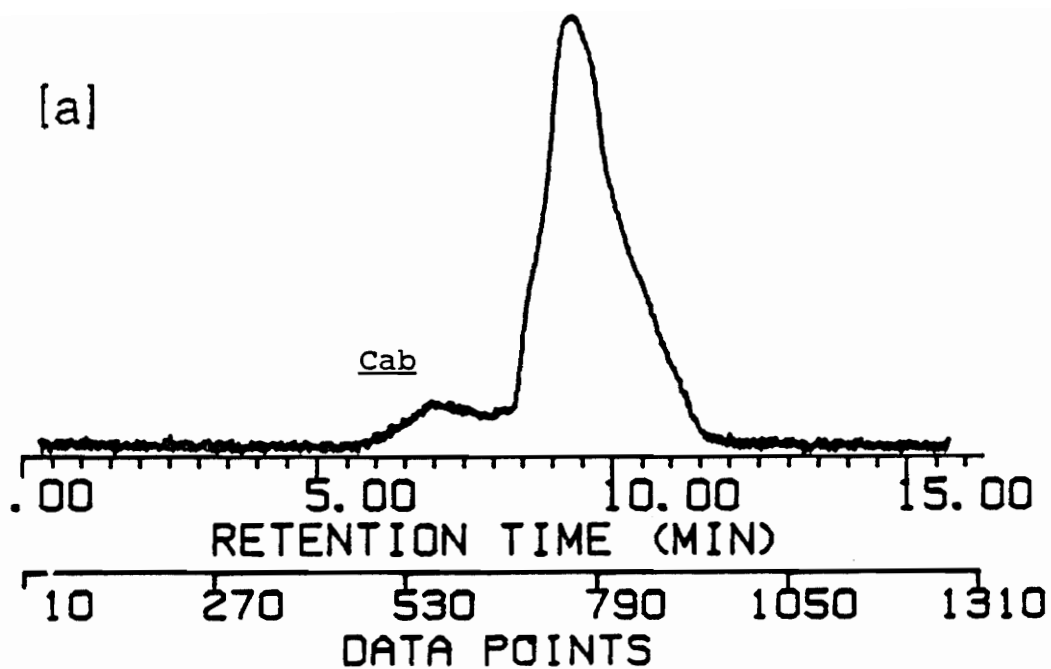
Figure 77. GPC of LOVA propellant [a] GSR, [b] 1759-
1747 cm^{-1} reconstruction

identifiable. Looking at the spectra from the early eluting portion of the CAB peak and the tailing region where it is overlapped by other components, we see that while identification of CAB is possible, quantitation of the acetyl and butyryl content is not due to inter-fering absorption from the other components (Figure 78). These components are primarily the energetic nitramines RDX and HMX. Thus, to quantitate the substi-tution of CABs in mixtures, complete chromatographic separation is necessary. This could be achieved by the use of a set of banked GPC columns, each containing a gel of decreasing pore size.

We can calculate the acetyl and butyryl substitu-tion in the earlier portion of the peak however, and these results are shown in Figures 79 and 80 respec-tively. The only observation of note is that average butyryl content appears to be slightly below what would be expected (1.78).

In conclusion, the solution infrared spectra can be used to determine the degree of nitration of CNs. The loss of nitrate groups upon heating can be detected by this method as well. Additionally, the GPC of CNs is sensitive to subtle changes in the MWD of the CN. As the MWD of the CN increases, the chromatographic peak broadens.

The quantitation of substituents for CABs is not as precise as for CN, due to the overlap of spectral features in the 1100 to 1200 cm^{-1} range. This influence is most pronounced in calculations using the absorbance ratio method. This does not preclude obtaining useful information however, particularly concerning sample homogeneity. Variations among the different regions of the GPC peak were identifiable for CABs as they were for CN.
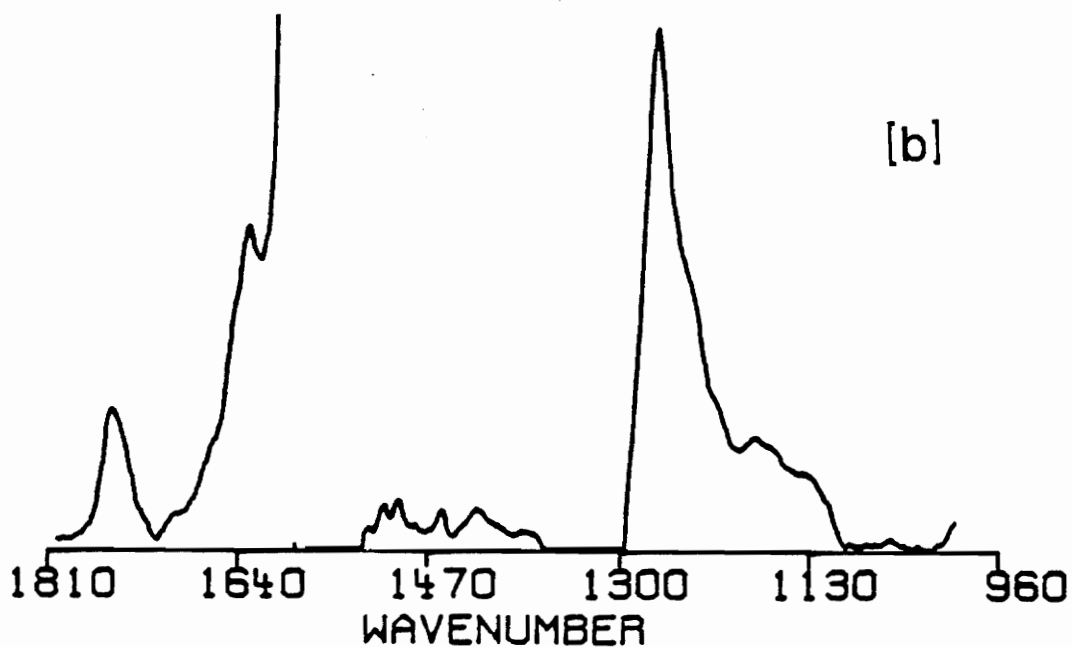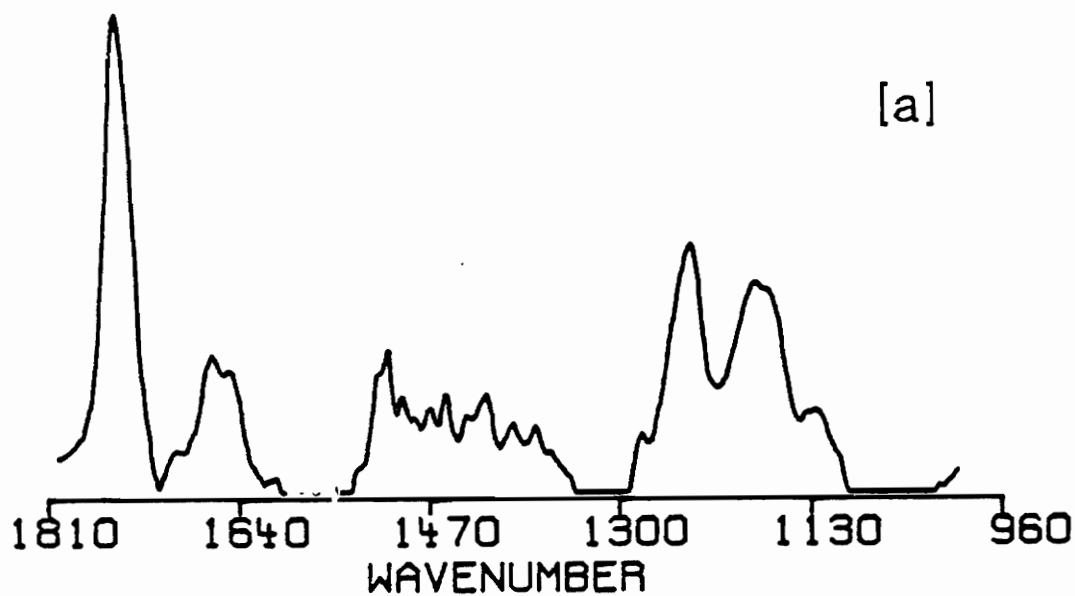
Figure 78. Infrared spectra from [a] early eluting and
[b] later eluting portion of LOVA GPC
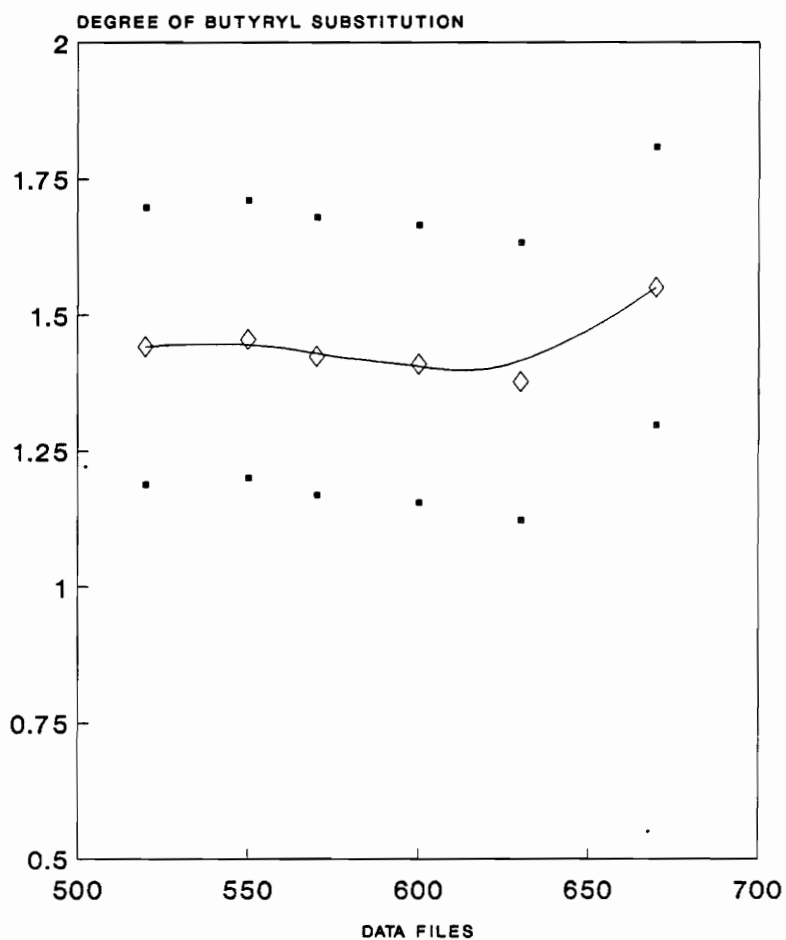
Figure 79. Calculated acetyl substitution for CAB in
LOVA

DEGREE OF BUTYRYL SUBSTITUTION
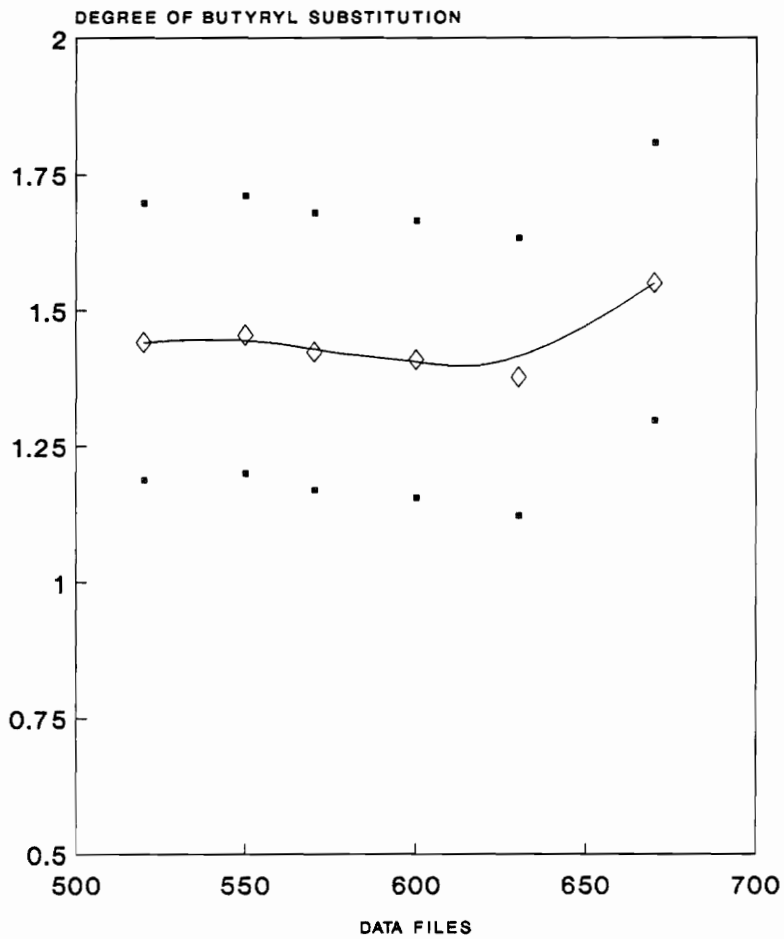
Figure 80. Calculated butyryl substitution for CAB in LOVA

Chapter 6

Conclusions

Conclusions

This research has focused upon the solution infra-
red spectra of the cellulose esters cellulose nitrate
(CN) and cellulose acetate butyrate (CAB). The objec-
tives were to explore the fundamental chemistry of the
solution behavior using FT-IR, and to develop methods
wherein this behavior might be exploited. The preceding
chapters have demonstrated that the infrared spectras
of cellulosics in solution are sensitive to the inter-
and intra-molecular interactions of the solvent/cellu-
losic pair. By selection of an appropriate solvent,
variations in the conformation of the cellulosic may be
evaluated, and also different portions of the function-
alities may be observed due to differences in solvent
infrared windows.

In Chapter 2 solvent-solute interactions of CN
with THF and acetonitrile were observed. These interac-
tions were explained by the electron donating and
accepting properties of the solvent-solute pair. Both
solvents were shown to exhibit donor type behavior
toward CN.

It was observed that primary and secondary nitrate
groups on CN have different IR absorptions. For ni-

trates in close proximity, as in the case of C_2 and C_3 dinitrated species, a shift of the infrared absorption frequency to higher energy was observed.. This shift was found to be the result of steric hindrance.

In Chapter 3 the nature of the various observed infrared spectra for CABs was explored. Here it was found that CAB behaved as a donor solute and the solvents THF, acetonitrile, and methylene chloride behaved as acceptors. Being a poorer acceptor solvent THF provided an environment wherein the CAB C=O moiety absorbed at a higher frequency than in the other solvents. It was found that in good acceptor solvents, such as acetonitrile and methylene chloride, that the influence of the ester group side chain could be observed. This was observed as a shift in the C=O frequency as a function of the acetyl content of the CAB.

The C-O-C absorption for CAB was also found to shift with changes in the ester side chain. These bands can be used to distinguish among the ester types, at least to side chain lengths of 3 carbons. A definitive trend was observed on going from acetate to propionate to butyrate for this absorption with frequencies of 1235 cm^{-1}, 1186 cm^{-1}, and 1176 cm^{-1} respectively.

In Chapter 4 methods were developed to quantitatvely idetermine the degree of nitration of CN con-

taining materials using the asymmetric nitrate stretch. This was applied successfully to both single and double base propellent formulations. The homogeneity of polymers was discernable as well as changes in the DN on heating the polymer for extended periods of time. Methods for determining the acetyl and butyryl substitution of CABs were also developed. These methods were applied to the examination of CABs prepared from different cellulose sources. Small differences in the substituent content of different molecular weight regions were observed.

In general, the applicability of on-line GPC/FT-IR as a technique for determining the degree of substitution of cellulose esters as a function of the polymer molecular weight has been demonstrated.

References

(1)   Reveley, A. In <u>Cellulose</u> <u>and</u> <u>Its</u> <u>Derivatives</u>,
      Kennedy, J.F., Phillips, G.O., Wedlock,D.J., Wil-
      liams, P.A., Eds., Ellis Horwood, Chichester

(2)   <u>Kirk-Othmer</u> <u>Encyclopedia</u> <u>of</u> <u>Chemical</u> <u>Technology</u>,
      3rd ed., Vol. 5, 1979; "Cellulose Derivatives,
      Esters"

(3)   Spurlin, H.M. In <u>High</u> <u>Polymers</u>, 1954, Vol. 5,
      Part II, "Cellulose", Chapter6, p 514

(4)   <u>Encyclopedia</u> <u>of</u> <u>Industrial</u> <u>Chemical</u> <u>Analysis</u>,
      1970, Vol.9, Snell, F.D., Ettre, L., Eds., In-
      terscience, "Cellulose Derivatives:Cellulose
      Nitrate"

(5)   Ibid, "Cellulose Derivatives:Cellulose Acetate"

(6)   <u>ASTM</u> <u>Annual</u> <u>Book</u> <u>of</u> <u>Standards</u>, 1988, Vol. 8.01,
      D 817-72 American Society for Testing and Materi-
      als

(7)   <u>Encyclopedia</u> <u>of</u> <u>Industrial</u> <u>Chemical</u> <u>Analysis</u>,
      1970, Vol. 5, Snell, F.D., Ettre, L., Eds.,
      Interscience, "Cellulose Derivatives:Esters"

(8)   <u>Fourier</u> <u>Transform</u> <u>Infrared</u> <u>Spectrometry</u>, Grif-

fiths, P.R., de Haseth, J.A., Chemical Analysis
Series Vol. 83, 1986, Wiley-Interscience, p 618

(9)   Chemistry and Technology of Explosives, Ubanski,
        T., 1985, Vol. 2, Pergamon Press, p 278

(10)   Siochi, E.J., Ph.D. Dissertation, Virginia Poly-
        technic Institute and State University, 1988

(11)   Mitchell, R.L., Ind. Eng. Chem., Anal. Ed.,1953,
        45,2526

(12)   Conrad, C.M., Ibid,2511

(13)   Meyerhoff, G., Makromol.Chem.,1965,89,282

(14)   Segal, L., J. Polym. Sci., Polym. Lett. Ed.,1966,
        4,1011

(15)   Segal, L.,J. Polym. Sci., Polym. Phys. Ed., 1968,
        21,267

(16)   Marx-Figini, M., Soubelet, O., Polym. Bull.,1984,
        11,281

(17)   Meyerhoff, G., Ber. Bunsenges. Phys. Chem.,1965,
        69,866

(18)   Meyerhoff, G., J. Chromatographic Sci.,1971,9,596

(19)   Marx-Figini, M,, Soubelet, O., Polym. Bull.,1982,
        6,501

(20)   Schurz, J.,Haas, J.,Cellul. Chem. Technol.,1970,
        4,633

(21)   Cunningham, A.F., Heathcote, C., Hillman, D.E.,
        Paul, J.I. In Liquid Chromatography of Polymers

and Related Materials II, Cazes, J., Delamare,
X., Eds., Chromatographic Science Series 13, 1979
Marcel Dekker

(22) Goldwasser, J.M., Carlson, D., Nauflett, G.W.,
Proceedings of the 1985 JANNAF Propellant Charac-
terization Subcommittee Meeting, C.P.I.A. Pub.
435,**1985**,291

(23) Carlson, D., Dow, T., Nauflett, G.W., Presented
at the 1988 JANNAF Propellant Characterization
Subcommittee Meeting, Las Cruces, N.M., Oct. 1988

(24) French, D.M., Nauflett, G.W., J. Liq. Chrom.,
1981,4,197

(25) Hillman, D.E., Paul, J.I., J. Chromatogr.,**1975**,
108,397

(26) Benoit, H., Grubisic, Z., Rempp, P, Polym. Lett.,
1967,5,753

(27) Holt, C., Mackie, W., Sellen, D., Polymer,**1978**,
19,1421

(28) Goetz, H., Elgass, H., Huber, L., J. Chromatogr.,
1985,349,357

(29) Meyerhoff, G., Makromol. Chem.,**1970**,134,129

(30) Spurlin, H.M. In High Polymers, Vol. 5 "Cellulose
and Its Derivatives", Part III, Interscience,
1955, Chapter 10, p 1094

(31) Lloyd, J.B.F., Anal. Chem.,**1984**,56,1907

(32) Lloyd, J.B.F., <u>J. Chromatogr.</u>,**1986**,<u>351</u>,323

(33) Raisor, R.C., Law, R.D., <u>Proceedings of the 1984 JANNAF Propellant Characterization Subcommittee Meeting</u>, C.P.I.A. Pub. 413,**1985**,39

(34) Prat, Y., Forestier, H., <u>Mem. Poudres.</u>,**1963**,<u>45</u>, 215; **CA** 64:1239d

(35) Elie-Calmet, J., Forestier, H., <u>Int. Crim. Police Rev.</u>,**1979**,<u>325</u>,38; **CA** 91:69406h

(36) Douse, J.M.F., <u>J. Chromatogr.</u>,**1982**,<u>234</u>,415

(37) Kamide, K., Okada, T., Terakawa, T., Kaneko, K., <u>Polym. J.</u>,**1978**,<u>10</u>,547

(38) Brewer, R.J., Tanghe, L.J., Bailey, S., Burr, J.T., <u>j. Polym. Sci., Polym. Chem. Ed.</u>,**1968**, <u>6</u>,1697

(39) Kamide, K., Miyazaki, Y., Abe, T., <u>Makromol. Chem.</u>,**1979**,<u>180</u>,2801

(40) Ibid, <u>Polym. J.</u>,**1979**,<u>11</u>,523

(41) Kamide, K., Saito, M., Abe, T., Ibid,**1981**,<u>13</u>,421

(42) Kamide, K., Terakawa, T., Miyazaki, Y., Ibid, **1979**,<u>11</u>,285

(43) Alexander, W.J., Muller, T.E., <u>Separation Sci.</u>, **1971**,<u>6</u>,47

(44) Levi, G.R., Giera, A., <u>Gazz. Chim. Ital.</u>,**1937**,<u>67</u>, 719; **CA** 32:4327[6]

(45) Okunev, P.A., Tarakanov, O.G., <u>Khim. Volokna.</u>,

1963,$\underline{6}$,44; **CA** 60:7018e

(46) Mano, E.B., Cunha Lima, L.C.O., <u>Anal. Chem.</u>,**1960**, $\underline{32}$,1772

(47) Wilson, S., Floyd, T., Presented at the 28th Eastern Analytical Symposium, New York N.Y., 1989

(48) Williams, R.J., Siggia, S., <u>Anal. Chem.</u>,**1977**, $\underline{49}$,2337

(49) Kuhn, L.P., <u>Anal. Chem.</u>,**1950**,$\underline{22}$,276

(50) Pristera, F., Halik, M., Castelli, A., Fredericks, W., <u>Anal. Chem.</u>,**1960**,$\underline{32}$,495

(51) Rosenberger, H.M., Shoemaker, C.J., <u>Anal. Chem.</u>, **1959**,$\underline{31}$,1315

(52) Levitsky, H., Norwitz, G., <u>Anal. Chem.</u>,**1962**, $\underline{34}$,1167

(53) Clarkson, A., Robertson, C.M., <u>Anal. Chem.</u>,**1966**, $\underline{38}$,522

(54) Norwitz, G., Chasan, D.E., <u>Talanta</u>,**1973**,$\underline{20}$,73

(55) Jutier, J., Harrison, Y., Premont, S., Prud'homme , R., <u>J. Appl. Polym. Sci.</u>,**1987**,$\underline{33}$,1359

(56) Brodman, B.W., Devine, M.P., Gurbarg, M.T., Ibid, **1974**,$\underline{18}$,943

(57) Ibid, **1975**,$\underline{19}$,2913

(58) Ibid, **1976**,$\underline{20}$,569

(59) Brodman, B.W., Devine, M.P., Schwartz, S., Ibid, **1976**,$\underline{20}$,2607

(60)   Brodman, B.W., Devine, M.P., Ibid, **1980**,25,1245

(61)   Brodman, B.W., Devine, M.P., Lampner, N., Ibid,
       1981,26,1739

(62)   Nauflett, G.W., Gill, R.C., U.S. Patent #
       4 457 791, 1984

(63)   Cangelosi, F., Shaw, T., Polym. Eng. Sci.,**1983**,
       23669

(64)   Panov, V.P., Zhbankov, R.G., Malakhov, R.A.,
       Polym. Sci. USSR, (Engl. Transl.) **1969**,11,2566 ;
       Vysokomol. Soyed.,**1969**,A11,2254

(65)   Ibid, (Engl. Transl.) **1970**,12,2007; Ibid, **1970**,
       A12,1768

(66)   Brown, L., Holliday, P., Trotter, I.F., J. Amer.
       Chem. Soc.,**1951**,73,1532

(67)   Mitchell, J.A., Bockman, C.D., Lee, A.V., Anal.
       Chem.,**1957**,29,499

(68)   Hilton, C.L., Anal. Chem.,**1959**,31,1610

(69)   Ivanova, N.V., Zhbankov, R.G., Vodorodnaya Svyaz,
       Akad. Nauk SSSR, Inst. Khim. Fiz., Sb. Statei,
       1964,149; **CA** 62:2906e

(70)   Marupov, R., Vestin. Akad. Navuk Belarusk SSR,
       Ser. Fiz.-Tekhn. Navuk,**1963**,3,128;
       CA 60:1236d

(71)   Low, M.J.D., Freeman, S.K., Anal. Chem.,**1967**,
       39,194

(72) <u>Fourier</u> <u>Transform</u> <u>Infrared</u> <u>Spectrometry</u>, Grif-
     fiths, P.R., de Haseth, J.A., John Wiley & Sons,
     1986, Chapters 18 and 19

(73) Ross, J.H., Casto, M.E., <u>J.</u> <u>Polym.</u> <u>Sci.,</u> <u>Polym.</u>
     <u>Phys.</u> <u>Ed.,</u>**1968,**<u>21</u>,143

(74) Terry, S.L., Rodriguez, F., Ibid, 191

(75) Vidrine, D.W., Mattson, D.R., <u>Appl.</u> <u>Spectrosc.,</u>
     1978,<u>32</u>,502

(76) Vidrine, D.W., <u>J.</u> <u>Chromatogr.</u> <u>Sci.,</u>**1979,**<u>17</u>,477

(77) Vidrine, D.W. In <u>Fourier</u> <u>Transform</u> <u>Infrared</u> <u>Spec-</u>
     <u>troscopy:</u> <u>Applications</u> <u>to</u> <u>Chemical</u> <u>Systems</u>,
     Ferraro, J.R., Basile, L.J., Eds., Vol. 2,
     Chapter 4

(78) Coffey, P., Mattson, D.R., Presented at the
     International Conference on Fourier Transform
     Infrared Spectroscopy, Columbia, S.C., 1977,
     paper MB6

(79) de Haseth, J.A., Isenhour, T.L., Ibid, paper MB7

(80) Coffey, P., Mattson, D.R., Wright, J.C., <u>Am.</u> <u>Lab.</u>
     ,**1978,**<u>10</u>(5),126

(81) de Haseth, J.A., Isenhour, T.L., <u>Anal.</u> <u>Chem.,</u>**1977**
     ,<u>49</u>,1977

(82) Spurlin, H.M. In <u>High</u> <u>Polymers</u>,Vol. 5 "Cellulose
     and Cellulose Derivatives", Part III, 1955,
     Interscience, Chapter 10, p 1074

(83) Segall, G.H., Purves, C.B., <u>Can. J. Chem.</u>,**1952**,
      <u>30</u>,860

(84) Falconer, E.L., Purves, C.B., <u>J. Am. Chem. Soc.</u>,
      1957,<u>79</u>,5308

(85) Wu, T.K., <u>Macromolecules</u>,**1980**,<u>13</u>,74

(86) Reeder, M.E., M.S. Thesis, Virginia Polytechnic
      Institute and State University, 1981

(87) Shearer, D.S., <u>JANNAF Propellant Characterization
      Subcommittee Workshop on Nitrocellulose Problems</u>
      ,**1985**,C.P.I.A. Pub. 438,1

(88) White, B.R., Richardson, A.C., Ibid,41

(89) Misra, N., Mandal, B.M., <u>Makromol. Chem. Rapid
      Commun.</u>,**1984**,<u>5</u>,471

(90) <u>Introduction to Modern Liquid Chromatography</u>,
      2nd ed, Snyder, L.R., Kirkland, J.J., 1979, John
      Wiley & Sons, Chapter 12, p 501

(91) Williams, K.W., <u>Lab. Pract.</u>,**1972**,<u>21</u>,667

(92) Clark, D.T., Stephenson, P.J., Heatley, F., <u>Poly-
      mer</u>,**1981**,<u>22</u>,1112

(93) <u>Chemistry and Technology of Explosives</u>, Urbanski,
      T., 1985, Pergamon Press, Vol. 4, Chapter 3, p 69

(94) Leider, H.R., Pane, A.J., <u>Proceedings of the
      ADPA Symposium on the Compatibility of Plastics
      and Other Materials with Explosives, Propellants,
      Pyrotechnics and Processing of Explosives, Pro-</u>

pellants and Ingredients, Oct. 1986, p 231

(95) Panov, V.P., Zhbankov, R.G., Malakhov, R.A.,
Polym. Sci. USSR (Engl. Transl.), **1970**,12,1738;
Vysokomol. Soyed.,**1970**,A12,1527

(96) Kuznetsova, Z.I., Ermolenko, I.N., Ivanova, V.S.,
Acad. Sci. USSR, Belorussian SSR (Engl. Transl.),
1968,6,1227; Izvestiya Akad. Nauk SSSR, Ser.
Khim.,**1968**,6,1301

(97) Urbanski, T., Witanowski, M., Trans. Faraday
Soc.,**1963**,59,1039

(98) Ibid, 1046

(99) Spurlin, H.M. In High Polymers, Vol. 5, "Cellu-
lose and Cellulose Derivatives", Part II, 1955,
Chapter 9, p 676

(100) Katritzky, A.R., Topsom, R.D., In Advances in
Linear Free Energy Relationships, Chapman, N.B.,
Shorter, J., Eds., 1972, Plenum Press

(101) Shorter, J. Ibid

(102) The Donor -Acceptor Approach to Molecular Inter-
actions, Gutmann, V., 1978, Plenum Press, p 3

(103) Wagniere, G.H. In The Chemistry of the Nitro and
Nitroso Groups, Feuer, H., Ed., 1969, Inter-
science, Part I

(104) Whitbeck, M.R., Appl. Spectrosc.,**1981**,35,93

(105) Urbanski, T., Witanowski, M., Trans. Faraday Soc.

,**1963**,<u>59</u>,1039

(106) <u>Chemistry</u> <u>and</u> <u>Technology</u> <u>of</u> <u>Explosives</u>, Urbanski,
       T., Vol. 4, 1984, Pergamon Press, Chapter 3

(107) Axenrod, T., Liang, B., Bulusu, S., <u>Magn.</u> <u>Reson.</u>
       <u>Chem.</u>,**1989**,<u>27</u>,925

(108) Bell, H.M., Virginia Polytechnic Institute and
       State University, Personal Communication

(109) Maddams, W.F., <u>Appl.</u> <u>Spectrosc.</u>,**1980**,<u>34</u>,245

(110) Kauppinen, J.K., Moffatt, D.J., Mantsch, H.H.,
       Cameron, D.G., Ibid,**1981**,<u>35</u>,271

(111) Holler, F., Burns, D.H., Callis, J.B., Ibid,
       1989,<u>43</u>,877

(112) Pierce, J.A., Jackson, R.S., Van Every, K.W.,
       Griffiths, P.R., Hongjin, G., <u>Anal.</u> <u>Chem.</u>,**1990**,
       <u>62</u>,477

(113) <u>Infrared</u> <u>Spectroscopy</u>, Conley, R., 2nd ed,
        Chapter 5

(114) Wohar, M.M., Seehra, J.K., Jagodzinski, D.W.,
       <u>Spectrochim.</u> <u>Acta,</u> <u>Part</u> <u>A</u>, **1988**,<u>44</u>,999

(115) Nyquist, R.A., Kirchner, T.M., Fouchea, H.A.,
       <u>Appl.</u> <u>Spectrosc.</u>,**1989**,<u>43</u>,1053

(116) Nyquist, R.A., Putzig, C.L., Hasha, D.L., Ibid,
       1049

(117) Nyquist, R.A., Chrzan, V., Houck, J., Ibid, 981

(118) Nyquist, R.A., Putzig, C.L., Yurga, L., Ibid, 983

(119) Strecker, R.A., Turngren, E.V., <u>Joint Symposium on Compatibility of Plastics and Materials with Explosives, and Processing of Explosives, Propellants, and Ingredients</u>, Oct 1980

(120) James, B.H., <u>Int. Jahrestag Fraunhofer-Inst. Treib Explosivst.</u>, 17th(Anal. Propellants Explos; Chem. Phys. Methods), 37-1

Vita

Charles William Saunders was born January 27, 1955 to Dr. Thomas D. and Virgie H. Saunders. He was raised in Newport News, Virginia where he graduated from H. L. Ferguson High School in 1972. He received his B. S. (cum laude) in chemistry from Christopher Newport College, Newport News, VA. in 1981. He received his M. S. in chemistry from Old Dominion University, Norfolk, VA. in 1986 under the direction of Prof. Patricia Pleban. Also in 1986 he began his studies at Virginia Polytechnic Institute and State University toward the Ph.D. in chemistry under the direction of Prof. Larry T. Taylor.

He is married to Dr. Mary Ellen Brown, currently a practicing veterinarian in Front Royal, VA.